Drug Eluting Hydrogels

Design, Synthesis and Evaluation

Lage Ahrenstedt

Doctoral Thesis

Department of Surgery

University of Cape Town

Cape Town

Aug 2012

The results in this thesis were produced in collaboration between the University of Cape Town (UCT; South Africa) and the Royal Institute of Technology (KTH; Stockholm, Sweden).

ROYAL INSTITUTE
OF TECHNOLOGY

Supervisor: Dr. Deon Bezuidenhout (UCT)

Co-supervisor: Prof. Anders Hult (KTH)

Department of Surgery
University of Cape Town
Chris Barnard Building
ZA-7925 OBSERVATORY
South Africa

ISBN 978-91-7501-071-7

PROLOGUE

In 1897 Josef Conrad wrote that an author must be like an artist in capturing the movement of a dart into stone or the magic intonation into a piece of music. In the same manner a scientist must use artistic abilities to grasp the complexity of his work and to interpret its content. But in contrast to the artist who works with ideas the scientist follows the path of facts.

Within this context the author, artist and scientist behind this work will take the reader on a journey through the development of drug eluting hydrogels and put those in the context of ameliorating the healing of cardiovascular diseases.

ABSTRACT

Hydrogels have successfully proved themselves useful for drug delivery applications and several delivery routes have been developed over the years. The particular interest in this work was to design, synthesise and evaluate *in situ* forming drug eluting hydrogels, which have the potential to ameliorate the healing of cardiovascular diseases.

With this aim the anti-inflammatory and immunosuppressant drugs rapamycin (Ra) and dexamethasone (Dex) were made water soluble by conjugation with polyethylene glycol (PEG). Ra was attached pendant from the terminal of PEGs while Dex was incorporated into dendritic structures grown from PEGs. These conjugates were further crosslinked into hydrogels by either conjugate or thiol-ene addition. The gel degradation was tuned to take between 5 and 27 days by using gel building block combinations that induced either 2 or 4 hydrolytically labile bonds per crosslink or by varying the number of crosslinking sites of the building blocks. The use of thiol-ene addition prolonged the degradation time nearly seven folded compared to conjugate addition as a more stable crosslink was formed.

Two different formulations for gelling via conjugate addition were used (acrylate-thiol or vinyl sulphone-thiol) to deliver Ra, which was carried by either a 4- or 2-armed PEG. The elution kinetic for the respective gel formulation was of zero order during 15 and 19 days of gel degradation. In addition, Ra was PEGylated via esters, with a distance of either one or two carbons to a nearby thio-ether functionality. The difference in ester conjugation resulted in a slight but significant change in drug-PEG conjugate stability, which was mirrored by the increased time to reach the half amount of total drug elution; from 9.3 to 10.2 days and from 5.1 to 9.7 days for the two gel formulations, respectively. Dexamethasone was incorporated via an ester into dendrons of first and second generation pending from 2- and 4-armed PEGs at loadings of 2, 4 or 6 Dex molecules per carrier molecule. The resulting elution kinetic was of zero order during degradation periods of 5-27 days. Released Dex still possessed biological activity as determined by an *in vitro* cell assay.

The novelties in this thesis are: (**A**) slow release of rapamycin obtained by covalent incorporation into hydrogels, (**B**) the use of unique PEG-based dendrimers to incorporate dexamethasone into a hydrogel and (**C**) zero order sustained release of dexamethasone at physiological pH.

SAMMANFATTNING

Hydrogeler har framgångsrikt visat sig användbara för att leverera läkemedel och ett flertal metoder har utvecklats de senaste 20 åren. Fokuset i den här avhandlingen ligger på att designa, framställa och utvärdera läkemedelsutsöndrande hydrogeler som spontanhärdar *in situ*, vilka har potential att förbättra läkningen efter kardiovaskulär sjukdom.

Med det syftet gjordes de anti-inflammatoriska och immunsänkande läkemedlen rapamycin (Ra) och dexametason (Dex) vattenlösliga genom att konjugeras med polyetylenglygol (PEG). Ra fästes kovalent längst ut på PEGar medans Dex inkluderades i dendritiska strukturer vilka byggdes från ändpunkten av PEGar. De här konjugaten tvärbands till hydrogeler via antingen konjugerad addition eller radikal polymerisation. Nedbrytningen av gelerna trimmades till att ta mellan 5 och 27 dagar genom att använda kombinationer av gelbyggstenar som bildar antingen 2 eller 4 hydrolyserbara estrar per tvärbindning eller genom att variera antalet tvärbindningspunkter hos byggstenarna. Användandet av radikal polymerisation i sig ledde till att nedbrytningen av geler tog nära sju gånger längre tid jämfört med geler gjorda via konjugerad addition eftersom stabilare tvärbindningar då formas.

Två olika kombinationer för härdning via konjugerad addition (akryl-tiol eller vinylsulfon-tiol) användes för att leverera Ra som bars av antingen en 4- eller 2-armad PEG. Utsöndringskinetiken av Ra för de två kombinationerna var av nollte ordningen under de 15 och 19 dagar som gelerna degraderade. Dessutom, Ra PEGylerades via estrar med ett avstånd på antingen ett eller två kol till en närliggande tioeter. Skillnaden i avstånd ledde till en liten men signifikant skillnad i stabiliteten hos Ra-PEG konjugaten, vilket speglades i den förlängda tiden att nå halva mängden av den totala läkemedelsutsöndringen; från 9.3 till 10.2 dagar och från 5.1 till 9.7 dagar för de två respektive gelkombinationerna. Dex kopplades in via en esterbindning till dendroner av första och andra generationen byggda från PEGar med 2 eller 4 armar, vilket resulterade i att 2, 4 eller 6 Dex levererades per bärarmolekyl. Dex eluerade med nollte ordningens kinetik under degraderingsperioder på mellan 5 och 27 dagar. Vidbehålllen biologisk aktivitet av eluerad Dex bekräftades genom cellexperiment *in vitro*.

Nyheterna i den här avhandlingen består av: (**A**) kontrollerad utsöndring av rapamycin uppnådd genom kovalent inbindning till hydrogeler, (**B**) användandet av unika PEGbaserade dendrimerer för kovalent inbindning av dexametason till hydrogeler och (**C**) nollte ordningens utsöndring av dexametason vid fysiologiskt pH.

LIST of PUBLICATIONS

The work in this thesis is presented or will be presented in the following publications.

Covalent Incorporation and Controlled Release of Active Dexamethasone from Injectable Polyethylene Glycol Hydrogels

Bezuidenhout D, Oosthuysen A, Davies N, **Ahrenstedt L**, Dobner S and Zilla P

2012, Submitted to J Biomed Mater Res A

Tailored Zero Order Rapamycin Release from Degradable PEG Hydrogels

Ahrenstedt L and Bezuidenhout D

2012, Manuscript in preparation

Hydrogels Made of PEG Didendrons with Pending Dexamethasone Result in Zero Order Sustained Release

Ahrenstedt L, Hed Y, Hult A, Zilla P, Malkoch M, Bezuidenhout D

2012, Manuscript in preparation

Dendritic Hydrogels for Controlled Drug Delivery

Ahrenstedt L, Hed Y, Malkoch M, Hult A, Zilla P, Bezuidenhout D

11th International Conference on Frontiers of Polymers and Advanced Materials

2011, Poster Presentation

ABBREVIATIONS

The abbreviations are listed in alphabetical order, regarding the left hand side column.

3D	Three-dimensional
Å	Ångström
Ac	Acrylate
AcCl	Acryloyl chloride
Acet	Acetonide protection
Act	Acetylene
At	Atorvastatin
CVDs	Cardiovascular deceases
d	Doublet
DCC	*N,N*'-dicyclohexylcarbodiimide
DCM	Dichloromethane
dd	Doublet of doublets
Dex	Dexamethasone
DMAP	4-Dimethylaminopyridine
DMF	Dimethylformamide
DMPA	2,2-dimethoxy-2-phenyl acetophenone
Dox	Doxorubicin
eq	Equivalent
ESI-MS	Electrospray ionisation mass spectroscopy
EtOAc	Ethyl acetate
EtOH	Ethanol
FI	Fold induction
g	Gram
HDC	Huisgen 1,3-dipolar cycloaddition
Hep	*n*-Heptane
Hex	*n*-Hexane
HPLC	High pressure liquid chromatography
I	Photo initiator
IAE	Iodoacetic ester
kDa	kilo Dalton
KTH	Royal Institute of Technology
m	Multiplet

MALDI	Matrix-assisted laser desorption ionisation time-of-flight mass spectroscopy
MeCN	Acetonitrile
MeOH	Methanol
mg	Milligram
MHz	Megahertz
MI	Myocardial infarct
ml	Millilitre
mm	Millimetre
mmol	Millimole
MMP	Matrix metalloproteases
mTOR	Mammalian target of rapamycin
nm	Nanometre
NMR	Nuclear magnetic resonance
NVP	*N*-vinyl-2-pyrrolidone
PBS	Phosphate buffered saline
PEG	Polyethylene glycol
PGA	poly(glycolic acid)
pH	$-\log[H^+]$
pKa	$-\log[K_a]$, K_a =acid dissociation constant
PLA	poly(lactic acid)
PLGA	poly(lactic-co-glycolic acid)
ppm	Parts per million
pTSA	Para toluene sulphonic acid
Ra	Rapamycin
s	Singlet
TEA	Triethylamine
THF	Tetrahydrofuran
TLC	Thin layer chromatography
Trizma	2-Amino-2-hydroxymethyl-propane-1,3-diol
UK	United Kingdom
UV	Ultraviolet
VS	Vinyl sulphone

TABLE of CONTENTS

1 INTRODUCTION

Over the last century the concept of hydrogels has been developed into an interesting branch of polymer science with enormous potential. Particularly fruitful is the use of hydrogels in medical research where gels are commonly used in a wide spectrum of applications. There are multiple parameters to consider in the design of a hydrogel, which must all individually be adapted to obtain desired gel properties. This broad register of choices is the origin of the success for hydrogel applications, since it allows for the preparation of gels with very divert but specific properties. Hence, with proper design and methodology it is possible to create gels that fulfil the strict demands of a biomaterial (Hoffman 2002) which can be used as wound covers, implant coatings, slow-release devices or materials that mimic *in vivo* functionality (Hubbell 1998; Lin *et al.* 2009). Commonly, drugs or growth factors are delivered with the hydrogels to obtain these properties in a biological system.

Many drugs however, are hydrophobic and therefore insoluble in the human aqueous media, which is a problem for drug delivery and efficiency. The non-solubility is a particular problem in cases where the drug is delivered from a solution, as only aqueous solutions should be introduced into living tissue. Therefore various approaches towards *in situ* delivery of hydrophobic drugs have been developed and a common method is to conjugate the drug to a water soluble polymer, such as PEG (polyethylene glycol). This conjugation does not only bring the drug into solution but also increases its circulation time and protects it, primarily in case of peptides and proteins, against proteolytic activity (Woghiren *et al.* 1993; Gombotz *et al.* 1995; Elbert *et al.* 2001; Roberts *et al.* 2002; Li *et al.* 2003; Frokjaer *et al.* 2005; Veronese *et al.* 2005).

Rapamycin (McMurray *et al.*), a macrolide compound originally developed as an antifungal agent, and Dexamethasone (Dex), a synthetic member of the glucocorticoid class of steroid drugs, both have immunosuppressant and anti-inflammatory properties. These drugs have high potential for ameliorating cardiovascular healing, which is of interest to our group, and have previously been used to prevent restenosis (Morice *et al.* 2002; Koenig *et al.* 2009), quench pathological cardiac hypertrophy (McMullen *et al.* 2004) and to reduce inflammation from implanted devices (Baeyens *et al.* 1998).

One approach to ameliorate cardiovascular recovery is by means of drugs and a crucial step in such approach is to develop suitable drug delivery devices. This thesis describes the development of methods to obtain controlled and sustained drug delivery of Ra and Dex via hydrogels and is part of a larger overall project (which describes healing post myocardial infarction using animal models and

other gel formulations than described here). The methods are based on drug PEGylation and the work shows the importance of proper design of the hydrogel formulation and drug incorporation methods to achieve desired properties.

1.1 Hydrogels

A hydrogel is formed by creating a sufficient number of crosslinks between polymeric building blocks so that a continuous three-dimensional (3D) network is created. The most representative feature of hydrogels is the ability to absorb large amounts of water.

In theory a multi-arm with only two functional groups (f_a =2) could be crosslinked by a 2-armed crosslinker (f_b =2), but then the hydrogel would not consist of an inter-crosslinked polymer network but a random entanglement of copolymers, which demands a conversion of 100% to form according to **Equation 1**. Practically however, a functionality of three is the minimum requirement for the multi-arm to form an infinitely connected network when crosslinked by a 2-armed crosslinker and according to **Equation 1** a conversion of 71% is needed for this combination to reach the gel point.

$$\textit{Critical conversion} = \sqrt{\frac{1}{(f_a - 1)(f_b - 1)}} \qquad (\mathbf{1})$$

The final degree of conversion is individual for each hydrogel system and increased by high polymer concentration and long gelling time (DuBose *et al.* 2005).

Figure 1 illustrates the resulting continuous network after crosslinking an 8-armed star shaped multi-arm with a 2-armed linear crosslinker. A stoichiometric ratio (1:1) for the functional groups of the two pregel components is fundamental for the gel to form. Only a few percent deviations may prevent the gelling, or at least drastically slow down the process. In the case where too many of the multi-arms are present mainly dimers are formed while an excess of crosslinker saturates the multi-arm and hence, no continuous network is formed. Nonetheless, even for a stoichiometric relation the crosslink efficiency is not 100% since the progressing network formation itself makes the forming gel more rigid, which lowers the possibility for remaining functional groups to come in close enough proximity to react, hence there will be unreacted groups in a gel.

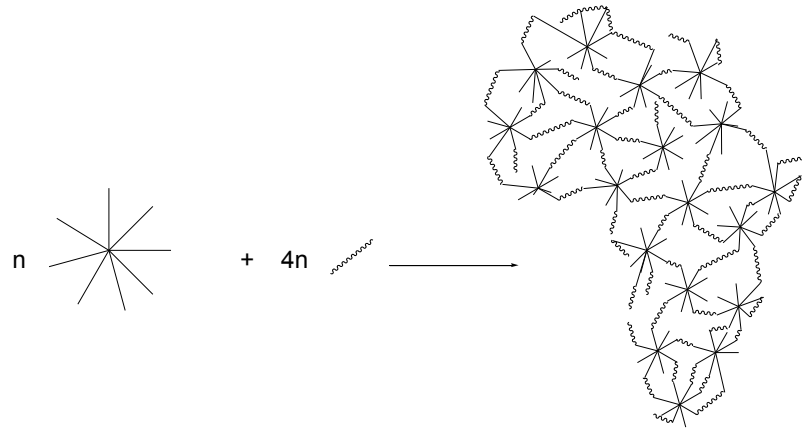

Figure 1: A continuous polymer network formed by crosslinking an 8-armed star shaped multi-arm with a 2-armed linear crosslinker.

One approach to categorise hydrogels is by their building blocks and a major distinction is usually made between natural and synthetic polymers, some of which are listed in **Table 1** (Gombotz *et al.* 1995; Hoffman 2002). Many of the naturally occurring polymers contain charged groups, signalling peptides or other functionalities, which make them useful for many applications but also unpredictable since different polymer sources may vary in the substitution pattern. Synthetic polymers on the other hand have greater potential to be tailored into desired properties with good repeatability.

Table 1: Common naturally occurring and synthetic building blocks used for hydrogel assembling.

Natural Polymers	**Synthetic Polymers**
Alginate	poly(acrylic acid), PAA
Chitosan	poly(ethylene glycol), PEG
Collagen	poly(glycolic acid), PGA
Dextran	poly(lactic acid), PLA
Fibrin	poly(lactic-co-glycolic acid), PLGA
Gelatine	poly(*N*-isopropyl acrylamide), PNIPAAm
Heparin	poly(*N*-vinyl-2-pyrrolidone), PVP
Hyaluronic acid	poly(vinyl alcohol), PVA

When hydrogels are required for *in vivo* use, biocompatibility is crucial. A biocompatible material should be inert to proteins and other substances in biological fluids as well as to receptors and other parts of cell membranes (Lee *et al.* 2000). Materials made of PLGA are hydrophobic, and in contact with blood the surface of such materials non-specifically adsorb a protein layer from the body fluids

(Miller *et al.* 2005). This protein layer possesses an intrinsic cell adhesive property, which might be the reason why hydrophobic polymers are more prone to initiate an inflammatory response than hydrophilic polymers. A general method to decrease the hydrophobicity and simultaneously increase backbone flexibility of PLA, PGA and PLGA polyesters is to incorporate them in block copolymers with PEG. These block copolymers and devices made thereof are degradable since the polyesters degrade by hydrolysis, and in addition enzymatically *in vivo* (Reeve *et al.* 1994). Even though these polyesters are hydrophobic, there is a widespread use of the PEG copolymers for the preparation of hydrogels (Qiao *et al.* 2005), micro/nano particles (Gombotz *et al.* 1995) and micelles (Song *et al.* 2011) in applications where degradability is essential.

In contrast, polymer coatings of the hydrophilic polymer PEG is known to increase platelet and bacterial repellence on implants and is thus a suitable material for biomedical applications (Lee *et al.* 2000). PEG hydrogels are also extremely non-adhesive towards blood proteins and cells and are approved by the Food and Drug Administration in the United States for various clinical uses such as biosensors, valves and surface mono layers in microarray devices (Peppas *et al.* 2006). *In vivo*, a degrading PEG material is slowly dissolved into the circulatory system and further cleared via both renal and hepatic pathways (Veronese *et al.* 2005). The "bio-inert" property of PEG-based gels can be explained by its extensive interaction with water (a typical hydrogel absorbs water until it contains only ~1-10% dry material), which acts like a camouflage for the immune system. A wide range of hydrophilic synthetic polymers have been thus used to create hydrogels for medical applications (Hoffman 2002).

Up to this point, the origin and some of the intrinsic properties of the polymeric building blocks used to assemble hydrogels have been presented. However, to obtain desired gel properties the geometry of the building blocks is as important as the polymer properties itself. The geometry determines the general gel properties, such as swelling (DuBose *et al.* 2005), mechanical strength (Anseth *et al.* 1996) and drug diffusion properties (van de Wetering *et al.* 2005). Polymer geometries which are often used include linear, star shaped and dendritic structures. In **Figure 2** a linear polymer is shown with the functional groups pending along its backbone. It is noticeable that this structure carries only one kind of functionality, consequently drug incorporation and hydrogel network formation must occur via the same chemistry, often simultaneously in a one-pot reaction. Also shown is a 4-armed star shaped dendritic structure of second generation. The dendrimer carries two different functionalities of orthogonal character (*i.e.* one can be reacted specifically without affecting the other). Therefore drug attachment is carried out in a separate reaction step prior gel formation, which is more controlled and repeatable.

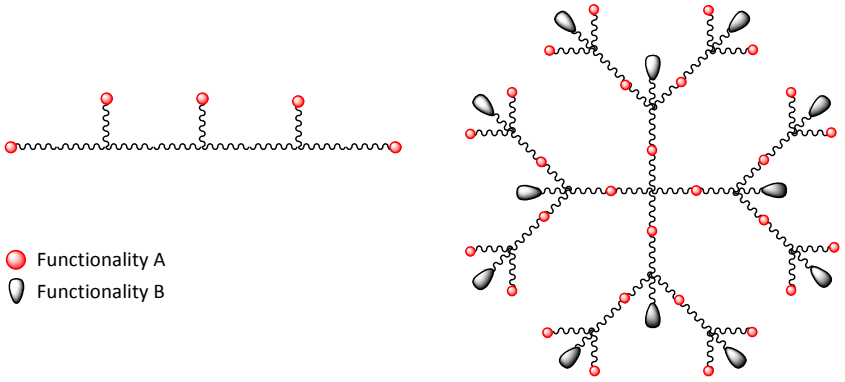

Figure 2: Examples of two PEG architectures; to the left a linear backbone with pending functional groups and to the right a 4-armed PEG dendrimer of second generation.

Dendritic materials have excellent intrinsic properties for drug delivery purposes and have successfully proved their usefulness in a number of delivery routes (Cheng *et al.* 2008). The specific advantages of dendritic structures compared to multi-arm polymers are the increased multivalency and the possibility of making them bi-functional. Recent developments of dendritic structures allow for a higher number of functional groups in fewer synthetic steps (Antoni *et al.* 2009), which for drug delivery purposes can be used to obtain high drug loading densities. An example of such material is the 2-Amino-2-hydroxymethyl-propane-1,3-diol (trizma) based dendrimer of third generation, synthesised by Antoni *et al*. in 6 steps, with 24 functional A groups and 21 B groups, where A and B are orthogonal. For dendritic materials in drug delivery applications functionality A is used to incorporate the drug while B is conjugated to tissue targeting molecules, polymers to increase water solubility or used for crosslinking to form a hydrogel (Ihre *et al.* 2002; Cheng *et al.* 2008). Even though dendritic materials have shown low cytotoxicity (Padilla De Jesus *et al.* 2002; Antoni *et al.* 2009) these carriers tend to accumulate in various organs within a few hours after intravenous administration. However, both the biodistribution and the retention time are improved by dendrimers PEGylation (Cheng *et al.* 2008).

The hydrogel scaffolds used in this thesis were constructed from PEG building blocks of several geometries. One approach used mono-functional 2- or 4-armed PEGs with terminal functional groups used for both drug incorporating and crosslinking. Alternatively, dendritic 2- or 4-armed bi-functional structures of first and/or second generation were used (**Figure 3**).

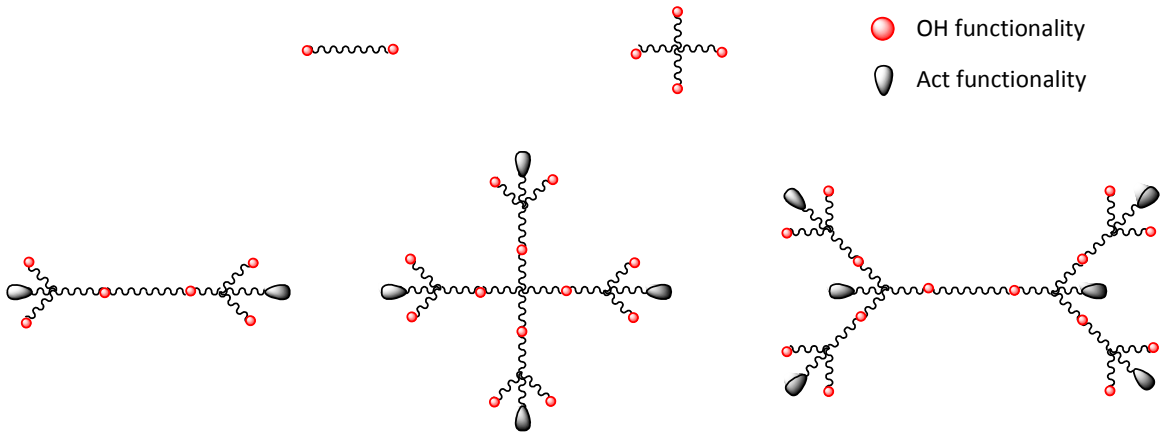

Figure 3: The geometries used for the work in this thesis. Top structures; 2- and 4-armed mono-functional PEGs. Lower structures; 2- and 4-armed dendritic PEGs of first generation followed by a 2-armed dendritic PEG of second generation.

1.1.1 Gelling Methods

Gelling occurs by establishing several crosslinks between the participating polymeric building blocks. The connections could be of either non-covalent character (electrostatic or solvent induced) as for "physical hydrogels" or covalent bonds, making "chemical hydrogels".

1.1.1.1 Physical Gels

For physical gels the polymer is either functionalised by charged groups, which are crosslinked by species of the opposite charge, or made of blocks that associate to minimise the contact with the surrounding media. Physical gels could also form from hydrogen bonding of functional groups along the backbone of the polymer. For example, a solution of alginate (a brown algae polysaccharide highly substituted with anionic carboxylic acid groups) gels upon addition of cationic polymers like chitosan or divalent cations, such as Mg^{2+} or Ca^{2+} (**Figure 4**).

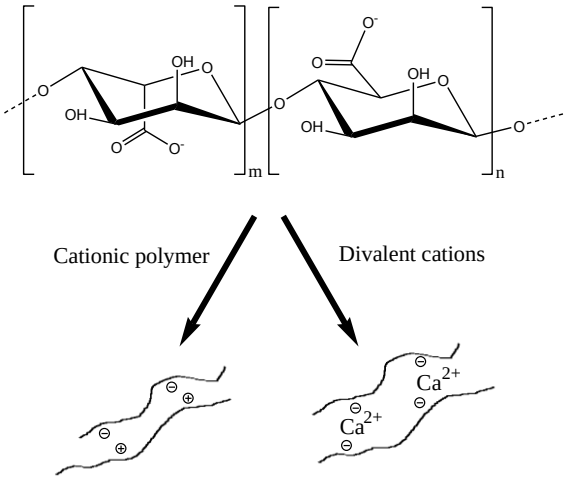

Figure 4: Formation of a physical hydrogel from alginate by crosslinking with either charged polymers or ions.

A potential niche of physical hydrogels is polymer-clay composite gels where clay particles are used as crosslinkers in free radical polymerisation of monomers. Those composites have shown extraordinary mechanical properties such as a 3 300 times higher fracture energy than conventional chemically crosslinked hydrogels (Haraguchi 2007).

1.1.1.2 Chemical Gels

In contrast to physical gels, polymers used to form a chemical gel carry functional groups which react by free radical reactions, or with a crosslinker carrying complementary functionality, to form covalent bonds (Hennink *et al.* 2002). Chemical gels have the advantage over conventional physical gels of being both stronger and more easily tailored to obtain desired properties, while physical gels benefit from their reversibility.

The work in this thesis is based on chemical gels formed by free radical polymerisation reactions or conjugate addition between PEG multi-arms carrying acrylate or thiol functionalities.

1.1.1.2.1 Photo-Polymerisation

Gelling through photo-polymerisation occurs when polymers containing olefinic groups are exposed to radicals, most commonly initiated by heat or ultraviolet (Sen *et al.*) irradiation. The resulting crosslinks are of carbon-carbon character (Srinivasan *et al.* 2010), which are considered non-degradable (the importance of this is explained later).

1.1.1.2.2 Thiol-ene Addition

To introduce covalent crosslinks other than carbon-carbon bonds during free radical polymerisation the concept of thiol-ene chemistry may be used. In this concept the propagating radical is formed on a thiol species which then reacts with the "ene" (double bond). **Scheme 1** pictures the general mechanism of the thiol-ene addition reaction. In the initiation step a photo initiator (I) is activated to produce radicals, which immediately abstracts a thiol hydrogen to form a thiyl radical.

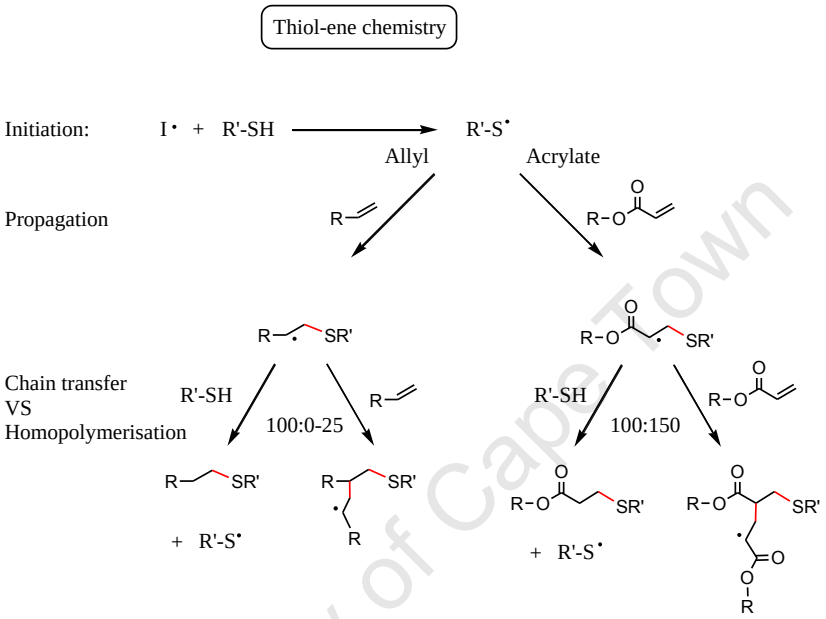

Scheme 1: General thiol-ene reaction mechanisms for allyl-thiol and acrylate-thiol systems, respectively. Red colour indicates bonds formed during thiol-ene addition.

Most often the olefin in thiol-ene reactions is an allyl, but in this thesis acrylates were used instead. Therefore the propagation and chain transfer steps of both groups are shown. In the propagation step the initially formed thiyl radical combines with the double bond to form a new bond, marked in red, while transferring the radical into the former double bond. The following reaction step is crucial for the gel properties (explained later) since the radical could react either via chain transfer by abstracting the hydrogen from a thiol or via homo-polymerisation to form a dimer. For a stoichiometric thiol-acrylate system the chain transfer step is slow compared to the propagation step (Cramer *et al.* 2003), hence the acrylate radical intermediate is rather stable and has the opportunity to undergo both reactions. Cramer and Bowman measured the rate constants for chain transfer (K_{CT}) and homo-polymerisation (K_H) respectively for a stoichiometric thiol-acrylate system and calculated the ratio (K_H /K_{CT}) to be 1.5 while for allyls the amount of homo-polymerisation was only a few percent up to 25% depending on the allyl character (Cramer *et al.* 2001). The consequence of homo-

polymerisation is that carbon-carbon bonds are formed on the expense of thio-ether bonds. Thiol-ene reactions ends by radical termination, which occur when two radicals of any origin recombines.

A general advantage of thiol-ene crosslinking methods is that many solvents can be used, also aqueous, and that no leaving groups are formed. A disadvantage is the large degree of side-reactions, which form non-degradable carbon-carbon bonds, and the need of a potentially toxic initiator.

However, thiol-ene addition is a versatile method to form hydrogels and many different "thiol" and "ene" combinations are reported (Rydholm *et al.* 2007; Aimetti *et al.* 2009; Benton *et al.* 2009; Diaz *et al.* 2010; Lundberg *et al.* 2010). The use of those systems for drug delivery purposes is described later.

1.1.1.2.3 Conjugate Addition

A gelling method, which does not rely on radical chemistry, is the conjugate addition reaction (in some texts referred to as "Michael-type addition"). In this reaction, an α,β-unsaturated carbonyl reacts with a nucleophile (**Scheme 2**). The conjugating feature of the double bond, making the terminal carbon electrophilic and liable for a nucleophilic attack, renders this reaction possible. The selectivity of the nucleophile to react via conjugation, instead of an attack of the carbonyl carbon, can be explained by the "hard/soft" concept, which is outside the scope of this thesis (LoPachin *et al.* 2008).

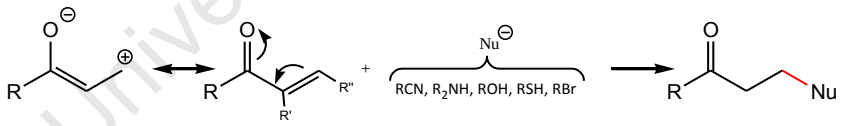

Scheme 2: General conjugate addition mechanism where an α,β-unsaturated carbonyl reacts with a nucleophile. Red colour indicates the formed bond.

From here on only conjugate addition of acrylates (R' and R'' = H) and thiols (RSH) will be considered. Acrylates are the least sterically hindered species among all α,β-unsaturated carbonyls, a feature which makes them easily accessible towards conjugate addition (McCarthy *et al.* 1994). Reactivity of thiols is determined by their individual pKa, which is a result of the surrounding structure. Adjacent electron withdrawing atoms or functional groups lowers the pKa, thereby making the proton easier to abstract and the thiol a better nucleophile, while an electron donating atmosphere has the opposite influence on the thiol reactivity (Lutolf *et al.* 2001). Since thiol reactivity is closely related to

the pKa it is crucial to control the pH of the reaction mixture during conjugate addition in order to control the reaction rate.

Conjugate addition holds many potential advantages over other gel formation chemistries, such as photo-polymerisation and thiol-ene addition, as it can be performed without the addition of initiator or radiation and does not produce a leaving group. In addition, a solution of mixed pregel components spontaneously turns into a solid gel within minutes at physiological conditions (pH 7.4 and 37° C). This feature has been used to design injectable hydrogels from PEG (Elbert *et al.* 2001) and PVA (Ossipov *et al.* 2008) to mention some synthetic hydrophilic polymers.

The concept of using conjugate addition to form degradable hydrogels for drug delivery was essentially developed by Hubbell and co-workers during the last ten years (Elbert *et al.* 2001; Lutolf *et al.* 2001; Schoenmakers *et al.* 2004; Fittkau *et al.* 2005; Metters *et al.* 2005; van de Wetering *et al.* 2005; Jo *et al.* 2009). Since then, others have adopted and developed the methodology to obtain properties desired for their applications.

In this thesis conjugate addition was primarily used to form hydrogels from mono-functional or dendritic PEG based compounds bearing 4 or 8 acrylate groups crosslinked by 2- or 4-armed PEG thiols. In cases where the pregel compounds were not water soluble the related thiol-ene addition was employed instead.

1.1.2 Crosslink Density and Swelling

Following the gelling phase of a hydrogel, the gel is normally immersed in an aqueous phase, for *in vitro* or *in vivo* studies, where absorption of water swells the gel. The degree of swelling depends on factors such as molecular weight of the building blocks, concentration of building blocks during gelling and the number of crosslinking sites (DuBose *et al.* 2005; van de Wetering *et al.* 2005). Those parameters influence the level of crosslink density, which is a measure of the amount of covalent/ionic bridges between gel building blocks formed during gelling. Both the average molecular mass between crosslinks (M_c; g/mol) and the average mesh size (ζ; Å) are used to represent crosslink density and these are calculated from experimental data (Andreopoulos *et al.* 1998).

The mesh size represents the average distance between two crosslinks, in Ångström, and a short distance between crosslinks is equivalent to a high crosslink density. A normalised mesh size ($\zeta_{Swollen}/\ \zeta_{Gelled}$) larger than 1 indicates that the mesh size for a swollen gel has increased compared to its initial value, not necessarily due to bond breaking. Instead, the main reason for an

initial increase in mesh size is a result of swelling where polymers in the gel network are stretched. Any further increase, however, indicates a lowered crosslink density resulting from bond breaking. Flory and Rehner developed the first equation to predict swelling of hydrogels (Flory *et al.* 1943). The equation is based on an entropy concept were two opposing forces either favours or disfavours swelling.

The driving force for swelling is the entropy increase when water diffuses into the polymer network. This thermodynamic mixing of polymer and water is described by the Flory-Huggins interaction parameter (Horta *et al.* 2005). The interaction parameter is an individual constant for each polymer-solvent system and indicates to which extent the polymer chains are hydrated (Horta *et al.* 2005). A gel made of hydrophobic polymers have a non-favoured interaction with water and does not swell much while gels made from hydrophilic polymers absorb large amounts of water and consequently swells to a great extent. A typical hydrogel swells until it contains up to 90-99% water by mass.

The opposing force, which discourage further swelling, is a pure consequence from the swelling itself, since swelling brings tension into the gel network by stretching it and hence, lowers the entropy. Rubber-elasticity theories are used to describe this term in the equation. Swelling continues until equilibrium is reached, that is when the driving force of mixing polymer and water equals the contracting force of the elastic polymer network (Richter *et al.* 2008).

Since the crosslink density is very important for the gel characteristics (DuBose *et al.* 2005), the equation is rather rearranged to instead calculate crosslink density from experimental swelling data.

A disadvantage of the Flory-Rehner theory is that crosslinks are assumed to form in the absence of solvent. However, the original equation has since been developed to account for the presence of water during gelling (Peppas *et al.* 2006), different degrees of swelling, both ideal and non-ideal hydrogel network formation (Metters *et al.* 2005) and for ionic gels (Sen *et al.* 2000).

Importantly, these calculated numbers only gives an average of the cavity size within the gel but not the range; and there is a range of mesh sizes since drugs larger than the calculated network dimensions still find paths through the gel and diffuses through it.

1.1.3 Degradation

Depending on the structural feature of the gel building blocks the resulting crosslinks may be non-degradable or degradable. One method to obtain non-degradable gels is conjugate addition of vinyl sulphone (VS) and thiol moieties (**Scheme 3**).

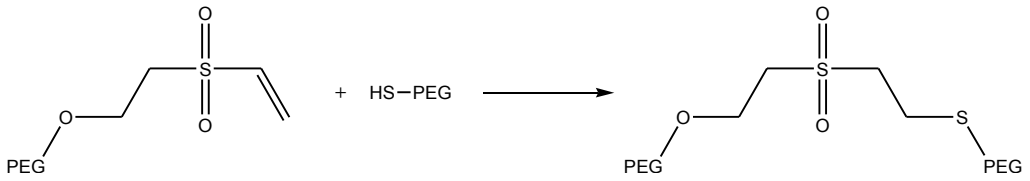

Scheme 3: Formation of a hydrolytically stable crosslink by conjugate addition.

Our group applied such hydrogel in a rat infarction model in order to improve pathological remodelling in the early healing phase (Dobner *et al.* 2009). The applied non-degradable gel acts as a mechanical support and resulted in initial benefits by increasing the wall thickness and reducing the wall dilatation, but there was also a substantial inflammatory response to the material.

For many *in vivo* applications, however, it is desired to remove the applied hydrogel by degradation of the gel network into its respective water soluble building blocks. The advantage of using degradable hydrogels is a lowered exposure to the gel and its potential risk to cause an inflammatory response. Degradation can be achieved by proper design of either the polymer backbone or the crosslinks between individual polymers. Since swelling results in an increased surface area of the polymer network exposed to water the introduction of hydrolytically labile bonds increases the degradation rate of the network. Such degradation can be designed to occur over days to months, depending on desired application.

1.1.3.1 Hydrolytic Degradation

The hydrogel crosslinks used for the work in this thesis were formed by connecting the gel building blocks via ester bonds, consequently the gels were degraded by ester hydrolysis (**Scheme 4**). Esters however, are relatively stable at near-neutral pH (Zacchigna *et al.* 2008), but can be weakened. For example, introduction of an adjacent thio-ether moiety decreases the ester stability and increases its degradation rate (Hiemstra *et al.* 2007; Rydholm *et al.* 2007). The electron withdrawing effect of the thio-ether is used to explain the weakening effect of thio-ethers on esters (Schoenmakers *et al.* 2004; Metters *et al.* 2005).

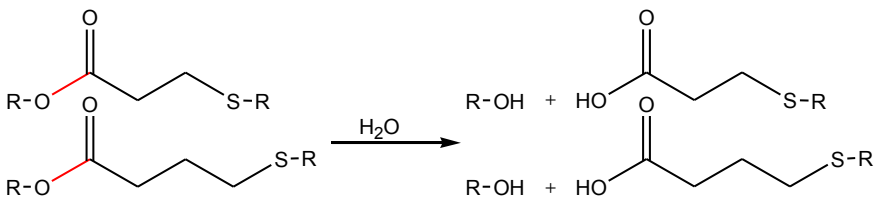

Scheme 4: Tailored degradation rate of hydrogel crosslinks, where red bonds are cleaved by hydrolysis.

The weakening effect is even greater if there are more electron withdrawing groups in the structure beyond the thio-ether (Jo *et al.* 2009). In addition to crosslink stability, the gel degradation rate is also related to crosslink density, where a higher density results in a slower degradation (DuBose *et al.* 2005).

Previously (chapter 1.1.1.2.2), during the introduction of free radical polymerisation as a crosslinking method, the formation of carbon-carbon bonds was mentioned as a disadvantage. **Scheme 5** shows the resulting bonds when acrylate-containing compounds are crosslinked via photo-polymerisation, thiol-ene addition and conjugate addition, respectively. The ester crosslinks produced by photo-polymerisation are not weakened by an adjacent electron-withdrawing group (**Scheme 5**, top reaction) and are consequently expected to hydrolyse very slowly.

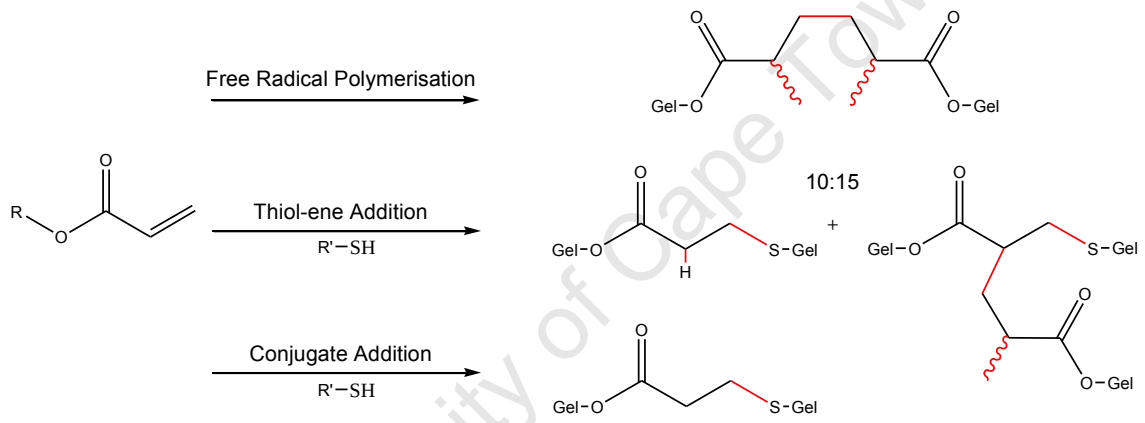

Scheme 5: Three alternative routes to form ester containing gel crosslinks, red bonds are formed during crosslinking.

Thiol-ene addition on the other hand introduces a thio-ether moiety, in this case at a distance of two carbons from the ester, which significantly increases the degradation rate of formed gels. However, the thiol-ene reaction of acrylates and thiols has a rather high degree of homo-polymerisation, which forms the more stable ester crosslinks (**Scheme 5**, middle right reaction product). The presence of those stable ester crosslinks makes the gel less degradable. Conjugate addition of acrylates and thiols (**Scheme 5**, lower reaction) on the other hand, results specifically in thio-ether weakened ester crosslinks and hydrogels formed by this method degrades readily.

In case of gels formed by thiol-ene or conjugate addition the degradability originates from hydrolysable crosslinks. Alternative routes for the introduction of degradability include the design of the crosslinker itself, which may consist of hydrolytically degradable polyesters or enzyme sensitive oligopeptides (Zisch *et al.* 2003; Ehrbar *et al.* 2005).

1.2 Approaches towards Controlled Drug Delivery

Introduction of drugs into the blood circulation can take place in multiple ways, either directly via intravenous injection or secondary via transdermal, suppository, intramuscular or oral routes from where the drug is absorbed into the circulation. One of many challenges of drug delivery is to control the drug concentration in the blood, since a too low concentration is inactive while a too high concentration is toxic. Therefore much effort has been dedicated to master the kinetics of drug release where a constant dosing over time is the goal.

When a drug enters the circulation it has the potential to come in contact with every single cell accessible to the blood system. Consequently, a large number of healthy cells in different organs are exposed to unnecessary treatment. This is a major cause for unwanted side effects of drugs. As an alternative, if the drug was delivered locally to the very spot in need of treatment, many side effects could be avoided. A highly potential delivery concept meeting the demands of both controlled and local release is drug delivery through hydrogels.

In such in vivo applications of hydrogels, the void of pathogens is of greatest importance. Depending on the hydrogel system, different sterilisation techniques are applicable. For UV cured implantable gels, UV sterilisation of the formed gel is suitable (Guvendiren et al. 2010), while for injectable gels it is possible to filter sterilise the gel precursor solutions prior mixing and injection (Bahney et al. 2011).

The following text describes the main hydrogel based drug delivery systems.

1.2.1 Encapsulation

The simplest concept for drug delivery through hydrogels is the encapsulation method where the drug is embedded, or trapped, within a hydrogel. There are numerous methods of drug encapsulation of which the most common will be described here. In general, a homogeneous distribution of drug molecules throughout the gel network is achieved upon crosslinking a solution of pregel polymers in which the drug is also dissolved (Peppas *et al.* 2006). The drug molecules are then captured within the cavities of the gel during its formation. In contrast to these matrix systems there are reservoir systems where the drug is stored in the interior of the gel surrounded by a second gel barrier.

Drug delivery using micro- or nano-particles combine the attractive features of both systems. The gel feature contributes with a high water content (biocompatibility) and flexibility while the particle feature adds availability and the possibility to control the drug release rate by choosing the appropriate particle size (Pan *et al.* 2002). Micro- and nano-spheres can be fabricated in multiple

ways, such as self-assembly of chitosan-PEG copolymers into micelle structures, precipitation of chitosan into nanoparticles or emulsion polymerisation methods to mention some. The delivered drug is either trapped in a reservoir system, homogeneously dispersed throughout the matrix or attached to the particle matrix (Hamidi *et al.* 2008).

Stimuli-responsive gels are characterised by their ability to react on changes in their physical environment, where the most studied systems respond to changes in pH (Sen *et al.* 2000) or temperature (Martellini *et al.* 1999). Other systems may respond to light, electric or ionic potentials or magnetic fields (Ahn *et al.* 2008). Some stimuli-responsive systems can be applied *in-situ* via injection, followed by gelling (He *et al.* 2008). Responsive behaviour could be designed for both chemical and physical gels, by the composition of the polymer backbone or the presence of pendant charged groups that bring the responsiveness. Gels made of poly(acrylic acid) are pH sensitive since a rise in pH deprotonates the acidic groups after which water diffuses into the gel to hydrate the charged groups and the gel starts to swell (Richter *et al.* 2008). For poly(acrylamide) a pH decrease protonates the amides, resulting in water covering the charged anions and the gel starting to swell (Richter *et al.* 2008). Poly(*N*-isopropylacrylamide) is the most commonly used polymer for thermo-sensitive gels and when the temperature rise above a critical level for such gels, the polymer backbone loses its bound water, which forces the hydrophobic polymers together to minimise the unfavourable polymer-water contact area upon the gel network deswells (Lin *et al.* 2006). There are also systems where swelling is trigged by an increase in temperature (Ganji *et al.* 2009).

Encapsulated drug molecules in those stimuli-responsive gels are released upon swelling since the growing network allows the drug to diffuse out of the gel. The swelling behaviour of those systems is reversible. Therefore, if the external stimulus ends the gel shrinks and the drug release diminish (He *et al.* 2008).

1.2.2 Covalent Incorporation

The drug delivery described hitherto constitutes systems where the drug is stored or dispersed within the gel by different methods and the release is controlled by designing the physical parameters of the gel, such as crosslink density, degree of swelling and degradation rate.

An alternative approach to controlled drug release is to covalently attach the drug to the hydrogel via a linker, thus, drug release is dependent on the breaking of a covalent bond. One of the main goals with drug release research is to deliver drugs into a biological system, hence when designing the *in vivo* breaking of such linker there is only a narrow range of chemistry available. The main approaches for releasing covalently bound drugs *in vivo* are hydrolysis, enzymatic digestion and reduction of disulphide bonds (West *et al.* 2005; Khandare *et al.* 2006).

1.2.2.1 Hydrolytically Labile Linkers

By connecting already existing functional groups on the drug, such as hydroxyl, carbonyl, amine or imine groups, with certain linkers release by hydrolysis is obtained, which can be tailored to occur at either acidic or physiological pH (West *et al.* 2005). Drug-gel linkers containing the acyl hydrazone moiety are acid-labile and used when drug delivery is directed to inflamed tissues, which are associated with acidic conditions (Farr *et al.* 1985), or other sites with lowered pH. Ulbricht *et al.* PEGylated the anticancer agent doxorubicin (Dox) via an acid labile acyl hydrazone containing linker (**Scheme 6**) and showed that release occurred exclusively at a lower pH (Ulbrich *et al.* 2004).

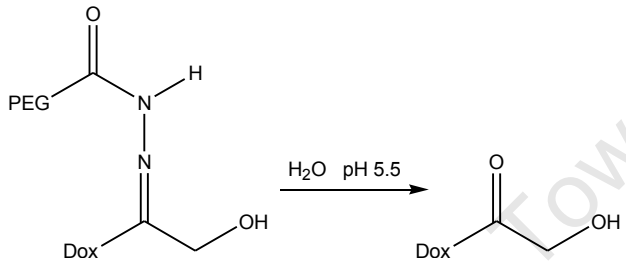

Scheme 6: Acid catalysed hydrolysis of an acyl hydrazone drug-PEG linker, which recreates the original Dox structure.

If instead the drug is attached via an ester, or ester in the vicinity of charged groups, the release can be tuned to occur at different rates at a physiological pH. In the work by Jo *et al.* release of covalently bound bovine serum albumin from a PEG hydrogel was obtained by hydrolysing the ester containing linker at a physiological pH (Jo *et al.* 2009). The release rate was furthered tailored by incorporating charged amino acids in line with the ester group.

1.2.2.2 Enzymatically Labile Linkers

Hydrogels in medical devices, such as dressings for improved wound healing, are specifically applied to the desired target, therefore the presence of certain cell types, such as epidermal, endothelial or inflammatory cells, is predictable (Singer *et al.* 1999). These cells secret enzymes, such as matrix metalloproteases (MMPs) and plasmin, which cleave specific peptide sequences within the surrounding fibrin network to provide passage for the migrating cells. By designing the drug-gel linker to contain particular peptide sequences corresponding to the substrate of these enzymes drug release mediated by enzymatic activity is obtained (Gombotz *et al.* 1995; Zisch *et al.* 2003; Benton *et al.* 2009).

Cell-demanded release of vascular endothelial growth factor (VEGF) was obtained by Zisch *et al.* by covalently attaching the factor via a MMP degradable linker (Zisch *et al.* 2003). In a similar approach Ehrbar *et al.* showed that the resulting proliferation of human umbilical vein

endothelial cells increased in a dose-dependent manner upon plasmin mediated VEGF release from fibrin matrices with different VEGF loads (Ehrbar *et al.* 2005).

1.2.2.3 Redox Labile Linkers

The difference in redox environment between the inside and outside of a cell is used to design redox-sensitive disulphide linkers. These are ideally stable in extra-cellular environments, but reduced as a result of cellular uptake resulting in intracellular drug release. The main agent considered for *in vivo* reduction of disulphides is the tripeptide glutathione, which is the most abundant thiol compound in the cytoplasm where the concentration is ~1-10 mM, compared to extracellular levels, ~2 µM (Hong *et al.* 2006). Importantly, the glutathione levels in some cancer tissues are significantly increased compared to healthy tissue (Yeh *et al.* 2006). Consequently, drug release depending on disulphide reduction can be used for targeted drug release.

In an *in vitro* study by Navath *et al.* glutathione mediated release of a model drug resulted in a 70% intracellular release of the drug load, while no release was detected extracellularly, from highly loaded (16 or 18 per carrier) dendritic drug conjugates (Navath *et al.* 2008).

Alternatively, the thiol containing model compound can be bound to a gold particle by self-assembly and exchanged by glutathione *in vivo (Hong et al. 2006)*.

1.3 Drug Release

1.3.1 Mechanisms and Kinetics

The elution of encapsulated or covalently attached drug may be controlled by different mechanisms and released with different kinetics, thus giving rise to different elution profiles.

The most commonly considered mechanisms for drug release are swelling, degradation, diffusion or the breaking of a covalent bond. To significantly ascribe experimentally obtained release data to any of these mechanisms mathematical models are used. To mathematically describe an elution process there are multiple parameters to consider, such as the change of matrix dimensions by diffusion of water into the gel matrix and its degradation and concentration dependant diffusion of the drug out of the gel (Siepmann *et al.* 2000). Each model makes certain assumptions and is therefore only suitable for systems that fit those criteria.

A commonly used model to describe diffusion controlled elution is the Higuchi equation, but is only valid for non-swelling and non-degrading thin films and is therefore not applicable to describe the elution from the gels in this work (Siepmann *et al.* 2011).

However, there are models that do consider swelling and degradation as a release mechanism, such as the Hixson-Crowell and Korsmeyer-Peppas equations (Shoaib *et al.* 2006). If experimentally obtained release data fits to the latter equation it may also be possible to distinguish whether the drug elution is primary controlled by the diffusion or swelling mechanisms or a combination thereof (Siepmann *et al.* 2001).

However, these equations were developed to describe the elution of entrapped drugs. The release of covalently incorporated drugs is generally determined by the degradation rate of the covalent linker. Most of these links are designed to degrade by hydrolysis and gives rise to unique zero order elution profiles, unattainable by diffusion controlled release mechanisms (Siepmann *et al.* 2001; DuBose *et al.* 2005; Lin *et al.* 2006). To distinguish between burst, first order or zero order release kinetics obtained release data is compared to representative equations. A significant curve fitting to those equations indicates whether the release rate is dependent (first order) or independent (zero order) on the drug concentration (Shoaib *et al.* 2006).

1.3.2 Controlled by Diffusion, Swelling or Degradation

Drug release from a hydrogel scaffold is controlled by a number of factors, such as the drug incorporation method, the drug diffusion coefficient and the gel architecture. No matter which method or what type of gel is used the drug must travel out of the gel boundaries by diffusion to accomplish any effect on the surroundings, unless release is controlled by surface degradation of the gel. This logic explains why the diffusion-controlled mechanism is the most applicable mechanism to describe drug release from hydrogels. Smart designs and methodologies thus aim to control diffusion barriers in order to render the drug delivery sustained over a longer time period than a purely diffusion-controlled system provides (Peppas *et al.* 2006). There are two main hydrogel types where drug release is diffusion-controlled, reservoir devices and matrix devices (**Figure 5**).

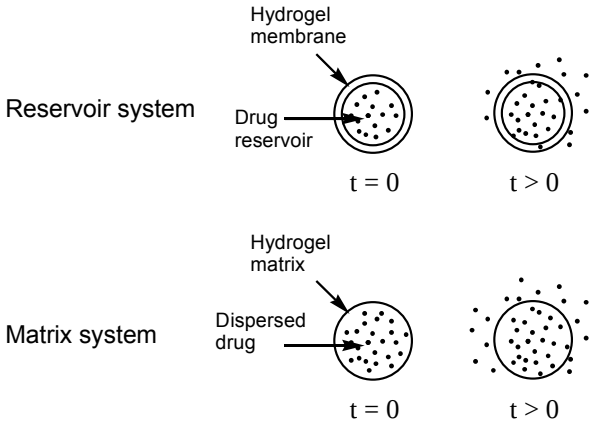

Figure 5: Diffusion controlled drug delivery from reservoir and matrix systems, t = time.

In the reservoir model a second hydrogel covers the drug-containing core as an effective diffusion barrier. In matrix systems the drug is homogeneously dispersed throughout the gel. In matrix systems affinity gels are smart expansions where the drug interacts with the gel network either through columbic or polar affinity, which lower the apparent diffusion coefficient and slows the drug elution.

To add complexity the gels made of hydrophilic polymers start to swell at t >0. For gels with high crosslink density the drug diffusion through the gel may be restricted making the drug release limited to the rate of swelling (**Figure 6**). Many stimuli-responsive gels belong to this category (He *et al.* 2008). The distinction between diffusion and swelling controlled drug delivery can be made using the Deborah number (De = λ/t) where the time scale of swelling, represented by the polymer relaxation time (*λ*), is compared to the time scale of diffusion (*t*). For a system controlled by swelling (De >1) the swelling is slow (big *λ*) and restricts the drug diffusion. For diffusion controlled systems the relation is the opposite (De <1), the diffusion is slow (large *t*) and limits the rate of drug elution (Lin *et al.* 2006). By varying the molecular weight (2-10 kDa) of 8-armed PEG acrylates van de Wetering *et al.* could control the gel swelling and regulate the release of a model compound from a burst release to sustained delivery over 25 days (van de Wetering *et al.* 2005).

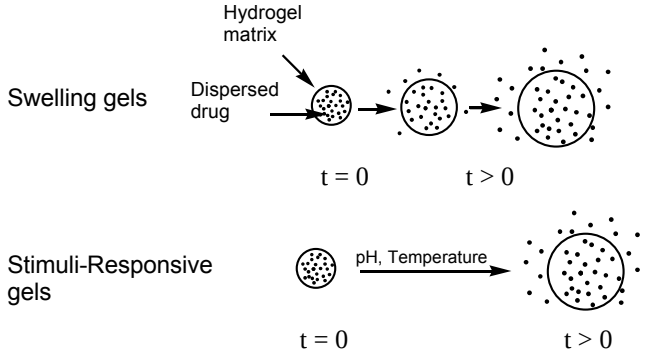

Figure 6: Swelling controlled drug delivery from a matrix system, t = time.

For degradable hydrogels, the degradation rate of the gel network effects the drug release and is in some cases the rate-limiting factor (**Figure 7**). Degradation occurs when labile bonds within the gel network are cleaved, either by hydrolysis or enzymatic activity. There are two modes of hydrogel degradation, surface erosion and bulk degradation. Surface erosion would occur in a hydrophobic gel where surrounding water degrades the gel surface, but this is a rather theoretical situation since hydrogels contain huge amounts of water per definition. Instead surface erosion takes place in a hydrogel crosslinked by peptide sequences or enzyme degradable polymers when the enzyme activity is faster than the transport of enzymes into the gel interior. Most degradable hydrogel systems, though, can be ascribed to bulk degradation, where the degradation is equally likely to occur throughout the entire gel. A general example of bulk degradation is for a hydrogel where either the monomer building blocks are hydrolytically labile or the non-degradable monomers are crosslinked by a degradable crosslinker, or a combination of both. Hydrogel degradation facilitates drug diffusion and is rate limiting if the drug diffusion is significantly slower than the gel degradation.

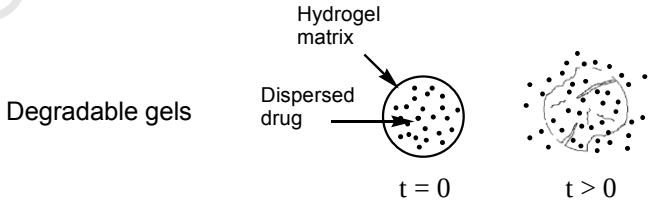

Figure 7: Degradation controlled drug delivery from a matrix system, t =time.

The reservoir and matrix hydrogel systems mentioned above may release the drug with an initial rapid burst followed by a prolonged release phase controlled by diffusion, swelling or degradation. Such burst may be decreased by increasing crosslink density or coating the drug containing gel with additional drug-free layers (Lin *et al.* 2006). Although no comprehensive theories have been put forth

to fully describe the phenomenon many possible causes have been identified including material/drug interactions, fabrication conditions and sample geometry (Huang *et al.* 2001).

1.3.3 Controlled by Hydrolysis

The complexity, and also the controllability of the drug eluting system, is taken to the next level by incorporating the drug covalently into the gel structure. Copolymerisation of drug and gel monomers incorporate the drug into the gel backbone, alternatively and more commonly used is the method to covalently attach the drug pendant from the polymer backbone. The character of the drug-polymer link determines whether the link degrades under acidic, alkaline or other conditions. Hydrazone bonds are acid-labile and drugs conjugated via these links are released in acid environment, such as certain inflammatory sites (Liu *et al.* 2010). Esters on the other hand degrade under slightly alkaline healthy *in vivo*-conditions (DuBose *et al.* 2005).

The drug release described in this thesis is controlled by ester hydrolysis, probably in combination with diffusion, swelling and gel degradation. The drugs used (described later) were incorporated into the pre-gel polymers by conjugate addition, nucleophilic substitution or the 1,3-dipolar cycloaddition (HDC) of azides and terminal acetylenes (Act), also known as one Huisgen of the click reactions. In all three cases ester links are formed between the drug and the polymer network of the gel (**Scheme 7**).

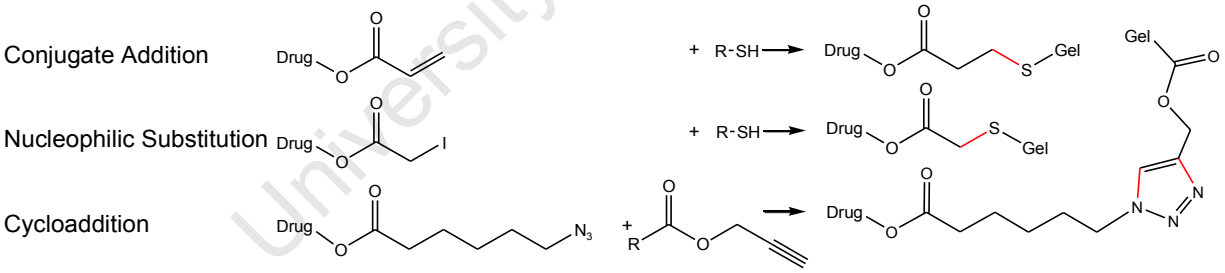

Scheme 7: Conjugate addition, nucleophilic substitution and cycloaddition were used for drug incorporation in this thesis. Red bonds are formed during drug incorporation.

As already stated in the case of gel degradability, esters in the vicinity of electron withdrawing groups are readily hydrolysed at a physiological pH. This is also the case for the drug-gel conjugates formed by conjugate addition and nucleophilic substitution depicted above. Schoenmakers *et al.* synthesised the drug-PEG conjugates shown in **Scheme 8** which differ in the number of methylene groups spacing the carbonyl and the thio-ether moieties. The measured hydrolysis rate of the two conjugates turned out to be approximately 3.3 times slower for the longer linker (Schoenmakers *et al.* 2004).

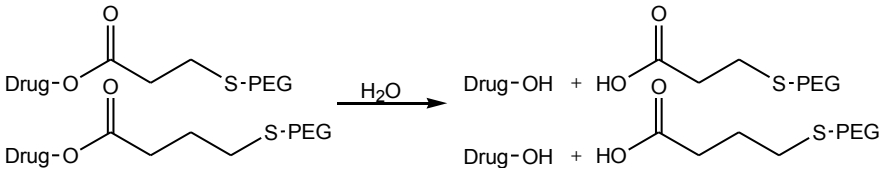

Scheme 8: Two drug-PEG conjugates with different release rates.

To explain this feature molecular modelling experiments were conducted in order to calculate the atomic charge on the carbon of the carbonyl group. Calculations were performed for the above structures (**Scheme 8**) and also for the case where only one methylene group separates the ester and the thio-ether. The results revealed that the positive charge of this carbon decreases with an increased number of methylene spacers (Schoenmakers *et al.* 2004), which is a clear indication why the hydrolysis rate is also decreased. Later research has shown that even the structure beyond the thio-ether moiety affects the ester degradation rate. In experiments where different amino acids were incorporated in line with the thio-ether it was obvious that the presence of electron withdrawing groups act to decrease the ester stability in the same fashion as the thio-ether itself (Jo *et al.* 2009).

Using the HDC reaction instead results in a triazole moiety connecting the drug and the polymer network (**Scheme 7**, lower reaction). The ester closest to the drug is formed in a separate reaction prior to incorporation and is not weakened by electron withdrawing species.

Normally cycloadditions proceed through a concerted mechanism. However, molecular modelling and experimental data favours a stepwise catalytic cycle for the HDC reaction. Roughly, the cycle can be described by four major steps (**Scheme 9**); an initial formation of a π-complex between the alkyne and the Cu(I) catalyst dimer whereupon the alkyne is deprotonated, the introduction of the azide into the complex followed by intra-complex rearrangements to form the triazole and a terminating protonation to release the product and reform the catalyst (Hein *et al.* 2008).

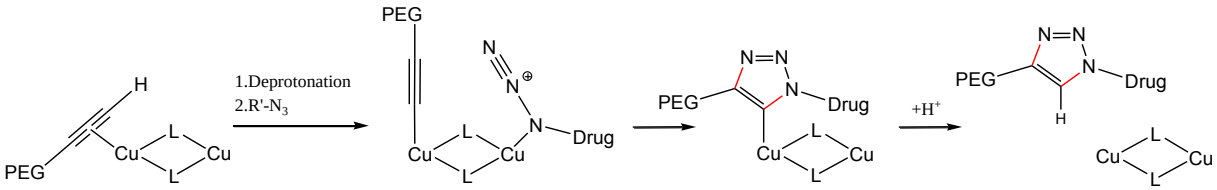

Scheme 9: A simplified catalytic cycle of HDC reactions, red bonds are newly formed.

The HDC reaction is unusually robust as it tolerates a wide range of pH values (5-12), can be performed over a wide range of temperatures (0-160° C) and tolerates the presence of water and oxygen. In addition the HDC always give 1,4-substituted products and proceeds approximately 10^7 times faster than the uncatalysed counterpart (Hein *et al.* 2008).

A disadvantage with this particular click reaction is the requirement of a copper catalyst. Although copper is an essential element to maintain normal body functions and has also been used with success to treat tumours, excessive amounts lead to the development neurological disorders such as Parkinson's disease and Alzheimer's disease (Wang, T. *et al.* 2006). However, the copper catalyst can be reduced to undetectable levels from click formed hydrogels by washing with ethylenediaminetetraacetic acid (EDTA) solution (Malkoch *et al.* 2006).

Two alternative mechanisms for release of tethered drugs by hydrolysis are proposed by Dubose *et al.* The dominant mechanism is primary release where the ester connecting gel and drug is hydrolysed and the drug released in its unmodified form. Alternatively, by cleaving esters further away along the PEG chain, or a combination of esters within the gel network, a drug-PEG conjugate is released, making it secondary or higher order release (DuBose *et al.* 2005). For the PEG gels studied by DuBose *et al.* (PEG-acrylate crosslinked by dithiothreitol with simultaneous incorporation of a thiolated dye) the amount of primary release was higher than 90%.

1.4 Cardiovascular Diseases

The specific interest of our research group (Cardiovascular Research Unit) concerns the treatment of cardiovascular diseases (CVDs). Therefore drugs with potential to ameliorate the healing of different aspects of CVDs were chosen to benchmark the hydrogel concepts developed in this work. Additionally, the use of drugs with combined anti-inflammatory and cardioprotective properties is beneficial in case the implanted gels would produce an inflammatory response.

CVDs is a collection term for a number of pathologies concerning the heart and the arteries supplying it with oxygen rich blood, but in a wider interpretation CVDs also include the general vascular system throughout the body. Statistics for the United Kingdom (Stojkovic *et al.*) revealed that 0.2% of the population suffered from a heart attack in 2010 and one third of all deaths in the UK was a result of CVDs (Scarborough *et al.* 2010). In fact, CVDs are the major cause of death worldwide accounting for 29% of all deaths (Mathers *et al.* 2004).

Several risk factors for developing CVDs have been identified giving a sad picture of the general awareness since most are self-inflicted. The risk factors are obesity, smoking, low

physical activity, high blood pressure, dyslipidaemia, diabetes and genetic factors (Blom *et al.* 2005; Brunzell *et al.* 2008). The positive aspect would be that irrespective of which high risk group an individual belongs to, going from a low to a moderate fitness level would approximately half the relative risks for CVDs (Blair *et al.* 1989).

The extreme of CVDs is when a blood vessel gets blocked as a consequence of the eruption of atheroma, resulting in an ischemic region with reduced access to oxygen. If such an event occurs in the coronary arteries, supplying the heart muscle with oxygen, it is called a myocardial infarct (McMurray *et al.*), generally known as a heart attack. The heart muscle cells lacking oxygen will not survive this state, causing a reduced access of pumping force for the heart. If adequate help is available the affected area of the heart can be minimised. But the time window for such rescue of viable myocardium is narrow, only a few hours (Ertl *et al.* 2005).

A heart attack initiates an intensive activity in the infarcted region in order to heal and minimise the damage. The mechanical response to an infarct may involve hypertrophy which is an attempt to compensate for lost heart muscle tissue but at the end may result in heart failure (Katz 2002). The biological wound healing has three major but overlapping phases, an initial inflammation which starts within hours, followed by tissue formation and tissue remodelling starting after days and weeks respectively (Singer *et al.* 1999; Ertl *et al.* 2005). The wound healing phases all have in common the migration of cells that produce growth factors to coordinate the healing procedure (Singer *et al.* 1999; Vanhoutte *et al.* 2006). However, for wound healing in the heart post MI, the lack of blood supply aggravates the situation since cells cannot migrate in an ischemic region. At the end, the inherent wound healing mechanism has repaired the wound but not regenerated its original functions. It is at this stage cardiovascular researches want to change the natural proceedings of the biological wound healing routs by gentle manipulation with drugs and controlled delivery methods (Andreadis *et al.* 2006; Gurtner *et al.* 2008). As an alternative to drug treatments, the use of stem-cells for cardiac recovery is currently under investigation (Segers *et al.* 2008).

At present, the clinical treatments to prevent further CVD related complications are of surgical or medical character, or a combination thereof, depending on the nature of the MI. The surgical interventions consist of percutaneous angioplasty, with or without the placement of a stent. If several of the coronary arteries, supplying the heart muscle with oxygen rich blood, are narrowed, there may instead be the need of an open chest by-pass operation for one or more of the blocked arteries.

The three main drug classes for medical treatment of post MI patients are angiotensin-converting enzyme inhibitors (Greenberg *et al.* 1995; Køber *et al.* 1995; McMurray *et al.* 2003),

angiotensin receptor blockers (Cohn *et al.* 2001) and β-blockers (Freemantle *et al.* 1999; Cruickshank 2010). These drugs are particularly used for the management of cardiac arrhythmias, cardioprotection post MI in order to prevent congestive heart failure and to prevent stroke for patients with hypertension.

1.4.1 Rapamycin

Rapamycin is a naturally occurring macroloid drug with a broad range of anti-inflammatory and immunosuppressant action. All documented effects of Ra action origins from its inhibition of the mammalian target of Ra (mTOR). By doing so a wide range of therapeutic effects is set off. A visual effect is the striking similarity between rapamycin-treated and starved cells, which is due to the mTOR signalling pathway being responsible for cell growth in response to nutrients. The complex is responsible to keep a balance between protein synthesis and degradation such that the cell can rapidly adjust mass accumulation to a level appropriate to the nutrient supply (Schmelzle *et al.* 2000). The mTOR also up-regulates the mammalian translational machinery upon elevated levels of amino acids and growth factors.

1.4.1.1 The Effect of Rapamycin on Cardiovascular Diseases

By inhibition of mTOR, the hub of the protein synthetic machinery, Ra exerts an avalanche of activity whereof many routes improve the detrimental effects of most stages of CVDs.

The starting point of many CVDs is vascular inflammation, which is reduced upon Ra treatment (Zhao *et al.* 2009). The mechanism of this involves inhibition of mTOR that regulates the response of major inflammatory cell types (Weichhart *et al*. 2008) and alters protein expression (Ma *et al.* 2007).

If vascular inflammation progress and the diseased vessels become occluded, grafting or by-pass surgery might be necessary. A common problem at the site of surgical injury and implanted stents is deposition of crosslinked fibrin, which may give rise to restenosis. Traditionally Ra is used to coat stents (Venkatraman *et al.* 2007), where the drug inhibits migration and proliferation of vascular smooth muscle cells (Sakakibara *et al.* 2005; Yallapu *et al.* 2008) -the main cause of restenosis. Formation of in-stent neointimal hyperplasia, the initial stage of restenosis, was eliminated in Ra treated stents (~2 mm^2) compared to standard uncoated stents (~37 mm^2) at six months (Morice *et al.* 2002). Rapamycin also improves long-term graft survival by lowering the immune response towards the graft. More specifically Ra influences the population of T-cells and Dendritic cells, which are the two main inflammatory cell lines when it comes to controlling alloimmune response (Bestard *et al.* 2009). T-cell activity is reduced by Ra inhibition of mTOR

activation. Dendritic cells produce interleukin-18 that is a pro-inflammatory cytokine closely connected with allograft rejection and vascular diseases. Rapamycin treatment inhibits the production of this inflammatory marker *in vivo (Ko et al. 2008)*.

If grafting or by-pass surgery could not prevent a MI, there is still potential in Ra treatment, which has shown excellent ability to quench pathological coronary hypertrophy post MI (Shioi *et al.* 2003; McMullen *et al.* 2004; Shiojima *et al.* 2005), due to mTOR inhibition (Boluyt *et al.* 2004; Proud 2004). Moreover, mTOR inhibition post MI also attenuates adverse left ventricular remodelling expressed as a significantly smaller infarct size (Buss *et al.* 2009).

The effects on post MI events of mTOR inhibition are truly powerful. Treatment initiated as late as 3 days post MI significantly attenuated myocardial remodelling and reduced hypertrophy. And after ending a one-month lasting treatment, there was still clear evidence of the improvements from mTOR inhibition after an additional two months (Buss *et al.* 2009). Finally, Ra treated mice increased their median and maximal lifespan by approximately 10% (Harrison *et al.* 2009).

No matter how potentially useful a drug is, the desired therapeutical effects will only be reached with the correct application of the drug. Prolonged systemic treatment with Ra resulted in side effects in as many as ~20% of the participating patients (Stojkovic *et al.* 2010). In contrast, when locally applied in a drug eluting stent application no adverse effects were attributable to the Ra coating of stents (Morice *et al.* 2002). These findings encourage the development of targeted drug delivery systems such as *in situ* forming hydrogels

1.4.1.2 Controlled Release of Rapamycin

The anti-inflammatory and immunosuppressant properties of Ra were investigated in numerous studies of stent coating (Venkatraman *et al.* 2007) and anti-rejection of transplanted organs (Gaumann *et al.* 2008). For improvement of implanted materials the standard approach is to blend Ra with a polymer carrier, prior to application to stents or other devices. Such approaches were developed by Wang *et al.* and Alexis *et al.* where Ra was homogeneously dispersed within a degradable PLGA matrix (Alexis *et al.* 2004; Wang, X. *et al.* 2006). The resulting elution profiles where biphasic for the two cases with an initial diffusion controlled release followed by a more rapid release when coat degradation was more substantial (**Figure 8**).

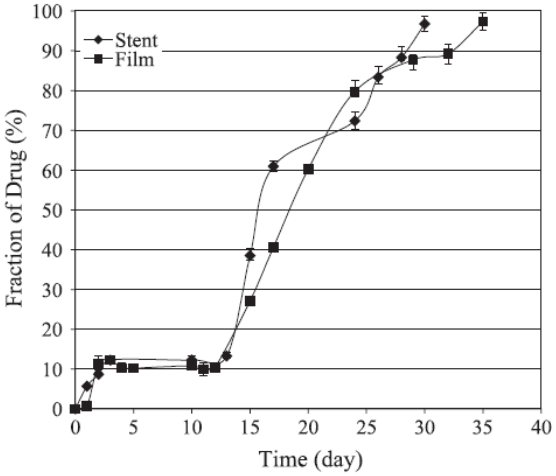

Figure 8: Rapamycin release from a PLGA coated stent. The graph is adapted from Alexis *et al.* (2004).

To prolong the elution time of Ra Chen and co-workers trapped the drug in PEG containing triblock micelles, which were further embedded in a chitosan and PEG based hydrogel. Stents coated with this hydrogel maintained drug elution during a period of 190 days with a non-zero order profile (Chen *et al.* 2009).

A range of both systemic and local delivery formulations of Ra, with potential to be used for anti-rejection therapy, has been developed. These approaches include the entrapment of Ra in various micelles or nanoparticles. Micelles made from diblock PEG-PCL resulted in a 6 day release controlled by diffusion (Forrest *et al.* 2006). **Figure 9** shows the elution profile from photo-polymerised poly(*N*-isopropylacrylamide) hydrogel nanoparticles carrying entrapped Ra (Reddy *et al.* 2008). The profile is representative for many of the reported Ra delivery approaches in the literature (Forrest *et al.* 2006; Venkatraman *et al.* 2007; Reddy *et al.* 2008; Chen *et al.* 2009; Lu *et al.* 2011).

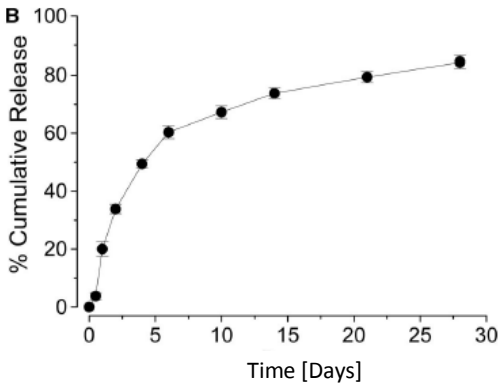

Figure 9: Rapamycin release from poly(N-isopropylacrylamide) nanoparticles. The graph is adapted from Reddy *et al.* (2008).

Apart from two commercially available synthetic derivatives of Ra, Everolimus and Temsirolimus, introduced between 2007 and 2011 for prevention of organ rejection and treatment of cancer (**Figure 10**), there are very few reported investigations where Ra is covalently modified.

Figure 10: Everolimus and Temsirolimus are Ra prodrugs substituted by the hydroxyl group at position 40.

However, one patent reports on PEGylation of Ra (Lee *et al.* 1998), and the Ra-PEG derivative was further used for applications such as anti-tumour treatment in combination with PEGylated 17-hydroxywortmannin (Yu *et al.* 2005). Other related patents describe the use of Ra trapped in sugar coatings (Nagi 1998) or in the hydrogel core of microcapsules (Sharp *et al.* 2012) for oral and topical administration, dissolved in aqueous *N*-*N*-dimethylacetamide for intravenous injection (Waranis *et al.* 1996), or trapped in polymeric coatings to be used with implantable devices, such as stents (Castro *et al.* 2010; Hossainy *et al.* 2012), to mention some applications.

As pointed out in the text above, a sustained Ra elution is obtainable by intelligent design of the drug entrapment, but the release is controlled by diffusion and/or degradation and the resulting elution profiles are not of zero order character. A zero order drug dosing elution profile is desired since the resulting drug concentration is more or less constant during the elution period, and the potentially toxic levels first order and burst release may result in are avoided. Thus, the apparent lack of controlled Ra release gives rise to a demand for devices showing both a sustained and zero order release.

1.4.2 Dexamethasone

Dexamethasone (Dex), a synthetic steroid hormone binding to the glucocorticoid receptor, acts through slow genomic (Cole 2006) or rapid non-genomic (Lowenberg *et al.* 2007) mechanisms to exert a wide range of activities in the human body. Due to its anti-inflammatory and immunosuppressant properties, Dex is regularly used for clinical treatment of anaphylactic shock and inflammatory diseases such as rheumatoid arthritis and asthma. However, prolonged systemic use of the drug has undesirable side effects such as obesity, diabetes, immune suppression and osteoporosis (Ng *et al.* 2004). To come around the undesired effects, Dex has also been delivered

locally to reduce inflammation from implanted devices such as screw-in pacemaker leads and ocular inserts (Baeyens *et al.* 1998), to prevent restenosis in vascular stents (Koenig *et al.* 2009) and is also available in a variety of topical ointments/gels/solutions (McGuigan *et al.* 1986; Chandra *et al.* 2000).

1.4.2.1 Controlled Release of Dexamethasone

As Dex has been shown to be effective also in a variety of applications, it is not surprising that there is a growing body of literature describing its controlled release. Dex has been incorporated in and released from PLGA microspheres (Kim, D. H. *et al.* 2006; Zolnik *et al.* 2008), polypyrrole coatings (Wadhwa *et al.* 2006), PEG containing copolymers crosslinked by photo-polymerisation (Norton *et al.* 2007), PLGA nanoparticles in PVA-gels (Cascone *et al.* 2002; Patil *et al.* 2007) and from degradable PLGA scaffolds made by gas-foaming/salt leaching (Yoon *et al.* 2003).

On the patent side, Dex has been incorporated and released from; drug delivery reservoirs filled with hydrogels based on hyaluronic acid (Jolly *et al.* 2009), PVA-gels for administration via transdermal or transmucosal routes (Kuribayashi *et al.* 2006) or hydroxymethyl methacrylate-based gels in combination with a growth factor in order to improve wound healing (Schultz 2003), to mention some applications.

In these and many other examples, Dex was incorporated by physical entrapment and was released by a diffusion/swelling mechanism and/or with degradation of the matrix. A representative elution profile for such release is shown in **Figure 11** where Dex is released from a silicone polymer matrix, which in a rat model inhibited neointimal proliferation after balloon vascular surgery (Villa *et al.* 1994).

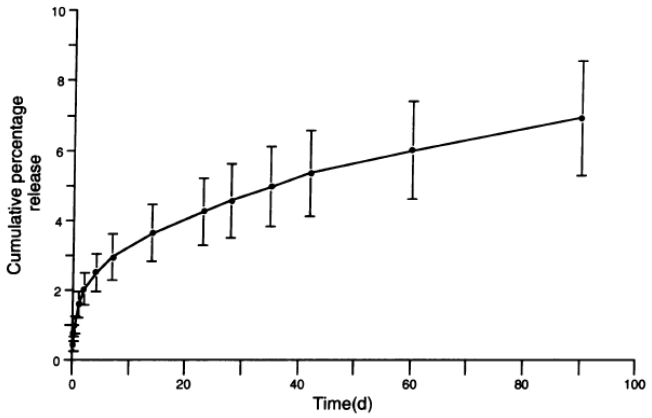

Figure 11: Release of Dex from a silicone polymer matrix. The graph is adapted from Villa *et al.* (1994).

In contrast, Zacchigna *et al.* studied the effect of covalent PEGylation of Dex by conjugating Dex-succinate with mono-PEG-NH_2, more than 65% of the drug was released by esterase action within 24 hours (Zacchigna *et al.* 2008). To obtain long term sustained drug delivery Nuttelman *et al.* covalently coupled Dex to methacrylated PEG, via a linker containing 2, 4 or 6 degradable lactic acid units, which were formed to hydrogels by photo-polymerisation. By encapsulating human mesenchymal stem cells in the gels an induced osteogenesis was verified as Dex was hydrolytically released (Nuttelman *et al.* 2006). The hydrogels eluted less than 27% of the load in approximately 30 days.

Dex has also been conjugated with molecules for targeting specific tissues. Both Dex-succinate-dextran and Dex-21-sulphate sodium are colon-specific pro-drugs, which release Dex in contact with colon or cecum specific enzymes (Pang *et al.* 2002; Kim, I. H. *et al.* 2006)

Controlled release by making use of local conditions in inflamed tissues was obtained by PEGylating Dex via an acyl hydrazone linker and forming micelles with a PEG containing block polymer (Howard *et al.* 2011). Alternatively, a Dex-acyl hydrazone-$2N_3$ derivative was copolymerised by the HDC click reaction with a mixture of mono-PEG-Act and PEG-2Act to obtain an injectable conjugate which released Dex over approximately 17 days in an acidic environment mimicking rheumatoid arthritis (Liu *et al.* 2010). The obtained acid catalysed zero order release of Dex is shown in **Figure 12**. A significantly lower anti-inflammatory response was proved in a subcutaneous mouse model for implanted hyaluronic acid hydrogels covalently linked via a hydrazide moiety to Dex compared to control gels (Ito *et al.* 2007).

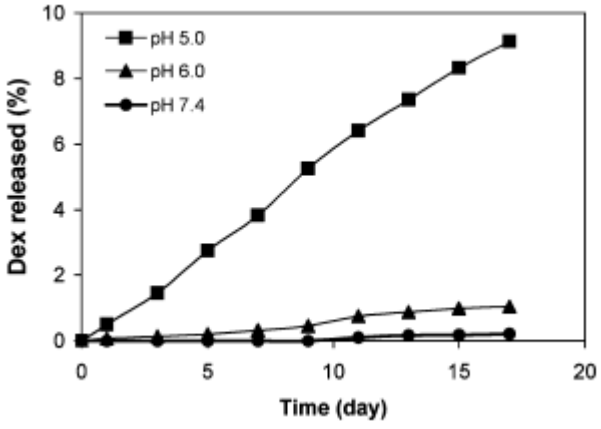

Figure 12: Hydrolytically released Dex from a PEG-Dex conjugate at different pH. The graph is adapted from Liu *et al.* (2010).

These reports show the possibility to elute Dex over a prolonged period of time by encapsulating the drug, while site specific release of Dex, either by enzymatic activity or hydrolysis in an acidic environment is less sustained. Therefore, methods for a sustained and controlled release at physiological pH remain to be developed.

1.5 Hypothesis and Aims

As noticed by the reader, in these opening chapters, drug release from hydrogels is a complex subject and controlled zero order release is not often observed in the literature.

To obtain such release, the author behind this thesis worked according to the following hypothesis; controlled, zero order release, of rapamycin, dexamethasone and atorvastatin from injectable and degradable hydrogels can be achieved by covalent attachment of the drugs to the hydrogel matrices via hydrolytically degradable bonds.

The specific aims with the work in this thesis are;

Regarding hydrogels:

- To produce acrylated and thiolated PEG-based building blocks, which render injectable hydrogel formulations that solidifies spontaneously under biological conditions.
- To obtain gels that degrade hydrolytically under biological conditions and that the degradability is tuneable by the crosslinking chemistry and by varying the number of crosslinking sites.

Regarding drug elution:

- To render the hydrophobic drugs Ra, Dex and atorvastatin water soluble by covalent conjugation with PEG, and that covalent incorporation into hydrogels and the subsequent hydrolytically controlled release of these drugs leads to a sustained elution.
- To obtain drug release, which follows zero order kinetics and that the released drugs retain their biological activity.
- To tune the rate of drug elution by the chemical environment next to the drug-gel linker.
- To distinguish between zero and first order or burst release kinetics by using the zero order and first order rate equations.

1.6 Strategy

To produce a biocompatible slow release drug delivery system there are many parameters to consider. The following text will take the reader through the strategic decisions made regarding the options of building blocks to drug eluting mechanisms, while briefly repeating the most important arguments on how to achieve the set out aims at each particular level (**Figure 13**, Level 1-6).

Level 1 and 2:

The polymers used to build a hydrogel scaffold could be of natural origin or synthetically produced, hydrophobic or hydrophilic to mention the fundamentals. The synthetic hydrophilic polymer PEG is a well-favoured material in pharmaceutical applications due to its inertness, non-toxicity and its elimination via both renal and hepatic pathways (Veronese *et al.* 2005) and was thus chosen. The strategy was to produce biocompatible hydrogel scaffolds, suitable for drug delivery, by co-gelling PEG based multi-arms and crosslinkers with PEGylated drugs.

Level 3:

The mode of gelling determines gel properties such as swelling degree, degradation rate and mechanical strength. The aim with this thesis was to produce a solid gel that keeps intact for a desired period of time, but eventually degrades and is cleared from the body. The strategy to obtain these properties was to gel the PEG building blocks by chemical gelling methods and the introduction of hydrolytically labile ester crosslinks rendered the gels degradable.

Level 4:

The choices of gel architecture (linear, star shaped, dendritic etc.) and assembling mode (matrix, reservoir, micro/nano-spheres, embedded spheres etc.) affect gel properties and drug elution kinetics. In order to obtain a range of drug eluting properties the strategy was to develop two different matrix approaches towards controlled drug delivery; one using either 2- or 4-armed mono-functional PEGs where the drug is pending at the terminal of the polymer and the other approach using bi-functional 2- or 4-armed PEG-based dendritic structures of first or second generation.

Level 5:

To obtain formulations, which solidify spontaneously at biological conditions, and thus can be injected for *in situ* formation, the conjugate addition reaction was preferred for the gelling step. In the case where the compounds were not water soluble thiol-ene crosslinking was utilised instead.

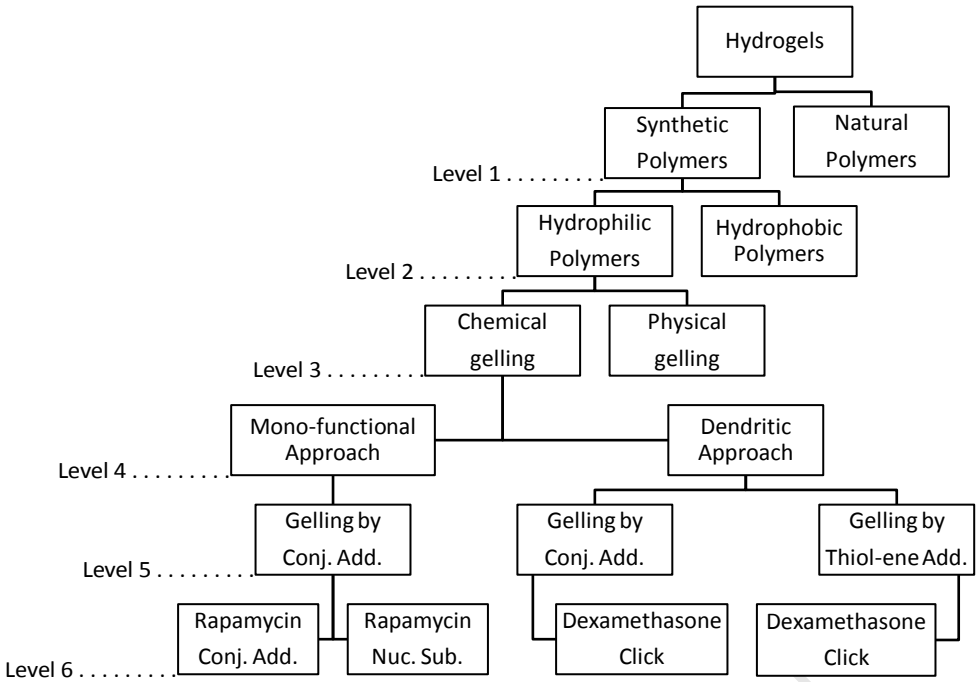

Figure 13: The main choices made to develop the drug eluting systems described in this thesis.

Level 6:

Drugs delivered by hydrogels can be released by different mechanisms (diffusion, swelling, degradation, hydrolysis, enzymatic activity etc.) resulting in various elution profiles (burst, zero or first order etc.). The sustained and constant drug release described by zero order kinetics is desired in many applications. To obtain such release for the chosen drugs, Ra and Dex, the strategy was to covalently incorporate these drugs into the pregel polymers, via hydrolytically labile esters, by conjugate addition (Conj. Add.) or nucleophilic substitution (Nuc. Sub.) in the mono-functional approach and by click chemistry (Click) in the dendritic approach.

In addition, atorvastatin, an HMG-CoA reductase inhibitor, was initially investigated for the mono-functional approach (Appendix I), but was put on hold in favour of development of Ra and Dex delivery.

Using biocompatible PEG building blocks gelled by conjugate addition opens up for the possibility to locally inject the pregel solution into the targeted tissue making these gels very useful in applications where localised anti-inflammatory action and/or immunosuppression is required, but especially where *in situ* gel formation is an additional requirement. By applying these gels *in situ* at the very site in need of stimulus, the drug elution is limited to the surrounding tissue, thus, avoiding systemic exposure, which is often associated with a range of unwanted side effects.

By creating such a hydrogel platform, the ground is laid for the further development of applications such as an injectable treatment for improvement of MI recovery and coatings for improved wound healing and patency of vascular grafts and stents.

2 MATERIALS and METHODS

All chemicals were obtained from commercial sources and of reagent grade or higher, except where otherwise stated. The two drugs and some of the polymers were obtained from particular sources and will therefore be specified. Dexamethasone was obtained from Pharmacia & Upjohn and the following chemicals were purchased: rapamycin (Zhou Fang Pharm Chemical, Shanghai, China), 10PEG-4OH (Shearwater Polymers, Huntsville, USA) 20PEG-8OH (Nektar Therapeutics, Huntsville, USA) and 10nPEG-4SH (Creative PEGworks, Winston Salem, USA).

2.1 Nomenclature

*m*PEG-*n*OH	*n* armed polyethylene glycol (PEG) with a molecular mass of *m* kilo Dalton (kDa)
*ms*PEG-*nX*	PEG conjugates with *n* arms and a molecular mass of *m* kDa where *X* is either acrylate (Ac), vinyl sulphone (VS) or thiol (SH) groups, *s* denotes whether the thiols are attached via an ester linkage (*s*= d for degradable) or not (*s*= n for non-degradable)
Ra-*nX*	mono (*n*= 1) or di (*n*= 2) functionalised rapamycin (Ra) where *X* is either acrylate (Ac) or iodoacetic ester (IAE) groups
Ra*X*-dPEG-2SH/3SH	mono functionalised RaX conjugated with 2dPEG-2SH or 10dPEG-4SH, *X* is either acrylate (Ac) or iodoacetic ester (IAE) groups
PEG-*G*-nX_1-nX_2	dendritic compounds of first (*G*= G1 or 4arm-G1) or second (*G*= G2) generation where *n* is the number of functional groups; X_1= acetylene (Act) or Dex, X_2= acetonide protection (Castro *et al.*), OH or Ac

2.2 Syntheses of Gel Building Blocks

2.2.1 Preparation of the Multi-arms

The multi-acrylate and multi-vinyl sulphone were the bulk materials for Ra containing gels and their synthesis protocols were adapted from the literature (Elbert *et al.* 2001; Dobner *et al.* 2009).

Synthesis of 20PEG-8Ac (1): Star shaped 20PEG-8OH (10 g, 4.0 mmol OH) was dissolved in toluene (500 ml) and dried by azeotropic distillation. The residue (~400 ml) was cooled on ice and diluted with DCM (200 ml). Freshly distilled triethylamine (TEA; 10 ml, 10 mmol, of a stock solution of 7 ml TEA in 50 ml dichloromethane; DCM) was added. Acryloyl chloride (AcCl; 10 ml of a stock solution of 4 ml in 50 ml DCM, 10 mmol) was added in portions (2 ml every 10 min) during 50 minutes. The

reaction was left with stirring overnight. The reaction mixture was filtered to remove insolubilities and the volume reduced (to ~60 ml) prior to precipitation in ice cold diethyl ether (600 ml). The precipitation was repeated twice from DCM (60 ml) into ice cold diethyl ether (600 ml). The product was further purified by dialysis (cut off value =1 kDa) and freeze dried to obtain a slightly off white powder (6.9 g, 68%, 94% purity by nuclear magnetic resonance; NMR).

^{1}H NMR (300 MHz, $CDCl_3$): δ= **3.43-3.80** (m; PEG), **4.29** (t, J= 5.5 Hz, 16H; -PEGOCH_2CH_2Ac), **5.81** (dd, J= 10.4 and 1.3 Hz, 8H; Ac_{Cis}), **6.13** (dd, J= 17.4 and 10.5 Hz, 8H; Ac) and **6.40** (dd, J= 17.4 and 1.2 Hz, 8H; Ac_{Trans}) parts per million (ppm).

Both the product purity and a high degree of substitution were verified by a gelling test where **1** (200 mg/ml PBS-2) was mixed with a solution of 2dPEG-2SH (**3**) at a stoichiometric ratio and a final concentration of 14% (w/v PBS-2). A gel (50 µl) was formed from the pregel solution and incubated (37° C). The gelling was assessed at regular intervals and was considered to occur when the gel was solid enough to maintain in one piece when removed from its surface.

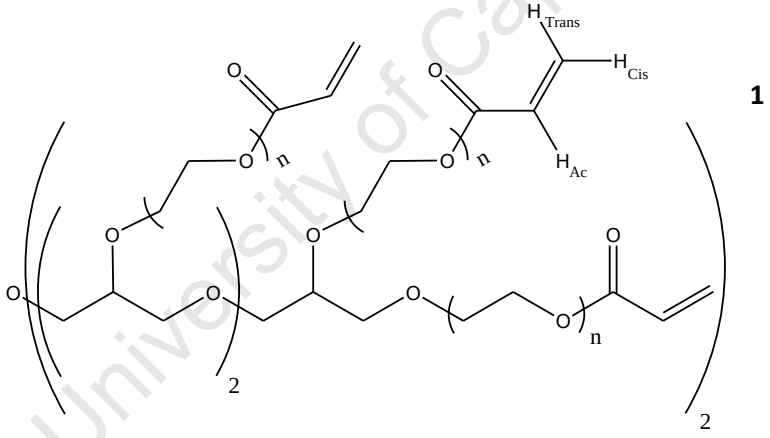

1

Synthesis of 20PEG-8VS (2): Star shaped 20PEG-8OH (20 g, 8.0 mmol OH) was dissolved in DCM (200 ml) and dried over molecular sieves (4 Ångström; Å) overnight. The molecular sieves were removed by filtration and NaH (65 % in oil; 1.5 g, 41 mmol) was added in portions followed by addition of DCM (300 ml). The solution was then purged with argon gas for five minutes by bubbling. Divinyl sulphone (40 ml, 398 mmol) was added in one portion, the solution was bubbled with argon (30 min) and left to react for two days in darkness. Addition of glacial acetic acid (2.5 ml, 44 mmol) quenched the remaining NaH and protonated the product. The volume was reduced (to ~100 ml) prior to precipitation in cold diethyl ether (1 l). The product was collected on a filter and remaining solvent

removed by vacuum. The precipitation was repeated twice to obtain a slightly off white powder (6.8 g, 32%, ~100% purity by NMR).

^{1}H NMR (300 MHz, $CDCl_3$): δ= **3.25** (t, J= 5.7 Hz, 16H; -PEGOCH_2CH_2VS), **3.58-3.72** (m; PEG), **3.89** (t, J= 5.7 Hz, 16H; -PEGOCH_2CH$_2$VS), **6.07** (d, J= 9.9 Hz, 8H; VS_{Cis}), **6.38** (d, J= 16.7 Hz, 8H; VS_{Trans}) and **6.80** (dd, J= 9.9 and 16.7 Hz, 8H; VS) ppm.

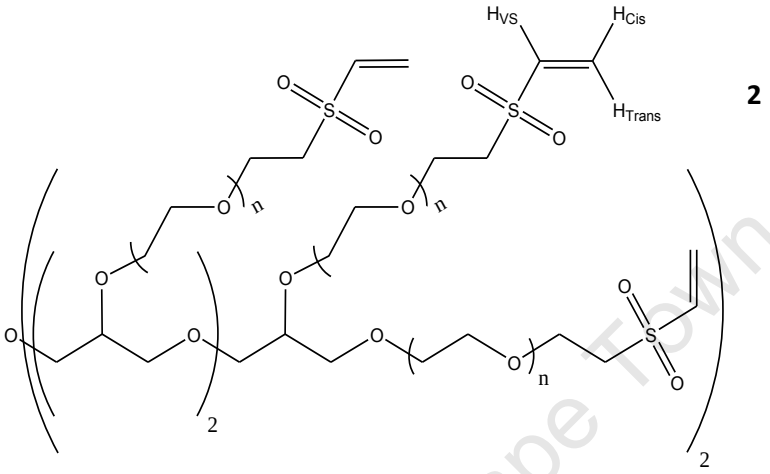

2

2.2.2 Preparation of the Thiol Crosslinkers

PEG-2OH with various molecular masses (0.6, 0.9, 1.5 and 2 kDa) were conjugated with 3-mercaptopropionic acid using the same method, as previously described (Nie *et al.* 2007). Details are given in the case of 2PEG-2OH.

Synthesis of 2dPEG-2SH (3): Linear 2PEG-2OH (10.0 g, 10 mmol OH), 3-mercaptopropionic acid (4.3 ml, 49 mmol) and para toluene sulphonic acid (pTSA; 95 mg, 0.50 mmol) were dissolved in toluene (150 ml). The reaction mixture was heated (140° C) and refluxed in a Dean-Stark apparatus set up overnight. The solution was cooled on ice and the volume reduced prior to precipitation in cold diethyl ether. The precipitation was repeated, this time from DCM (20 ml) into cold diethyl ether (200 ml) and the collected product was vacuum dried (9.9 g, 90%, 99% purity by NMR).

^{1}H NMR (300 MHz, $CDCl_3$): δ= **1.62** (t, J= 8.1 Hz, 2H; -S*H*), **2.59-2.64** (m, 4H; -OCOCH_2CH$_2$SH), **2.67-2.75** (m, 4H; -OCOCH$_2$CH_2SH), **3.32-3.82** (m; PEG) and **4.20** (t, J= 4.7 Hz, 4H; PEG-CH$_2$CH_2OCO-) ppm. ^{13}C NMR (75.5 MHz, $CDCl_3$): δ= **19.50** (-CH$_2$*C*H$_2$SH), **38.21** (-*C*H$_2$CH$_2$SH), 63.53, 68.84, 70.35 and **171.26** (-*C*OO-) ppm.

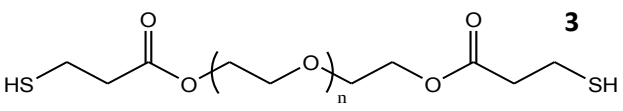

3

Synthesis of 10dPEG-4SH (4): Star shaped 10PEG-4OH (9.5 g, 3.8 mmol OH), 3-mercaptopropionic acid (3.5 ml, 40 mmol) and pTSA (77 mg, 0.40 mmol) were dissolved in toluene (150 ml). The reaction mixture was heated (135° C) and refluxed in a Dean-Stark apparatus set up over the day. Toluene was removed by evaporation and the crude product was precipitated twice from DCM (20 ml) into cold diethyl ether (250 ml). The collected product was vacuum dried (8.7 g, 88%, 99% purity by NMR).

^{1}H NMR (300 MHz, $CDCl_3$): δ= **1.64** (t, J= 8.4 Hz, 4H; -S*H*), **2.61-2.67** (m, 8H; -OCOC*H*$_2$CH$_2$SH), **2.69-2.78** (m, 8H; -OCOCH$_2$C*H*$_2$SH), **3.35-3-85** (m; PEG) and **4.23** (t, J= 4.7 Hz, 8H; PEG-CH$_2$C*H*$_2$OCO-) ppm.

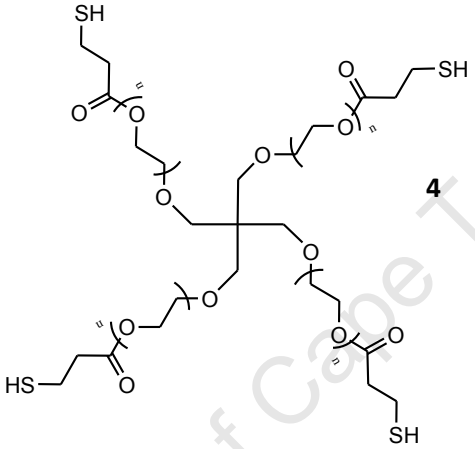

4

2.2.3 Mono-functional Approach

2.2.3.1 Preparations of Rapamycin Derivatives

The precipitation protocol of RaAc (Viswanath *et al.* 2008) and the synthesis and PEGylation protocols of RaIAE (Plattsburgh *et al.* 1998; Yu *et al.* 2005) were adapted from the literature.

RaAc was synthesised several times using different amounts of AcCl. The methodologies were similar in all cases, but details are only given for the batch further used for the PEGylation and gel incorporation steps.

Synthesis of RaAc (5): Rapamycin (Ra; 278 mg, 304 µmol) and TEA (85 µl, 610 µmol) were dissolved in DCM (20 ml). AcCl (49 µl, 606 µmol) was separately dissolved in DCM (10 ml) and slowly added to the reaction mixture from a dripping funnel resulting in the formation of hydrochloric gas. The two reaction solutions were always kept in an argon atmosphere. The reaction was followed by thin layer chromatography (TLC; 70% ethyl acetate in *n*-hexane) and if Ra (R_f≈ 0.3) was not consumed within 2 hours of reaction, additional amounts of AcCl and TEA were added (total addition: 8 eq/Ra). The solvent was evaporated and the crude product loaded to silica (1 g) by evaporating the solvent from

a chloroform mixture of the product and silica. The product/silica mixture was then loaded to a column packed with silica (30 g) in hexane which was washed with an increasing gradient of ethyl acetate (EtOAc) in *n*-hexane (Hex), the product eluted at 50%. All fractions containing the product (R_f ≈0.7) were pooled and the solvents co-evaporated with chloroform. The product was further dissolved in *tert*-butyl methyl ether, filtered and precipitated in *n*-heptane (Hep) to yield a slightly off-white powder (102 mg, 35%, 100% purity by NMR).

High pressure liquid chromatography (HPLC) retention times for the Ra reference: 37.64 min and for compound **5**: 40.95 min.

Electrospray ionisation mass spectrometry (ESI-MS) of Ra: found (assigned) *m/z*= 814.5 (Ra-frag1), 832.6 (Ra-frag1 + H_2O), 846.6 (Ra-frag2), 864.6 (Ra-frag2 + H_2O), 882.6 (Ra-frag2 + $2H_2O$), 931.6 (Ra + H_2O), 936.6 (Ra + Na^+), 952.6 (Ra + K^+) and 994.6 (Ra-adduct). ESI-MS of compound **5**: found (calculated, assigned): *m/z*= 886.6 (886.6, Ra-frag1-Ac + H_2O), 900.6 (900.6, Ra-frag2-Ac), 918.6 (918.6, Ra-frag2-Ac + H_2O), 936.6 (936.6, Ra-frag2-Ac + $2H_2O$), 990.6 (990.6, Ra-Ac + Na^+) and 1006.6 (1006.6, Ra-Ac + K^+).

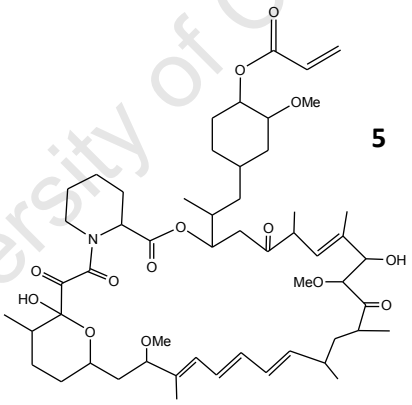

5

Synthesis of RaIAE (6a and 6b): Rapamycin (250 mg, 273 µmol), 4-dimethylaminopyridine (DMAP; 2.0 mg, 16 µmol), iodoacetic acid (61 mg, 328 µmol) and *N,N'*-dicyclohexylcarbodiimide (DCC; 67.7 mg, 328 µmol) were dissolved in DCM (15 ml), placed on ice and left with stirring overnight. The reaction was followed by TLC (70% EtOAc in Hex) and the incomplete consumption of Ra (R_f ≈0.3) led to the addition of more iodoacetic acid (0.2 eq/Ra) and DCC (0.2 eq/Ra). The solvent was evaporated and the crude product absorbed on silica (1 g) by evaporating a chloroform mixture of the product and silica. The product/silica mixture was then loaded to a column with silica (20 g) packed in Hex and washed with an increasing gradient of EtOAc, the products eluted at 40% with only a small overlap. All fractions containing product **6a** (R_f ≈0.7) and product **6b** (R_f ≈0.9) were pooled separately

and the solvents co-evaporated with chloroform to yield an off-white powder (**6a**: 192 mg, 65%, 100% purity by NMR; **6b**: 142 mg, 100% purity by NMR).

HPLC retention times for the Ra reference: 37.64 min, compound **6a**: 41.07 min and compound **6b**: 42.63 min.

ESI-MS of compound **6a**: found (calculated, assigned): *m/z*= 1000.5 (1000.5, Ra-frag1-monoIAE + H_2O), 1014.5 (1014.5, Ra-frag2-monoIAE), 1032.5 (1032.5, Ra-frag2-monoIAE + H_2O), 1050.5 (1050.5, Ra-frag2-monoIAE + $2H_2O$), 1099.6 (1099.5, Ra-monoIAE + H_2O), 1104.5 (1104.5, Ra-monoIAE + Na^+), 1120.5 (1120.5, Ra-monoIAE + K^+) and 1162.5 (1162.5, Ra-adduct-monoIAE). ESI-MS of compound **6b**: found (calculated, assigned): m/z= 1014.5 (1014.5, Ra-frag2-monoIAE), 1182.4 (1182.4, Ra-frag2-diIAE), 1200.4 (1200.4, Ra-frag2-diIAE + H_2O), 1218.4 (1218.4, Ra-frag2-diIAE + $2H_2O$), 1267.5 (1267.4, Ra-diIAE + H_2O), 1272.4 (1272.4, Ra-diIAE + Na^+), 1288.4 (1288.4, Ra-diIAE + K^+) and 1330.4 (1330.4, Ra-adduct-diIAE).

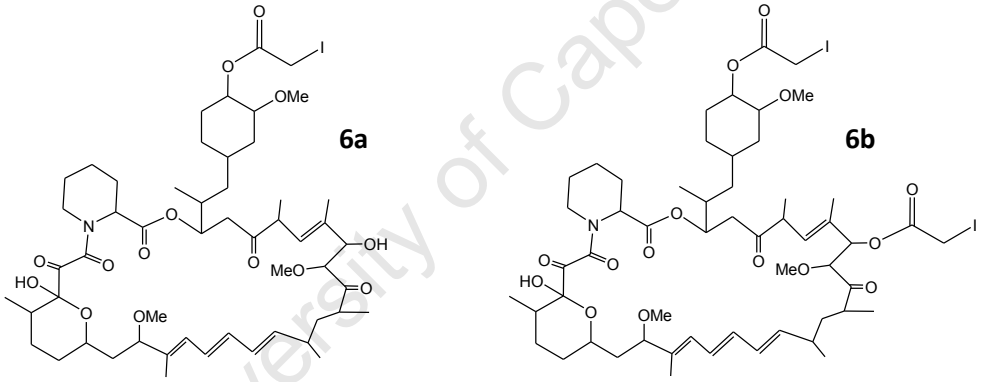

2.2.3.2 Preparations of Ra-PEG conjugates

The RaAc and RaIAE derivatives were conjugated with 2nPEG-2SH, mercaptoethanol, 0.6dPEG-2SH, 0.9dPEG-2SH, 1.5dPEG-2SH, 2dPEG-2SH or 10dPEG-4SH using similar methods. Details are given for conjugation with 2dPEG-2SH and 10dPEG-4SH.

Synthesis of RaAc-dPEG-3SH (7): RaAc (**5**; 25.9 mg, 26.8 µmol) was dissolved in MeCN (1.5 ml) and a solution of 10dPEG-4SH (**4**; 750 µl of 288.6 mg in 793 µl of 0.1 M $NaHCO_3$, 26.8 µmol) was added. The reaction mixture was incubated at 37° C for 1 hour prior to freeze drying. The crude reaction mixture was redissolved in DCM (2.2 ml) and precipitated in cold diethyl ether (25 ml) to yield the product (285 mg, 94%).

The amount of Ra per gram product was determined by dissolving compound **7** (11.9 mg) in 100 ml of a 1:1 mixture of phosphate buffered saline (PBS-1) and ethanol (EtOH), reading the absorbance on a spectrophotometer (λ =279 nm) and calculating the amount of Ra using a standard curve made from serial dilutions of Ra.

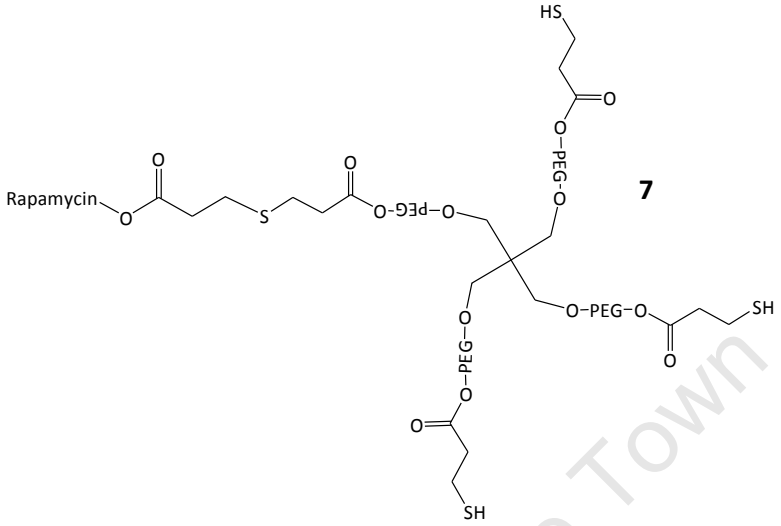

7

Synthesis of RaIAE-dPEG-3SH (8): Compound **6a** (31.9 mg, 29.5 µmol) was dissolved in MeCN (1.6 ml) and diluted with of a solution of 10dPEG-4SH (**4**; 800 µl of 302.9 mg in 806 µl of 0.1 M $NaHCO_3$, 29.5 µmol). The reaction mixture was incubated at 37° C for 1 hour prior to freeze drying. The crude reaction mixture was redissolved in DCM (3 ml), filtered through a cotton plug and precipitated in cold diethyl ether (25 ml) to yield the product (289 mg, 87%).

The amount of Ra per gram mixture was determined by dissolving compound **8** (15.6 mg) in 50% PBS-1 in EtOH (100 ml), reading the absorbance on a spectrophotometer (λ =279 nm) and calculating the amount of Ra using a standard curve made from serial dilutions of Ra.

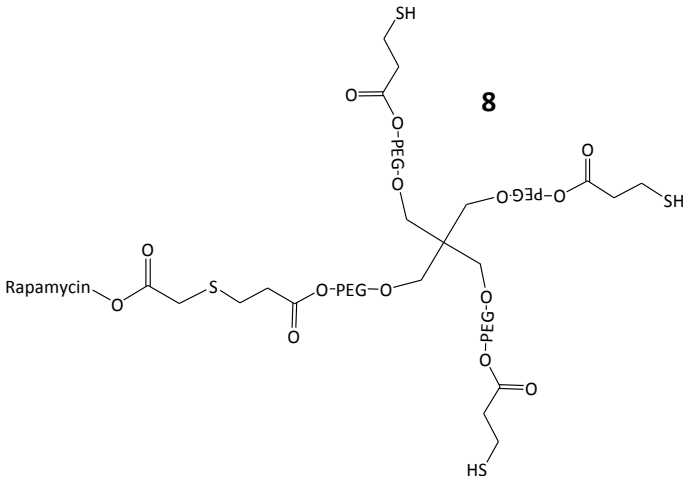

8

Synthesis of RaAc-dPEG-SH (9): RaAc (**5**; 7.5 mg, 7.7 µmol) was dissolved in acetonitrile (MeCN; 200 µl) and a solution of 2dPEG-2SH (**3**; 17.0 mg, 7.7 µmol, in 100 µl of 0.1 M $NaHCO_3$) was added. The reaction mixture was incubated at 37° C for 1 hour prior to freeze drying. The crude reaction mixture was used without further purification for initial experiments.

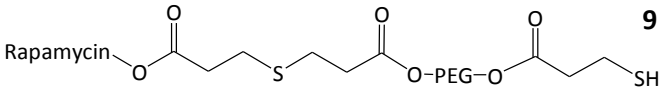

9

Synthesis of RaIAE-dPEG-SH (10): A mixture of RaMonoIAE and RaDiIAE (**6a** and **6b**; 9.9 mg, 8.5 µmol) was dissolved in a mixture of MeCN (200 µl) and methanol (MeOH; 200 µl) and a solution of 2dPEG-2SH (**3**; 18.5 mg, 8.4 µmol, in 200 µl of 0.1 M $NaHCO_3$) was added. The reaction mixture was incubated at 37° C for 2 hours prior to freeze drying. The crude reaction mixture was used without further purification for initial experiments.

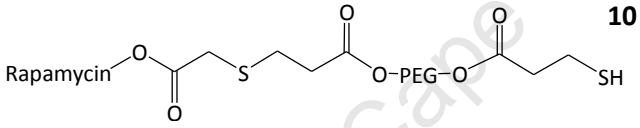

10

2.2.4 Dendritic Approach

2.2.4.1 Preparations of Acetylene monomer anhydride

The acetylene monomer anhydride was the main building block for the dendritic structures and was synthesised similarly to existing methods (Antoni *et al.* 2009) as follows:

Synthesis of acetonide protected trizma (11): The hydrochloride salt of 2-amino-2-hydroxymethyl-propane-1,3-diol (Trizma; 100 g, 635 mmol), 2,2-dimethoxypropane (118 ml, 963 mmol) and pTSA (5.2 g, 27 mmol) were dissolved in dimethylformamide (DMF; 600 ml) and stirred overnight. The acid was neutralised by TEA (4 ml, 29 mmol) followed by rotary evaporation of 2,2-dimethoxypropane and DMF at 60° C. The crude reaction mixture was redissolved in DMF (50 ml) and then diluted with EtOAc (950 ml). The hydrochloride salt of the product was neutralised by adding TEA (100 ml, 717 mmol) and the precipitate was removed by filtration. The volume was reduced (to ~150 ml) and the product was precipitated in cold diethyl ether (1.5 l, cooled with dry ice) from a dripping funnel. The precipitate was collected on a filter and dried over vacuum to yield the product (75 g, 73%, 96% purity by NMR).

^{1}H NMR (400 MHz, D_2O): δ= **1.41** (s, 3H; -C*H*$_3$), **1.43** (s, 3H; -C*H*$_3$), **3.53** (s, 2H; -C*H*$_2$OH), **3.62** (s, J= 12.1 Hz, 2H; -OC*H*$_2$-) and **3.86** (d, J= 12.1 Hz, 2H; -OC*H*$_2$-) ppm. ^{13}C NMR (100.6 MHz, D_2O): δ= **22.53** (-*C*H$_3$), **24.51** (-*C*H$_3$), 50.96, 63.31, 65.67 and **99.99** ((CH$_3$)$_2$*C*OO-) ppm.

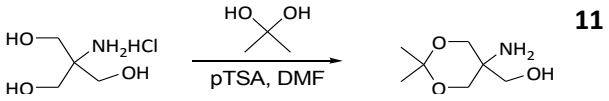

11

Synthesis of succinic propargyl ester (12): Propargyl alcohol (104 ml, 1.8 mol) and DMAP (43.6 g, 0.36 mol) were dissolved in DCM (1 l) and placed on ice prior to portion wise addition of succinic anhydride (214 g, 2.14 mol) which dissolved upon stirring overnight. NMR confirmed the complete consumption of propargyl alcohol (CHCC*H*$_2$OH, δ= 4.25 ppm) and the excess of succinic anhydride was quenched by addition of 200 ml distilled water. The crude reaction mixture was purified by extraction with weak acid (6X 200 ml 10% w/v $NaHSO_4$) whereupon the organic phase was dried with $MgSO_4$, filtered to remove the solids and evaporated to yield the product (227.4 g, 81%, 100% purity by NMR).

^{1}H NMR (400 MHz, $CDCl_3$): δ= **2.47** (t, J= 2.3 Hz, 1H; Act), **2.61** (m, 4H; COOHC*H*$_2$C*H*$_2$-), **4.62** (d, J= 2.3 Hz, 2H; -OC*H*$_2$CCH) and **10.95** (s, 1H, -COO*H*) ppm. ^{13}C NMR (100.6 MHz, $CDCl_3$): δ= 28.28, 28.47, **52.07** (-OCH$_2$CCH), 74.99, 77.16, **171.28** (-*C*OO-) and **177.90** (-*C*OOH) ppm.

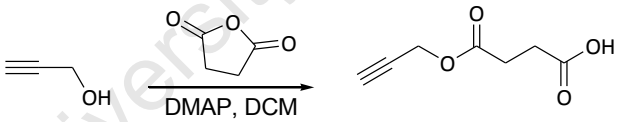

12

Anhydride formation of succinic propargyl ester (13): Compound **12** (227.4 g, 1.46 mol), was dissolved in DCM (350 ml) and cooled on ice. DCC (150.3 g, 0.73 mol) was added in portions and the reaction was stirred overnight. The precipitated dicyclohexylurea was removed by filtration and the solvent was evaporated to yield the product (129.1 g, 60%, 100% purity by NMR).

^{1}H NMR (400 MHz, $CDCl_3$): δ= **2.49** (t, J= 2.3 Hz, 1H; Act), **2.71** (t, J= 6.6 Hz, 2H; -CH$_2$C*H*$_2$-), **2.81** (t, J= 6.6 Hz, 2H; -C*H*$_2$CH$_2$-) and **4.70** (d, J= 2.2 Hz, 2H; -OC*H*$_2$CCH) ppm. ^{13}C NMR (100.6 MHz, $CDCl_3$): δ= 28.19, 29.98, **52.37** (-OCH$_2$CCH), 75.15, 77.22, **167.56** (-*C*OO*C*O-) and **170.82** (-*C*OOCH$_2$-) ppm.

13

Acetylene addition to acetonide protected trizma (14): Acetonide protected trizma (**11**; 39.7 g, 246 mmol), and TEA (51 ml, 368 mmol) were dissolved in DCM (1.8 l) and placed on ice. Compound **13** (58 g, 197 mmol), was dissolved in DCM (400 ml) and added to the reaction solution via a dripping funnel over 1h. After an additional hour ^{13}C NMR revealed the consumption of the anhydride and the volume was reduced (to ~1 l). The solution was extracted with weak acid (5X 400 ml, 10% w/v $NaHSO_4$) and mild base (5X 400 ml, 10% w/v Na_2CO_3) and stirred with $MgSO_4$ overnight. The solids were removed by filtration, the solvent was evaporated and the remaining product was dried over vacuum (48.7 g, 83%, 98% purity by NMR).

^1H NMR (400 MHz, $CDCl_3$): δ= **1.40** (s, 3H; -C*H*$_3$), **1.41** (s, 3H; -C*H*$_3$), **2.13** (s, 1H; -O*H*), **2.47** (t, J= 2.4 Hz, 1H; Act), **2.55** (t, J= 6.8 Hz, 2H; -C*H*$_2$CH$_2$CONH-), **2.68** (t, J= 6.8 Hz, 2H; ; -CH$_2$C*H*$_2$CONH-), **3.66** (s, 2H; -C*H*$_2$OH), **3.78** (d, J= 12.1 Hz, 2H; -CC*H*$_2$O-), **3.86** (d, J= 11.9 Hz, 2H; -CC*H*$_2$O-), **4.66** (d, J= 2.6 Hz, 2H; -OC*H*$_2$CCH) and **6.39** (s, 1H; -N*H*-) ppm. ^{13}C NMR (100.6 MHz, $CDCl_3$): δ= 19.90, 26.88, 29.12, 31.05, 52.15, 54.96, 63.69, 63.88, 75.01, 77.33, **98.72** ((CH$_3$)$_2$*C*OO-), **171.89** (-*C*OO-) and **172.39** (-*C*ONH-) ppm.

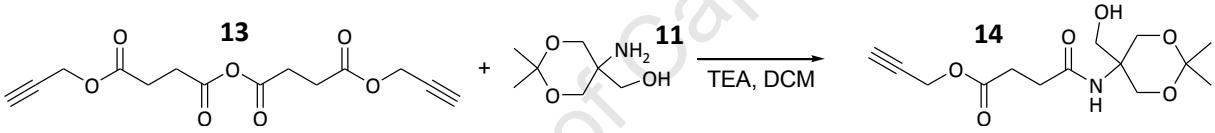

Synthesis of acetylene monomer (15): Compound **14** (48.7 g, 163 mmol), DMAP (4.0 g, 33 mmol) and TEA (27 ml, 195 mmol) were dissolved in DCM (230 ml) and placed on ice. Succinic anhydride (22.8 g, 228 mmol) was added in portions and the reaction was stirred overnight. Proton NMR confirmed the total consumption of **14** (δ= 3.66 ppm, -C*H*$_2$OH) and the reaction was quenched by addition of distilled water (200 ml). The crude reaction mixture was extracted with a weak acid (5X 300 ml, 10% w/v $NaHSO_4$) and brine (5X 300 ml), whereupon the organic phase was dried with $MgSO_4$, filtered to remove the solids and evaporated to yield the product (44.7 g, 69%, 100% purity by NMR).

^1H NMR (400 MHz, $CDCl_3$): δ= **1.33** (s, 3H; -C*H*$_3$), **1.40** (s, 3H; -C*H*$_3$), **2.44** (t, J= 6.8 Hz, 2H; -C*H*$_2$CH$_2$CONH-), **2.47** (t, J= 2.5 Hz, 1H; Act), **2.60-2.63** (m, 6H; -C*H*$_2$-), **3.74** (d, J= 12.2 Hz, 2H; -OC*H*$_2$-), **4.12** (d, J= 12.1 Hz, 2H; -OC*H*$_2$-), **4.41** (s, 2H; -CC*H*$_2$OCO-), **4.61** (d, J= 2.2 Hz, 2H; -C*H*$_2$CCH), **6.27** (s, 1H; -N*H*-) and **9.60** (s, 1H; -O*H*) ppm. ^{13}C NMR (100.6 MHz, $CDCl_3$): δ= 23.00, 23.60, 28.63, 28.83, 30.71, 52.07, 52.92, 62.13, 63.20, 75.05, 77.34, **98.69** ((CH$_3$)$_2$*C*OO-), 172.07, 172.16 and **175.63** (-*C*OOH) ppm.

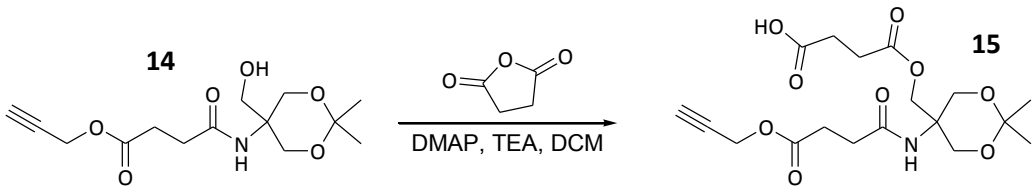

Synthesis of acetylene monomer anhydride (16): Compound **15** (44.7 g, 112 mmol) was dissolved in DCM (80 ml). DCC (11.5 g, 56 mmol) was dissolved in DCM (10 ml) prior to addition to the reaction mixture and left with stirring overnight. The precipitated dicyclohexylurea was removed by filtration and the solvent was evaporated to yield the product (30.0 g, 68%, 90% purity by NMR).

^{1}H NMR (400 MHz, $CDCl_3$): δ= **1.33** (s, 6H; -C*H*$_3$), **1.40** (s, 6H; -C*H*$_3$), **2.41** (t, J= 6.8 Hz, 4H; -C*H*$_2$CH$_2$CONH-), **2.46** (t, J= 2.3 Hz, 2H; Act), **2.59** (t, J= 6.7 Hz, 4H; -CH$_2$C*H*$_2$CONH-), **2.63** (t, J= 6.6 Hz, 4H; -OCOC*H*$_2$CH$_2$COO-), **2.75** (t, J= 6.2 Hz, 4H; -OCOCH$_2$C*H*$_2$COO-), **3.77** (d, J= 11.8 Hz, 4H; -OC*H*$_2$-), **4.07** (d, J= 12.1 Hz, 4H; -OC*H*$_2$-), **4.45** (s, 4H; -CC*H*$_2$OCO-), **4.61** (d, J= 2.0 Hz, 4H; -C*H*$_2$CCH) and **6.06** (s, 2H; -N*H*-) ppm. ^{13}C NMR (100.6 MHz, $CDCl_3$): δ= 22.61, 24.05, 28.25, 28.79, 30.00, 30.70, 51.91, 52.78, 62.34, 63.34, 74.92, 77.19, 77.44, **98.57** ((CH$_3$)$_2$*C*OO-), **168.07** (-*C*OO*C*O-), **171.31** (-*C*OO-), **171.65** (-*C*OO-) and **171.88** (-*C*ONH-) ppm.

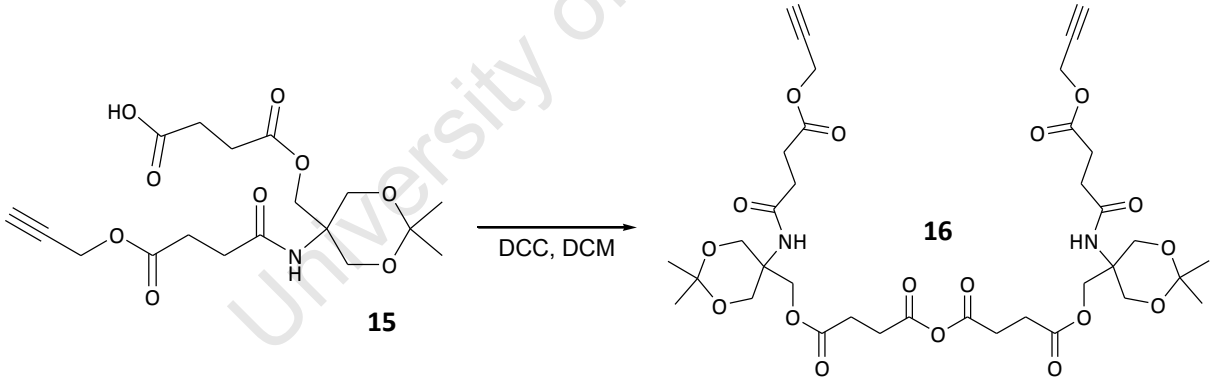

2.2.4.2 Preparation of Dex-azide conjugate

The azide anhydride (O(COCH$_2$CH$_2$CH$_2$CH$_2$CH$_2$N$_3$)$_2$) used for this synthesis was kindly provided by research associate Yvonne Hed (KTH, Stockholm, Sweden). For the full NMR assignment of dexamethasone (Dex) the reader is referred to the literature (Liu *et al.* 1995). The ^{1}H NMR assignment of the product will only consider effected shifts and compare those with corresponding shifts of Dex.

Synthesis of Dex-N_3 (17): Dex (6.9 g, 17.6 mmol) and DMAP (430 mg, 3.5 mmol) were dissolved in tetrahydrofuran (THF; 150 ml) and placed on ice. A solution of the azide anhydride (purity: 94 wt% by NMR, 7.2 g, 22.8 mmol) in THF (20 ml) was slowly dripped into the reaction solution, which was always kept in an argon atmosphere. The reaction was followed by TLC (80% EtOAc/20% Hep) and quenched with distilled water (20 ml) when Dex was consumed (R_f ≈0.6). THF was evaporated and replaced by DCM (200 ml) upon two phases were formed. The organic phase was purified by extraction with a mild base (4X 50 ml, 10% w/v Na_2CO_3) and a weak acid (4X 50 ml, 10% w/v $NaHSO_4$), dried with $MgSO_4$, filtered to remove the solids and evaporated to yield the product, which was further purified by gradient (EtoAc/Hep) flash chromatography to obtain the product (1.6 g, 17%, 100% purity by NMR).

^{1}H NMR (400 MHz, DMSO-d6) for Dex: δ= **3.96** (dd, J= 13.4 and 5.8 Hz, 1H; -C*H*$_2$OH), **4.41** (dd, J= 13.4 and 5.9 Hz, 1H; -C*H*$_2$OH) and **4.59** (t, J= 5.8 Hz, 1H; -CH$_2$O*H*) ppm. ^{1}H NMR (400 MHz, DMSO-d6) for the product: δ= **4.79** (d, J= 17.6 Hz, 1H; -C*H*$_2$OCO-) and **5.01** (d, J= 17.5 Hz, 1H; -C*H*$_2$OCO-) ppm.

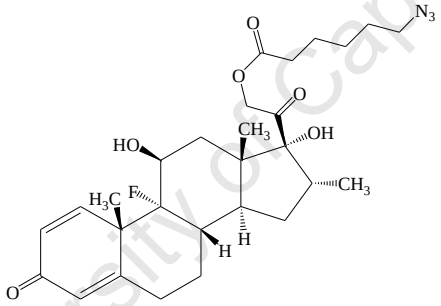

17

2.2.4.3 Preparations of First Generation Linear PEG-Dex Conjugate

Synthesis of PEG-G1-2Act-Acet (18): Linear 10PEG-2OH (30 g, 6.0 mmol OH), acetylene monomer anhydride (**16**; 9.4 g, 12 mmol), DMAP (147 mg, 1.2 mmol) and pyridine (4.8 mg, 0.06 mmol) were dissolved in DCM (100 ml) and left on stirring overnight. The reaction was followed by ^{13}C NMR (δ= 168.07 ppm; -*C*OO*C*O-) and if **16** was consumed an additional equivalent/OH was added. This was repeated twice to complete the reaction. The solvent was evaporated and the product redissolved in THF prior to precipitation in cold diethyl ether. The precipitation was repeated once more to yield the product (30.4 g, 94%).

^{1}H NMR (400 MHz, $CDCl_3$): δ= **1.31** (s, 6H; -C*H*$_3$), **1.40** (s, 6H; -C*H*$_3$), **2.45** (t, J= 2.4 Hz, 2H; Act), **4.14-4.18** (m, 8H; -OCH$_2$C*H*$_2$OCO- and -COC*H*$_2$C-), **4.42** (s, 4H; -CC*H*$_2$OCO-) and **4.60** (t, J= 2.2 Hz, 4H; -C*H*$_2$CCH) ppm. ^{13}C NMR (100.6 MHz, $CDCl_3$): δ= 22.19, 24.43, 28.70, 28.80, 30.68, 51.80, 52.81, 61.97,

63.30, 63.75, 68.68, 70.25 (PEG), 74.88, 77.19, **98.39** ($(CH_3)_2$*C*OO-), **171.44** (-*C*OO-), **171.63** (-*C*OO-), **172.04** (-*C*OO-) and **172.21** (-*C*ONH-) ppm.

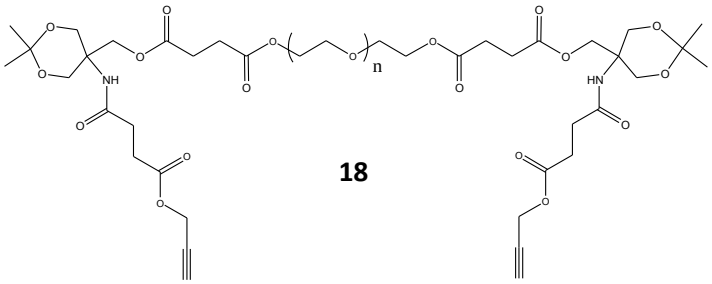

18

Synthesis of PEG-G1-2Act-4OH (19): Compound **18** (30.4 g, 2.8 mmol) was dissolved in MeOH (200 ml) and the acidic resin DOWEX 50W-X2 was added to the solution. The solution was heated to 30° C and stirred overnight. The deprotection was followed by ^{1}H NMR (disappearance of δ= 1.31 and 1.40 ppm). Since deprotection was incomplete the temperature was increased to 35° C and supplementary DOWEX resin was added. To drive the deprotection to completion the resin was removed by filtration and the solvent evaporated followed by continued deprotection with fresh MeOH (250 ml) and DOWEX resin at 35° C overnight with stirring. The resin was removed by filtration and the solvent evaporated prior to precipitation from THF into cold diethyl ether to yield the product (27.7 g, 92%).

^{1}H NMR (400 MHz, $CDCl_3$): δ= **2.47** (t, J= 2.4 Hz, 2H; Act), **4.17** (t, J= 4.6 Hz, 4H; -OCH_2CH_2OCO-), **4.24** (s, 4H; -CCH_2OCO-) and **4.61** (t, J= 2.3 Hz, 4H; -CH_2CCH) ppm.

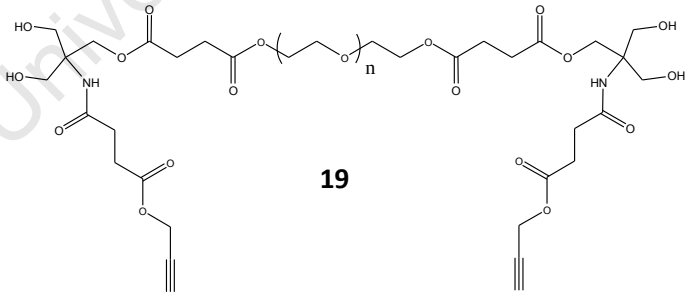

19

Synthesis of PEG-G1-2Act-4Ac (20): Compound **19** (3.8 g, 1.4 mmol OH), TEA (394 µl, 2.8 mmol) and hydroquinone (catalytic amount) were dissolved in DCM (40 ml) and placed on ice while kept in argon atmosphere. AcCl (232 µl, 2.8 mmol) was separately dissolved in DCM (20 ml) and slowly added to the reaction solution from a dripping funnel, the reaction was then left overnight on stirring. The solution was diluted with water and DCM evaporated prior to overnight dialysis (cut off

value ~1 kDa). Insolubilities were removed by filtration and the solution was freeze dried prior to precipitation from THF into cold diethyl ether to yield the product (1.2 g, 31%).

^{1}H NMR (400 MHz, $CDCl_3$): δ= **2.44** (t, J= 2.2 Hz, 2H; Act), **4.46** (d, J= 11.4 Hz, 4H; -CC*H*$_2$OCOCHCH$_2$), **4.56** (d, J= 9.8 Hz, 4H; -CC*H*$_2$OCOCHCH$_2$), **4.67-4.68** (m, 8H; -C*H*$_2$CCH and -CC*H*$_2$OCOCH$_2$CH$_2$-), **5.39** (dd, J= 10.3 and 1.3 Hz, 4H; Ac_{cis}), 6.12 (dd, J= 17.3 and 10.5 Hz, 4H; Ac) and 6.43 (dd, J= 17.2 and 1.3 Hz, 4H; Ac_{Trans}) ppm.

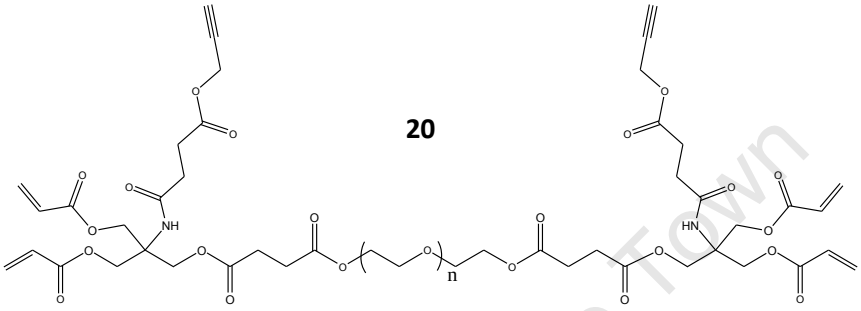

20

Synthesis of PEG-G1-2Dex-4Ac (21): Compound **20** (2.29 g, 420 µmol acetylene groups; Act) and Dex-N_3 (**12**; 268 mg, 504 µmol) were dissolved in THF (55 ml). Sodium ascorbate (166 mg, 838 µmol) and copper sulphate (105 mg, 421 µmol) were dissolved separately in distilled water (1 ml respectively) and added to the reaction mixture. Additional distilled water (1 ml) was added to keep the solution clear. The reaction was followed by ^{1}H NMR (δ =4.67-4.68 ppm) and when compound **20** was consumed the solution was diluted with THF (200 ml) and filtered to remove insolubilities. THF was evaporated and the solution diluted with water prior to freeze drying. The crude product was redissolved in THF (200 ml) and filtered through a column of activated neutral Al_2O_3 to remove the copper. The column was washed with DCM (100 ml) and the combined organic phases were removed by evaporation. The product was further purified by precipitation from THF (35 ml) and DCM (3 ml) into cold diethyl ether (250 ml) to yield the product (1.7 g, 68%).

^{1}H NMR (400 MHz, $CDCl_3$): δ= **5.22** (s, 4H; -NNCC*H*$_2$O-) and **7.65** (s, 2H; -NNC*H*-) ppm.

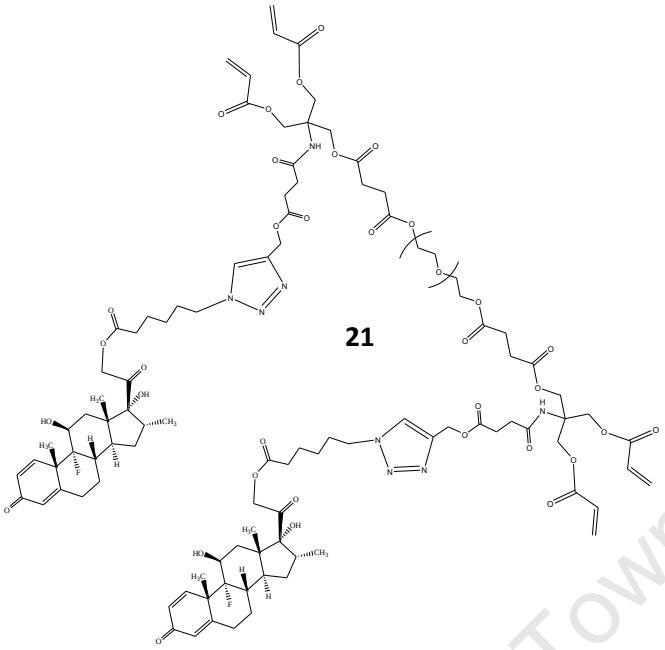

21

2.2.4.4 Preparations of First Generation 4-armed PEG-Dex Conjugate

Synthesis of PEG-4arm-G1-4Act-Acet (22): Star shaped 10PEG-4OH (10.0 g, 4.0 mmol OH), the acetylene monomer anhydride (**16**; 6.9 g, 8.8 mmol), DMAP (98 mg, 0.80 mmol) and pyridine (3.2 ml, 40 mmol) were dissolved in DCM (70 ml) and stirred overnight. The reaction progress was followed by matrix-assisted laser desorption ionisation mass spectroscopy (MALDI) and ^{13}C NMR (δ =168.07 ppm; -*C*OO*C*O-). An additional amount of compound **16** (2 eq/OH) was added after the first night and both compound **16** (2 eq/OH) and DMAP (0.2 eq/OH) were added after the second night. The volume was evaporated and the crude product redissolved in toluene prior to precipitation in cold diethyl ether. The precipitation was repeated once to yield the product (3.5 g, 30%, 91% purity by NMR).

^{1}H NMR (400 MHz, $CDCl_3$): δ= **1.36** (s, 12H; -C*H*$_3$), **1.45** (s, 12H; -C*H*$_3$), **3.73-3.77** (m, 8H; -CC*H*$_2$Acet), **4.24** (d, J= 11.1 Hz, 8H; -CC*H*$_2$Acet), **4.46** (s, 8H; -CC*H*$_2$OCO-) and **4.64** (d, J= 2.4 Hz, (H; -C*H*$_2$Act) ppm. ^{13}C NMR (100.6 MHz, $CDCl_3$): δ= 22.40, 24.40, 24.47, 25.05, 25.36, 28.79, 28.86, 28.94, 51.98, 52.10 52.97, 62.10, 63.89, 68.83, 70.38, 74.94, **98.56** ($(CH_3)_2$*C*OO-), **171.62** (-*C*OO-), **171.72** (-*C*OO-), **172.23** (-*C*OO-) and **172,40** (-*C*ONH-) ppm.

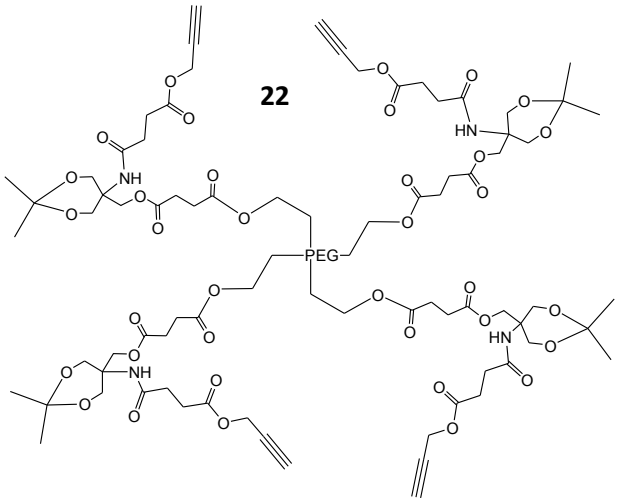

Synthesis of PEG-4arm-G1-4Act-8OH (23): Compound **22** was deprotected according to the same protocol as for compound **18**.

^{13}C NMR (100.6 MHz, $CDCl_3$): δ= 28.79, 28.83, 30.61, 45.17, 51.83, 60.95, 62.19, 62.50, 63.68, 68.62, 69.65, 69.99, 70.21, 70.61, 72.20, 74.98, 77.19, **171.63** (-*C*OO-), **172.03** (-*C*OO-), **172.19** (-*C*OO-) and **172.56** (-*C*ONH-) ppm.

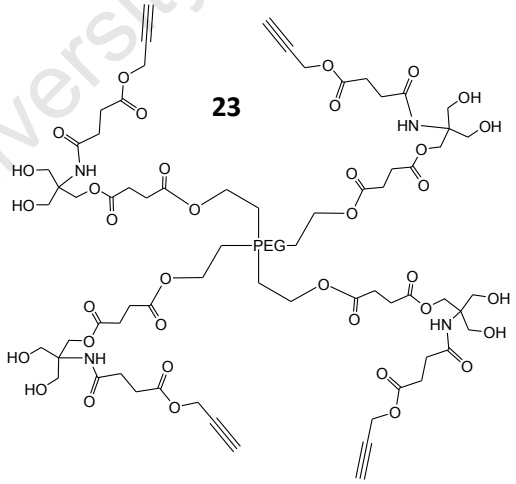

Synthesis of PEG-4arm-G1-4Act-8Ac (24): Compound **23** was acrylated according to the same protocol as for compound **19**.

^{1}H NMR (400 MHz, $CDCl_3$): δ= **4.47** (s, 8H; -CC*H*$_2$OCO-), **4.54** (s, 16H; -CC*H*$_2$OAc), **4.66** (d, J= 2.3 Hz, 8H; -OC*H*$_2$Act), **5.88** (dd, J= 10.3 and 1.3 Hz, 8H; Ac_{Cis}), **6.12** (dd, J= 17.3 and 10.5 Hz, 8H; Ac) and **6.42** (dd, J= 17.4 and 1.1 Hz, 8H; Ac_{Trans}) ppm.

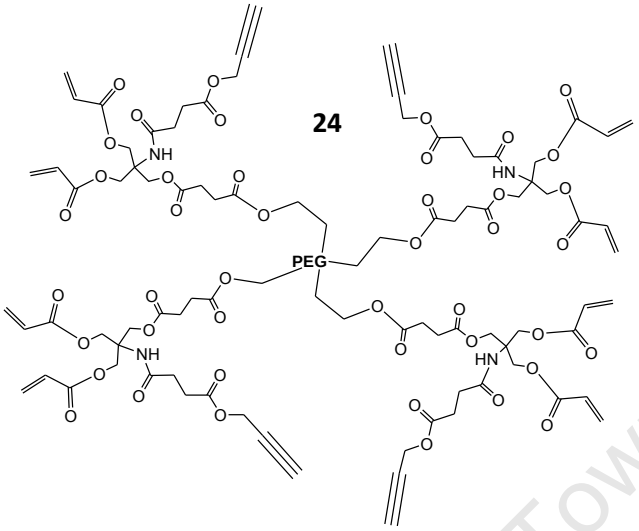

Synthesis of PEG-4arm-G1-4Dex-8Ac (25): Compound **24** (500 mg) was conjugated with Dex-N_3 (**17**) using the same protocol as for compound **20** to yield the product (180 mg, 31%).

^{1}H NMR (400 MHz, $CDCl_3$): δ= **5.21** (s, 8H; -NNCC*H*$_2$-) and **7.64** (s, 4H; -NNC*H*-) ppm.

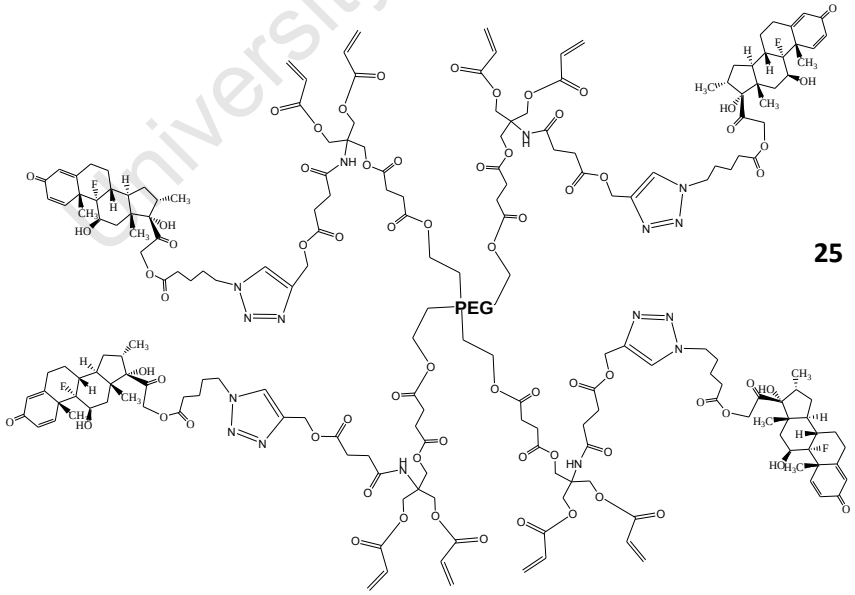

At the time for the volumetric swelling experiment compound **25** had undergone spontaneous crosslinking to some extent. Thus, the compound was redissolved in DCM, filtered and precipitated in ice cold diethyl ether.

2.2.4.5 Preparations of Second Generations Linear PEG-Dex Conjugate

Synthesis of PEG-G2-6Act-Acet (26): PEG-G1-2Act-4OH (**19**; 15.0 g, 5.62 mmol OH), the acetylene monomer anhydride (**16**; 13.2 g, 16.9 mmol), DMAP (137 mg, 1.12 mmol) and pyridine (4.5 ml, 55.8 mmol) were dissolved in DCM (100 ml) and left on stirring overnight. Complete reaction progress was confirmed by ^{13}C NMR (δ= 168.07 ppm). The solvent was evaporated and the crude product redissolved in THF prior to precipitation in cold diethyl ether. The precipitation was repeated once to yield the product (15.8 g, 92%, 86% purity by NMR).

^{1}H NMR (400 MHz, $CDCl_3$): δ= **1.39** (s, 12H; -C*H*$_3$), **1.48** (s, 12H; -C*H*$_3$), **3.78** (d, J= 11.4 Hz, 4H; -CC*H*$_2$OCO...Acet), **4.24** (d, J= 11.6 Hz, 4H; -CC*H*$_2$OCO...Acet), **4.43** (s, 8H; AcetCC*H*$_2$OCO-), **4.48** (s, 16H; -CC*H*$_2$Acet) and **4.68** (d, J= 2.2 Hz, 12H; -OC*H*$_2$Act) ppm. ^{13}C NMR (100.6 MHz, $CDCl_3$): δ= 21.65, 22.19, 24.12, 24.18, 24.76, 28.54, 30.52, 51.69, 52.49, 52.66, 57.49, 61.92, 62.21, 63.24, 68.52, 74.88, 74.94, **98.18** ((CH$_3$)$_2$*C*OO-), **98.25** ((CH$_3$)$_2$*C*OO-), **171.40** (-*C*OO-), **171.55** (-*C*OO-), **171.62** (-*C*OO-), **171.91** (-*C*OO-) and **171.95** (-*C*ONH-) ppm.

26

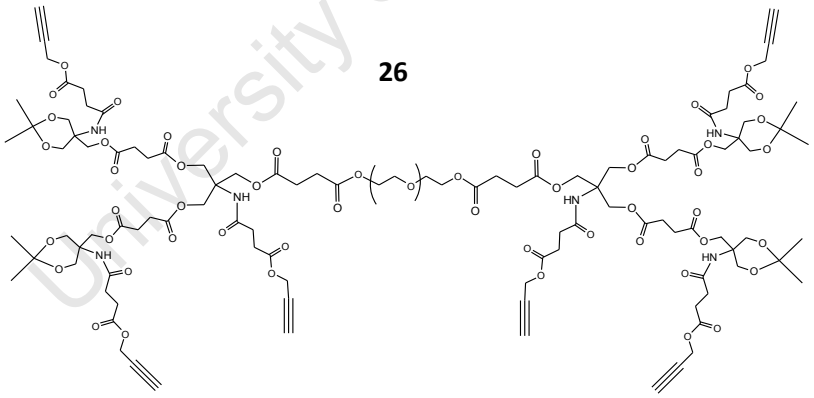

Synthesis of PEG-G2-6Act-8OH (27): Compound **26** (15.4 g) was deprotected following a similar protocol as for compound **18**, with the difference that the deprotection was restarted twice and the temperature was slightly elevated. The reaction mixture was heated to 35° C overnight and increased to 40 ° C for a few hours to ensure full deprotection. Precipitation yielded the product (12.4 g, 82%, ~100% purity by NMR).

^{1}H NMR (400 MHz, $CDCl_3$): δ= **4.29** (s, 8H; -CH_2CCH$_2$OH), **4.40** (s, 4H; -CCH_2OCO...PEG), **4.42** (s, 8H; -CCH_2OCO...OH), **4.67** (d, J= 2.6 Hz, 4H; -OCH_2Act) and **4.68** (d, J= 2.6 Hz, 8H; -OCH_2Act) ppm.

27

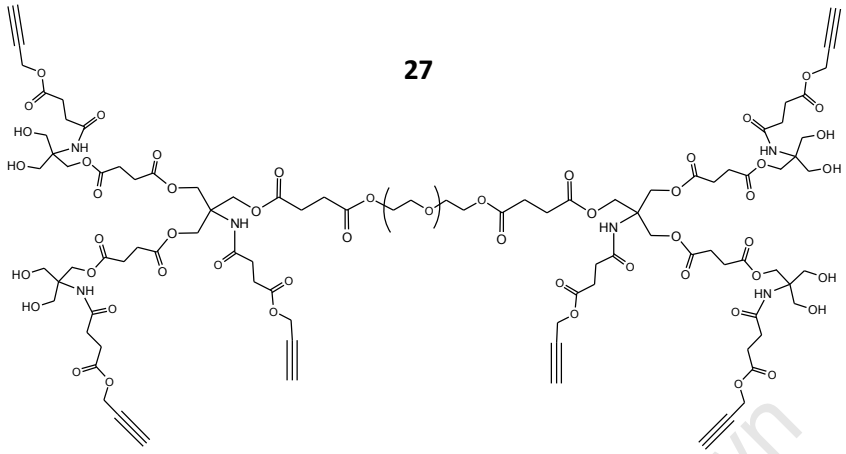

Synthesis of PEG-G2-6Act-8Ac (28): Compound **27** (12.0 g) was acrylated following a similar protocol as for compound **19**, but no precipitation was needed after dialysis to obtain the pure product. (11.1 g, 89%, ~100% purity by NMR)

^{1}H NMR (400 MHz, $CDCl_3$): δ = **4.67** (d, J= 2.3 Hz, 12H; -OCH_2Act), **5.89** (dd, J= 11.0 and 1.1 Hz, 8H; Ac_{Cis}), **6.12** (dd, J= 17.3 and 10.5 Hz, 8H; Ac), **6.26** (s, 2H; -N*H*-), **6.28** (s, 4H; -N*H*-) and **6.43** (dd, J= 17.3 and 1.1 Hz, 8H; Ac_{Trans}) ppm.

28

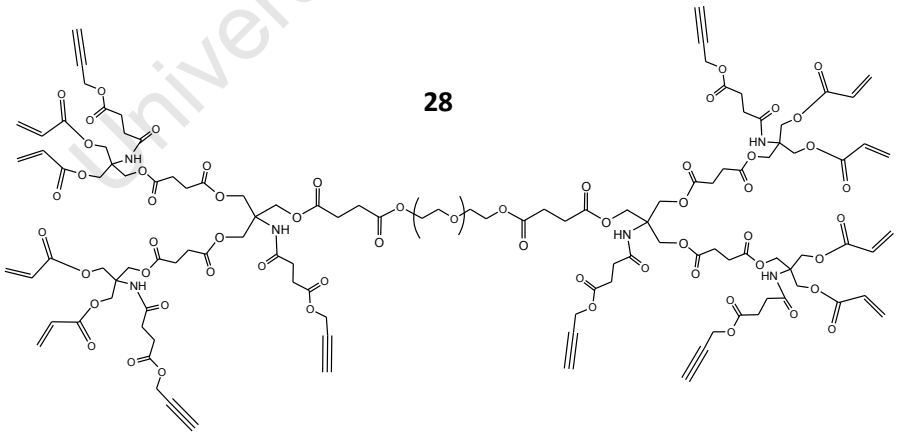

Synthesis of PEG-G2-6Dex-8Ac (29): Compound **28** (2.0 g) was conjugated with Dex-N_3 (**17**) in the presence of hydroquinone (catalytic amount), but otherwise using the same protocol as for compound **20** to yield the product (1.3 g, 52%).

^{1}H NMR (400 MHz, DMSO-d6): δ= **5.52** (dd, J= 62.9 and 3.6 Hz; 12H; -NNCC*H*$_2$O-) and **8.68** (s, 6H; -NNC*H*-) ppm.

29

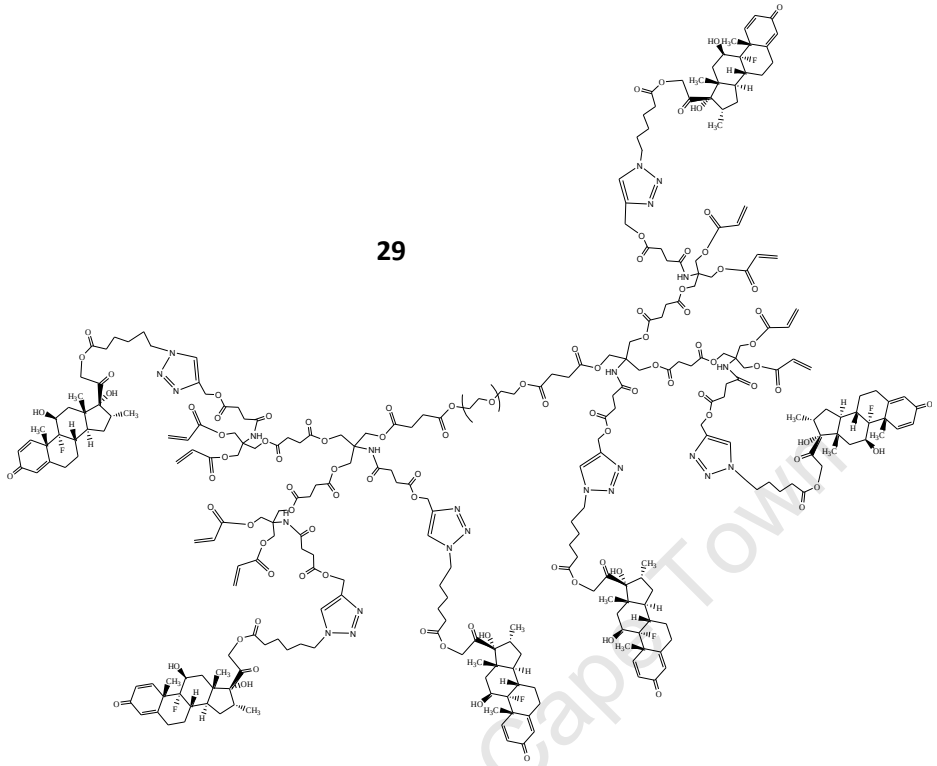

2.3 Atorvastatin

Isolation of Atorvastatin (30): Lipitor tablets (n =20, 1.6 g atorvastatin; At; obtained from Merck) were pulverised and soaked in THF (350 ml) and water (5 ml) overnight prior to Soxhlet extraction (85 cycles). The solvent was evaporated and the crude extract loaded to silica (3 g) by evaporating the solvent from a chloroform mixture of the product and silica. The product/silica mixture was then loaded to a column packed with silica (10 g) in Hex which was washed with an increasing gradient of EtOAc in Hex. Ring closed At eluted at 50% and ring open At at 70%. All fractions containing ring open At (TLC R_f ≈0.7, 100% EtOAc) were pooled and the solvents co-evaporated with chloroform. The product was further dissolved in EtOH (15 ml), filtered and precipitated in cold diethyl ether (150 ml) to yield the product (248 mg, 16%).

ESI-MS of compound **30**: found (calculated, assigned) *m/z*= 559 (559.3, At + H^+), 581 (581.2, At + Na^+), 1118 (1117.5, 2 At + H^+) and 1139 (1139.5, 2At + Na^+).

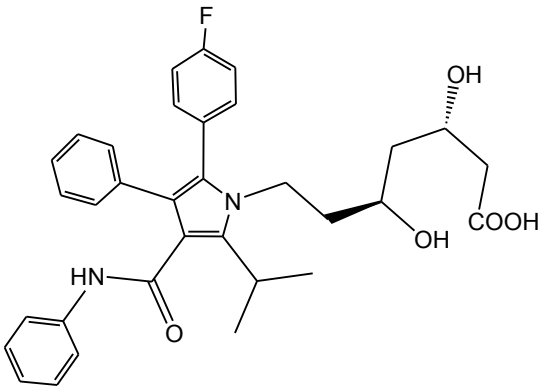

30

Synthesis of AtAc (31): At was acrylated according to the same protocol as for compound **5**.

2.4 General Procedures

2.4.1 Dendritic Synthesis

The assembling of the dendritic structures were based on a previously reported method (Malkoch *et al.* 2006). Only the key ^{1}H NMR shifts are given for the drug conjugate and the dendritic compounds, normally terminal protons for which the shifts were changed during the actual or following reaction. ^{13}C NMR peaks are reported when available.

2.4.2 DOWEX Purification

The DOWEX resin was heated (45 ° C) in MeOH and collected on a filter. This procedure was repeated until the filtrate was colourless.

2.4.3 NMR Analysis

All nuclear magnetic resonance (NMR) spectra were recorded on a Varian spectrometer (300 MHz) except for the dendritic compounds for which a Bruker spectrometer (400 MHz) was used instead.

2.4.4 mHPLC Analysis

RaAc (**5**)**,** RaMonoIAE (**6a**) and RaDiIAE (**6b**) were analysed with high pressure liquid chromatography (HPLC) on an Agilent 1200 series with respect to purity. The samples were loaded (5 µl, 1 mg/ml MeOH), separated into their constituents on a Jupiter C18 column (dimensions: 250 x 4.6 mm, porosity: 300 Å, particle size: 5 µm) from Phenomenex using a linear gradient of MeCN in distilled water (0-100% in 35 min, 0.7 ml/min) and detected with a diode array detector. The data was processed with the "Chemstation for LC 3D systems" software.

2.4.5 MS Analysis

The molecular weights of RaAc (**5**), RaMonoIAE (**6a**) and RaDiIAE (**6b**) were confirmed by mass spectrometry (MS) on a Waters API Q-TOF Ultima mass spectrometer. The samples were dissolved in MeCN, diluted with 50% MeCN in water to 20 µg/ml and introduced (2 µl) to the MS using a Waters UPLC pump at a flow rate of 0.2 ml/min in a mixture of MeCN and 0.1% formic acid (80:20). The samples were ionised by electro spray ionisation (Baeyens *et al.*) in the positive mode (capillary voltage: 3.5 kV, cone voltage: 35, RF1: 40, source temperature: 100 °C, desolvation temperature: 350 °C, desolvation gas flow: 350 l/h and cone gas flow: 50 l/h). Data was acquired at a mass/charge window of 300-1500 and processed with the "Masslynx 4.1" software. Only peaks with an intensity of 1% or more of the respective main peaks are reported except for Ra for which all peaks are reported.

The amount of mono-, di- and tri-substitution of compound **5** was quantified by separating the crude reaction mixtures on an Xbridge C18 column (dimensions: 50 x 2.1 mm, Waters) in line with the ESI-MS system. The substituted compounds were washed out from the column by an increasing gradient of MeCN in 0.1% formic acid (20-100% in 12 min, 0.35 ml/min), quantified by UV absorption at 280 nm and assigned by ESI-MS.

2.4.6 MALDI Analysis

Matrix-assisted laser desorption ionisation time-of-flight mass spectroscopy (MALDI) was initially used to identify drug-PEG conjugates. The analyses were performed on a Voyager DE PRO mass spectrometer fitted with delayed extraction (PerSeptive Biosystems) and operated by the PerSeptive Biosystems Time-of-Flight Mass spectrometer software (version 4.51). Samples were dissolved in MeOH (10 mg/ml) and mixed in a 1:1 ratio with a freshly prepared matrix solution (α-Cyano-4-hydroxycinnamic acid, 10 mg/ml in 50% MeCN and 50% H_2O), 1µl was then applied to the plate which were inserted into the instrument and analysed in the linear mode. The obtained data were processed with PerSeptive GRAMS/32 software (version 4.14).

2.4.7 Phosphate Buffered Saline

Two different buffers were used throughout the gel work, both with a molarity of 150 mM and iso-osmotic with blood. Phosphate buffered saline formula 1 (PBS-1) was used as supernatant during the swelling and drug elution experiments and phosphate buffered saline formula 2 (PBS-2), which has a higher buffering capacity than PBS-1, was used as solvent during gelling through conjugate addition.

PBS-1 was prepared by dissolving disodium hydrogen phosphate ($Na_2HPO_4 \cdot 12H_2O$, 2.89 g, 8.1 mmol), potassium dihydrogen phosphate (KH_2PO_4, 0.20 g, 1.5 mmol), potassium chloride (KCl, 0.20 g, 2.7 mmol) and sodium chloride (NaCl, 8.0 g, 136.9 mmol) in deionised water (1.00 l).

PBS-2 was prepared by mixing solution A (65 ml), solution B (435 ml) and solution C (500 ml). Solution A: sodium dihydrogen phosphate ($NaH_2PO_4 \cdot 2H_2O$, 2.34 g, 15.0 mmol, 100 ml). Solution B: disodium hydrogen phosphate (Na_2HPO_4, 10.65 g, 75.0 mmol, 500ml). Solution C: sodium chloride (NaCl, 4.5 g, 77.0 mmol, 500 ml). All solutions were made in deionised water.

2.4.8 Gel Formation

The synthetic approaches were divided into categories referring to the main structure of the involved compounds. The categories (main structure) are; **RaX-d4** (RaAc/IAE, 4-armed PEG carrier), **RaX-d2** (RaAc/IAE, 2-armed PEG carrier), **RaDiIAE** (RaDiIAE, no carrier), **G1** (first generation, 2-armed backbone), **4arm** (first generation, 4-armed backbone) and **G2** (second generation, 2-armed backbone).

The elution experiments included three gel formulations; "**Bound**" gels made by crosslinking compounds containing covalently attached drug, "**Trapped**" gels made by crosslinking the corresponding drug deficient compounds in the presence of free drug (equivalent to the amount in the corresponding "Bound" formulation) captured within the gel network and "**Blank**" gels made by crosslinking the corresponding drug deficient compounds.

The multi-arm building blocks for the RaX-d4 and RaX-d2 categories were dissolved at a nominal concentration of 200 mg/ml and the following addition of crosslinker and RaPEG conjugate diluted these solutions to different degrees.

The concentrations of building blocks for the G1, 4arm and G2 categories were obtained by considering solubility, amount of initiator, irradiation time and comparability between the gel categories.

2.4.8.1 Photo-Polymerisation

20PEG-8Ac (**1**; 65.3 mg) was dissolved in PBS-2 (170 µl), followed by addition of Ra (170 µl of 2.8 mg in 170 µl EtOH) and 2,2-dimethoxy-2-phenylacetophenone (DMPA; 29 µl of 4.7 mg in 2.0 ml *N*-vinylpyrrolidone; NVP; 1 mol% DMPA and 1000 mol% NVP regarding Ac groups). Gels (100 µl, n =3) were formed from the pregel solution at a final concentration of 18% (mass of solids over added volume of PBS-2) and gelling occurred when irradiated by UV light (mercury lamp, 100 W) at a distance of 15 cm for 6 minutes.

Control gels were made by UV irradiation of; **1** (20%), a mixture of **1** and DMPA (1 mol%) or a solution DMPA in NVP (2.4 mg/ml).

2.4.8.2 Mono-functional Approach, RaMonoX Method 1

The multi-acrylate compound 20PEG-8Ac (**1**) was dissolved (200 mg/ml PBS-2) and individual PBS-2 solutions of the crosslinker compound 10dPEG-4SH (**4**; 7 SH/10 Ac) and either RaAc-dPEG-3SH (**7**) or RaIAE-dPEG-3SH (**8**) were added at a loading density of 1 Ra/10 Ac**.** For "Trapped" gels a Ra solution (1 Ra/10 Ac, 20 µl EtOH) replaced the solutions of **7** and **8**. The "Blank" gels were made of compound **1** and **4** only (stoichiometric relation). Gels (50 µl each, n =3) were formed from the pregel solutions at a final concentration of 20-22% (mass of solids per added volume of PBS-2) and gelling occurred during 45 minutes incubation (37° C, 100% relative humidity).

2.4.8.3 Mono-functional Approach, RaMonoX Method 2

The multi-vinyl sulphone compound 20PEG-8VS (**2**) was dissolved (200 mg/ml PBS-2) and solutions of either RaAc-dPEG-SH (**9**; 20 µl PBS-2) or RaIAE-dPEG-SH (**10**; 20 µl PBS-2) were added at a loading density of 1 Ra/10 VS**.** The mixtures were incubated (37° C) for 20 minutes in closed containers prior to addition of the 2dPEG-2SH crosslinker compound (**3**; 9 SH/10 VS, 82 mg/ ml PBS-2). For "Trapped" gels a Ra solution (1 Ra/10 VS, 20 µl EtOH) replaced the solutions of **9** and **10** and also the "Trapped" pregel mixtures were incubated (37° C) for 20 minutes in closed containers prior to addition of the 2dPEG-2SH crosslinker compound (**3**; stoichiometric ratio, 80 mg/ ml PBS-2). "Blank" gels were made of compound **2** and **3** only (stoichiometric ratio, PBS-2). Gels (100 µl each, n =3) were formed from the pregel solutions at a final concentration of 13-14% (mass of solids per added volume of PBS-2) and gelling occurred during 40 minutes incubation (37° C, 100% relative humidity).

2.4.8.4 Mono-functional Approach, RaDiIAE

Ra-diIAE (**6b**; 6.9 mg, 11.0 µmol IAE) was dissolved in MeCN (140 µl) and a solution of 10dPEG-4SH (**4**; 400 mg/ml 0.1 M $NaHCO_3$, 70 µl, 11.0 µmol SH) was added. Gels (50 µl each, n =3) were formed from the pregel solution in sealed containers at a final concentration of 17% (weight of solids over volume) and gelling occurred during 18 hours incubation (37° C).

2.4.8.5 Dendritic Approach, Conjugate Addition

PEG-G1-2Act-4Ac (**20**) or PEG-G1-2Dex-4Ac (**21**) were individually dissolved in PBS-2 and mixed with a PBS-2 solution of the crosslinker compound 10nPEG-4SH (stoichiometric ratio of thiol to Ac groups). For gels containing trapped Dex a solution (20 µl THF) of the unmodified drug (equivalent to the amount of covalently incorporated drug) replaced **21**. Gels (50 µl each, n =3) were formed from the pregel solutions at a final concentration of 19% (weight of solids over added volume of PBS-2) and gelling occurred during 20 minutes in an incubator (37° C, 100% relative humidity).

2.4.8.6 Dendritic Approach, Thiol-ene Addition

PEG-G1-2Act-4Ac (**20**), PEG-G1-2Dex-4Ac (**21**), PEG-4arm-G1-4Act-8Ac (**24**), PEG-4arm-G1-4Dex-8Ac (**25**), PEG-G2-6Act-8Ac (**28**) or PEG-G2-6Dex-8Ac (**29**) were individually dissolved by addition of separate THF solutions of the photo initiator Irgacure 2959 (5 or 10 mol% of the Ac groups) and the crosslinker compounds 2dPEG-2SH (**3**) or 10nPEG-4SH (stoichiometric ratio of thiol to Ac groups). For gels containing trapped Dex an additional THF solution (20 µl) of the unmodified drug (equivalent to the amount of covalently incorporated drug) was also added. Gels (15-25 µl each, n =3) were formed from the pregel solution at a final concentration of 38-69% (weight of solids over added volume of THF) and gelling occurred when irradiated by UV (ultraviolet) light (mercury lamp, 100 Watt) at a distance of 15 cm for 2 minutes.

A side effect of the UV irradiation was a substantial evaporation of solvent as noticed by low gel weights (W_{Gel}), which in turn resulted in increased swelling ratios ($W_{Swollen}/W_{Gel}$) compared to the conjugate addition gels. To minimise the evaporation effect the irradiation time was kept short. But, by decreasing the irradiation time the concentration of pregel compounds and initiator must be increased.

The protocol was developed by carefully balancing the needs of a short irradiation time with the demands of a low concentration of both pregel compounds (similar to the conjugate addition gels) and initiator. Thus, the concentrations of building blocks were not equal for the three dendritic categories (38, 69 or 50% respectively) which are higher than for the mono-functional approach (20%).

2.4.9 Drug Elution

The formed gels (n= 3) were weighed, individually immersed in PBS-1 (2 ml, pH 7.4) and placed in an incubator (37° C) for swelling and drug elution. At regular intervals the supernatant was replaced by fresh buffer and at the same time the swollen gels were carefully blotted and weighed. The collected supernatant was diluted with EtOH (1:1), the absorbance (λ_{Ra}= 279 nm and λ_{Dex}= 241 nm) read in a spectrophotometer and the amount of released drug calculated using a standard curve made from serial dilutions of a PBS-1/EtOH (1:1) solution of respective drug. Supernatant from the "Blank" gels (n =3, pooled) were used as background readings for every drug eluting experiment except for gels made from RaDilAE where a mixture of PBS-1 in EtOH (50%) was used instead.

The gel end points were considered to be reached when supernatant could no longer be replaced because of a too substantial degradation. The remaining amount of covalently attached drug was forced to be released by treating the gels with NaOH (1 ml, 1 M).

The theoretical drug content (mg /g gel), for the different gel formulations, was calculated using the weighed amount of drug-carrier conjugate compound, the molecular weight of the drug in relation to the drug-carrier conjugate compound and the measured volumes in each step of the mixing procedure. The calculated amount (mg drug/gel) was subsequently divided by the measured gel weight (average of 3; before swelling) of respective formulation.

2.4.10 Determination of pH dependence of gel formation

Gels (n =1) were made by crosslinking 20PEG-8Ac (**1**; 200 mg/ml) with 2nPEG-2SH in a Ac:SH ratio of 1:1 at a final concentration of 10% in PBS-2 of different pH (adjusted with dilute hydrochloric acid). Gelling was assessed to occur when the gel solutions were sufficiently solidified to be removed in one piece from the support.

2.4.11 Curve Fitting

The curve fitting application in Excel (Microsoft Office) was used to fit linear curves to the obtained elution data, either directly or after processing the data with any of the following equations. Neither the origin nor data after forced release with NaOH were used for the calculations and the Y-axis intersection of the fitted curves was not guided through zero.

To assign degradation as the primary release mechanism the Hixson-Crowell (Shoaib *et al.* 2006) equation was used (**Equation 2**).

$$\sqrt[3]{Q_0} - \sqrt[3]{Q_t} = k_{HC}t \qquad (\mathbf{2})$$

The rate constant for the Hixson-Crowell rate equation is described by k_{HC}. To differentiate between diffusion and swelling as the primary release mechanism the Korsmeyer-Peppas equation (Siepmann *et al.* 2001; Shoaib *et al.* 2006) was used (**Equation 3**).

$$\frac{Q_t}{Q_0} = kt^n \qquad (\mathbf{3})$$

The structural/geometric constant for a particular system is described by *k* and *n* is the release exponent. The experimentally obtained *n*-value is characteristic for the release mechanism and for a cylindrical drug eluting matrix an obtained value of (describes the release by); *n* =0.45 (diffusion), 0.45 < n < 0.89 (a mixture of diffusion and swelling), n =0.89 (swelling).

Zero order release was confirmed by fitting obtained data to the zero order rate equation (**Equation 4**).

$$Q_{rem} = k_0 t \qquad (4)$$

Q_{rem} is the remaining release at time *t* and k_0 is the zero order rate constant expressed in units of cumulated release per time. First order release was confirmed by fitting obtained data to the first order rate equation (**Equation 5**).

$$\ln Q_{rem} = \ln Q_0 - k_1 t \qquad (5)$$

Q_0 is the total cumulated amount of released drug and k_1 is the first order rate constant. In case exponential release was obtained an online curve fitting programme was used to find a proper equation for the profile (www.ZunZun.com).

The following plots were made for the "Trapped" formulations (to establish the release mechanism); cube root of normalised remaining amount of drug versus elution time (degradation controlled release), logarithm of normalised cumulated release versus logarithm of elution time (diffusion or swelling controlled release) and natural logarithm of normalised remaining amount of drug versus elution time (first order release and k_1). To calculate elution curves with first order release kinetics a modified version of **Equation 5** was used (**Equation 5b**).

$$Q_{rel} = Q_0(1 - e^{-k_1 t}) \qquad (5b)$$

The following plots were made for the "Bound" formulations (to establish the release mechanism); cumulated release versus elution time (zero order release) and natural logarithm of normalised remaining amount of drug versus elution time (first order release).

The fraction of the total squared error (commonly known as the R^2-value) was used to determine whether the applied curve fittings were significant or not and for a R^2 >0.95 an applied curve was considered significant. In contrast, if none of the applied curves fitted, the elution was considered to be of burst character.

2.4.12 Swelling

The swelling ratio Q for a hydrogel is normally defined as $V_{swollen}/V_{dried}$ but in this work it was decided for several reasons to mainly use a mass and wet gel based swelling ratio instead ($W_{swollen}/W_{gelled}$).

The primary reason to use the mass instead of the volume is because it is possible to follow the swelling trend for a longer period of time by weighing the gels in air only, since this is still possible when a gel is too degraded to be weighed in EtOH, which is necessary to establish $V_{swollen}$. Additionally, since the gels contain > 90% water their mass and volume are nearly identical (not shown).

The reason for using the mass of formed gels, instead of dried gels, as the denominator has a practical background, since it mirrors the degree of swelling compared to the formed gel and not to its dry content, which is an important parameter for *in vivo* applications. Additionally, weighing the same gels repeatedly instead of drying three gels for each data point, which is needed to calculate the volume, is an efficient way to economise a limited amount of material.

2.4.13 Volume Determination

In order to further calculate crosslink densities the volume of a limited number of gels were also measured.

Gels (n= 2 or 3 for each data point) were formed, immersed in buffer and placed in an incubator in the same manner as for the drug elution experiments describe above. At the same time points as for the respective drug elution experiment (including day 0) the supernatant was either changed or the gels were weighed both in air and EtOH, dried (60° C) overnight and then weighed in air and EtOH again. The volume of the just gelled (V_g), swollen (V_s) and dried (V_d) gels was calculated from the respective mass according to **Equation 6** and further used for the calculations of crosslink densities.

$$V = \frac{W_{air} - W_{EtOH}}{\rho_{EtOH}} \qquad (6)$$

Owing to limited resources of the dendritic compounds volumetric swelling of the G1 category was omitted and only duplicates were made for the 4arm and G2 categories.

2.4.13.1 Calculation of Crosslink Density

Equation 7 was used to calculate average molecular mass between crosslinks, M_c (Andreopoulos *et al.* 1998).

$$\frac{1}{M_c} = \frac{2}{M_n} - \frac{\bar{u}/V_1\left(\ln\left(1-u_{2,s}\right)+u_{2,s}+\chi u_{2,s}^2\right)}{u_{2,r}\left(\sqrt[3]{\left(u_{2,s}/u_{2,r}\right)}-\frac{1}{2}\left(u_{2,s}/u_{2,r}\right)\right)} \qquad (7)$$

The swelling data is represented by the $u_{2,s}$ and $u_{2,r}$ variables, which are the averaged volumetric ratios of dry gels over swollen and just gelled gels respectively. The constants are; M_n the molecular mass of the PEG building block, $\bar{u}$ (0.861 ml/g) the specific volume of the PEG building block before crosslinking, V_1 (18.1 ml/mol) the molar volume of water and χ (0.426) the polymer-solvent interaction parameter for a PEG-water system.

Equation 8 was used to calculate the average mesh size, ζ (Å), for the swollen hydrogels. The constants are; C_n (4.0) the characteristic ratio of PEG and l (1.48 Å) the bond length of the gel's polymeric backbone.

$$\zeta = \alpha_s l\sqrt{C_n n} \qquad (8)$$

The experimental data is represented by α_s and was calculated according to **Equation 9**. The number of bonds between two crosslinks n was calculated according to **Equation 10** where M_c is the previously calculated average molecular weight between crosslinks and M_r (44 g/mol) is the molecular mass of the repeating unit of PEG.

$$\alpha_s = \frac{1}{\sqrt[3]{u_{2,s}}} \qquad (9) \qquad\qquad n = \frac{3\overline{M}_c}{M_r} \qquad (10)$$

Equation 3 and **4** involve several system specific constants which are experimentally and computationally obtained. For the calculations presented here the specific volume of the pregel compounds were roughly assumed to be equal to unmodified PEG and the polymer-solvent interaction was assumed to be equal to a PEG-water system. These estimations are particularly coarse for the dendritic compounds, therefore the crosslink densities for the dendritic gels are

presented as relative mesh sizes where the mesh size for swollen gels are normalised by the value of respective gel prior swelling. The compounds in the mono-functional approach, however, predominantly consist of the PEG carrier (> 90% by mass) and therefore the actual mesh sizes are shown in this case.

2.4.14 Reporter Assays

The activity of released drugs were determined via cell treatments and quantified by pre-fabricated reporter assay kits resulting in luciferase mediated luminescence, which was measured on a Veritas Microplate Luminometer (Turner Biosystems) using the Veritas software (version 2.0.5101).

2.4.14.1 Rapamycin

The protocol for Ra treatment of cells was adopted from a previously reported method (Yallapu *et al.* 2008) and was implemented as follows:

Human aortic smooth muscle cells (Passage 3) were seeded in a clear 96-well plate with 10^4 cells per well in 100 µl sodium bicarbonate buffered MCDB medium with 10% fetal calf serum and left to attach for 6 hours at 37° C in a humidified atmosphere with 5% CO_2. The medium was then replaced by 100 µl of sterile filtered medium-based treatment solutions containing either gel supernatant (10% v/v) or Ra (1-2000 µg/l). The Ra solutions were made from serial dilutions with medium of a stock solution (20 mg Ra/ml MeOH). All treatment solutions had a final concentration of 10% v/v PBS-1 and 0.01% v/v MeOH. Cell deficient wells (*Empty*) were given the same treatment as cell containing wells (*Cell*) and were used as background readings for the calculations in **Equation 11**. On second day and every alternate day the medium was replaced by fresh medium without further addition of treatment.

Inhibition of cell proliferation was monitored on the 8th day by leaving the plate reach room temperature and adding a cell viability reagent (Promega, CellTiter Glo) that induces luminescence proportional to the amount of living cells. The assay reagent (100 µl) was added to each well, incubated (15 min, T_{room}) with shaking at regular intervals (1 min at t= 0, 5, 10 min) and placed in the luminometer (1 sec reading/well) where the luminescence was measured.

$$\%Growth = \frac{Cell - Empty_{Average}}{\left(Cell_{Sham} - Empty_{Sham,Average}\right)_{Average}} \qquad (11)$$

The reduced cell proliferation resulting from Ra treatment is presented in terms of percent cell growth where the background luminescence for all treatments was subtracted prior to normalisation by a sham treatment only containing media and solvent (**Equation 11**).

2.4.14.2 Dexamethasone

The protocol for determination of Dex activity in gel supernatants was adopted from a previously reported method (Wilson *et al.* 2002). The method is based on using a breast cancer cell line which is genetically transformed to induce luciferase expression upon binding of glucocorticoid receptor agonists, such as Dex and was implemented as follows:

MDA-kb2 cells (Passage 3) were seeded in a white 96-well plate with 10^4 cells per well in 100 µl Leibovitz L-15 Hepes buffered medium with 10% fetal calf serum and left to attach for 6 hours at 37° C in a humidified atmosphere. The medium was then replaced by 100 µl of sterile filtered treatment solution consisting of 1 ml buffer/medium/serum mixture plus 1 µl of either Dex containing PBS-1 supernatant, Dex dissolved in EtOH or pure solvent (PBS-1 or EtOH) and incubated at 37° C for 24 hours. Cell deficient wells (*Empty*) were given the same treatment as cell containing wells (*Cell*) and were used as background readings for the calculations in **Equation 12**. The plate was left to reach room temperature and treated with a luciferase reagent (100 µl/well; Promega), shaken (10 seconds) and immediately placed in the luminometer (1 sec reading/well) where the luminescence was measured.

$$FI = \frac{Cell - Empty_{Average}}{\left(Cell_{Sham} - Empty_{Sham,Average}\right)_{Average}} \qquad (\mathbf{12})$$

The Dex induced luciferase expression is presented in terms of fold induction (FI) where the background luminescence for all treatments was subtracted prior to normalisation by a sham treatment containing only media and solvent (**Equation 12**).

3 RESULTS and DISCUSSION

The main goal of the work in this thesis was to obtain tailored and sustained drug delivery systems. To achieve such systems both mono- and di-functional PEG based approaches were embraced and developed. The synthesised compounds were used to form hydrogels, using either conjugate or thiol-ene addition, which were further evaluated with respect to their drug elution profile, swelling ratio and degradation rate.

Ultimately, the aim is to use these hydrogel systems to improve post MI recovery by injecting the gels into the affected myocardium. The beneficial effect of such injection has previously been proved by our group (Dobner *et al.* 2009; Kadner *et al.* 2012) and is reviewed by Nelson *et al.* 2011). Furthermore, the aim with these gels is to represent a foundation for the further development of coatings to improve patency and to decrease restenosis of vascular grafts and stents.

However, the focus in this thesis was to develop the chemistries for hydrogel platforms, from which the abovementioned aims can be achieved. Therefore, the evaluation of drug elution kinetics was limited to *in vitro* methods in PBS, which are previously well documented, as well as generally accepted in the literature as initial experiments prior evaluation in serum and *in vivo (Alexis et al. 2004; Nuttelman et al. 2006; Wang, X. et al. 2006; Ito et al. 2007; Jo et al. 2009; LU et al. 2011)*.

The following results are presented together with relevant discussion, starting from the synthetic work and followed by gel formation and the characterisation thereof.

3.1 Synthesis of Gel Building Blocks

The synthesis of gel building blocks was the part of the thesis that presented the most opportunities for problem solving and also provided the most opportunities to develop new hydrogel concepts as presented here.

3.1.1 Multi-arms

The PEG acrylate multi-arm (20PEG-8Ac; **1**) was obtained as a white powder in good yields (68%), which was slightly lower then previously reported (86%) by (Elbert *et al.* 2001). The lower yields are explained by a more extensive purification protocol compared to Elbert *et al.* (3 subsequent precipitations plus dialysis compared to only one precipitation step). The purity of **1** was determined

by NMR and a high degree of Ac substitution was also confirmed by a gelling test with a 2-armed crosslinker where the gel point was reached within 5 minutes.

The PEG vinyl sulphone multi-arm (20PEG-8VS; **2**) was obtained in a low yield (32%) compared to previous reports (65%) by (Dobner *et al.* 2009), probably as a result of spontaneous crosslinking of the vinyl sulphone groups. The formation of solids during synthesis supports this assumption. A possible explanation for the occurrence of spontaneous crosslinking of αβ-unsaturated double bonds in the synthesis of **2** but not for **1** could be the different polymer concentrations in the reaction medium. The concentrations during synthesis of **2** and **1** were 40 and 17 mg/ml respectively.

3.1.2 Crosslinkers

In this work two different crosslinkers were used, one with built-in hydrolytic degradability (dPEG-SH) and the other without (nPEG-SH). The dPEG-SH crosslinkers were readily synthesised in one step and good yields were obtained (~90%) in the same range as previously reported (Nie *et al.* 2007). Their built-in degradability was verified by the degradation of gels formed with non-degradable crosslinks (**Figure 14**).

Gels were formed by crosslinking 20PEG-8VS with either dPEG-SH or nPEG-SH (**Figure 14,** green plots). The former combination was too disintegrated for further measurements on day 18 while the latter showed no visible degradation by day 20, as assessed by a non-significant increase in post equilibrium swelling (23 ±3 to 26 ±1) and mesh size (156 ±15 to 169 ±8 Å). Since previous experiments in our laboratory (not shown), for gels made with the PEG-VS + nPEG-SH combination, did not indicate degradation while incubated for more than a year it was decided to only measure the corresponding gel formulation in this experiment for a similar period of time as the PEG-VS + dPEG-SH combination.

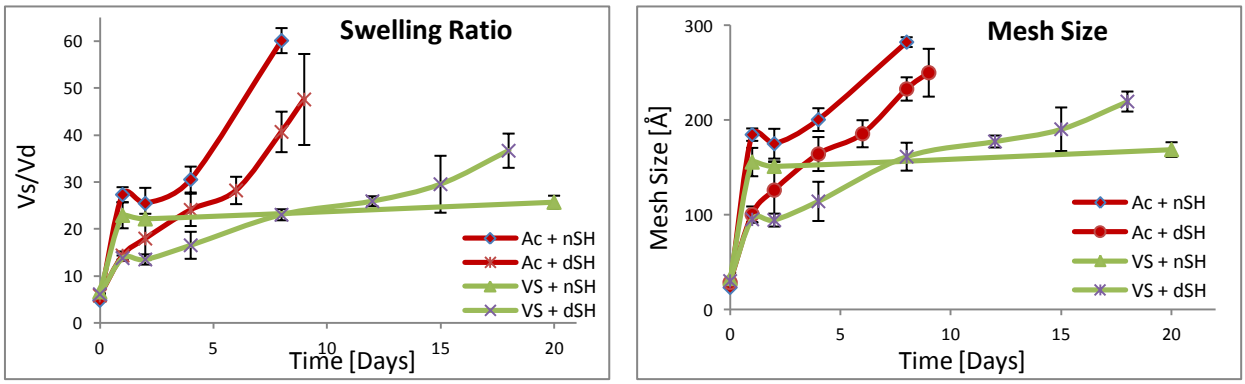

Figure 14: Swelling ratio and mesh size for gels formed by crosslinking either 20PEG-8Ac (**1**) or 20PEG-8VS (**2**) with 2dPEG-2SH or 2nPEG-2SH respectively.

Observed degradation of gels made from crosslinking 20PEG-8VS with either dPEG-SH or nPEG-SH followed the expected trend since the former crosslinker introduces hydrolytically degradable thio-ether weakened ester linkages while the latter does not (**Figure 15**).

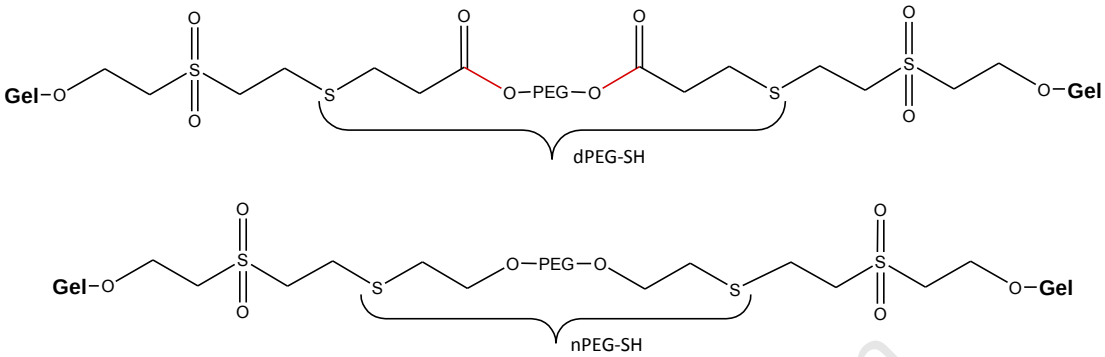

Figure 15: Gel-Gel crosslinks formed by reacting PEG-VS and dPEG-2SH or nPEG-2SH, respectively, red bonds are hydrolytically labile.

When considering the gels made from crosslinking 20PEG-8Ac with either dPEG-SH or nPEG-SH (**Figure 14**, red plots) it was observed that the two gel formulations degraded within a similar time period (9 and 8 days, respectively). This observation is not in line with the expected outcome since the former crosslink contain four weakened esters while the latter contains only two (**Figure 16**). Therefore the nPEG-SH crosslinked gels should last longer than gels crosslinked by dPEG-SH. The discrepancy could however be explained by the equilibrium swelling in **Figure 14**.

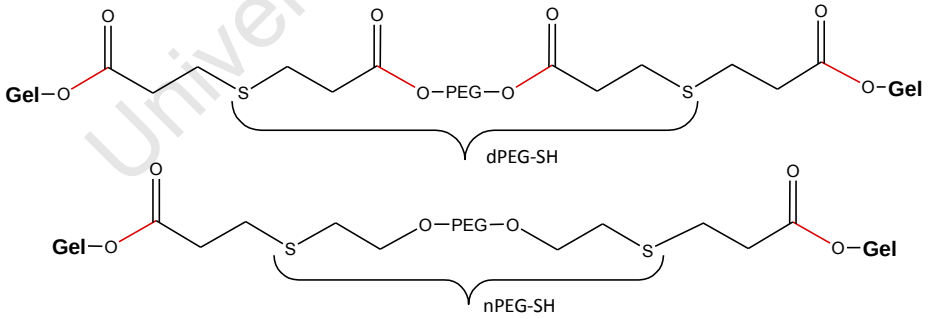

Figure 16: Gel-Gel crosslinks formed by reacting PEG-Ac and dPEG-2SH or nPEG-2SH, respectively, red bonds are hydrolytically labile.

For both multi-arms the gel formulations crosslinked by nPEG-SH displayed a much higher level of equilibrium swelling than the respective gels crosslinked by dPEG-SH. In theory the crosslink density, and hence the equilibrium swelling, should be similar for the two systems. The unexpected and elevated equilibrium swelling of gels crosslinked by nPEG-2SH may be explained by a low degree of thiol substitution of this compound. Such HO-PEG-SH impurity would consume crosslinking sites of

the multi-arms, but without forming crosslinks. The presence of a considerable amount of this impurity was confirmed by ^{13}C NMR (not shown) and a decreased crosslink density was verified by the calculated mesh sizes in **Figure 14**.

3.1.3 Mono-functional Approach

The mono-functional approach is a two-step method, which resulted in rapamycin (Ra) covalently pending from the hydrogel network. The method is referred to as "mono-functional" since one thiol of the dPEG-4SH or dPEG-2SH crosslinkers, which were used as drug carriers, was conjugated to Ra and the remaining thiols/thiol were used for gel incorporation. Thus, the same type of functionality was used for two purposes.

The method development of the mono-functional approach includes valuable problem solving, therefore a summary is given. However, the summary is placed after the method presentation since the chemistry used during the problem solving is explained here.

In the first step Ra was substituted with either Ac or IAE functionality in order to be susceptible to conjugate addition or nucleophilic substitution by the drug carrier. The hydroxyl groups of Ra were targeted for addition of these functional groups, but since there are three hydroxyl groups there is a possibility of several product combinations. Three of these combinations (mono-, di- and tri-substituted Ra) were identified by TLC and liquid chromatography in combination with ESI-MS. In **Table 2** the resulting substitution patterns from the reaction of Ra and 2, 4 or 6 equivalents of AcCl are shown.

Table 2: Product compositions of crude RaAc products after reacting Ra and increasing equivalents of acryloyl chloride. Amounts are given in per cent. For the lowest excess of AcCl di- and tri-substitutions were not detected (n.d.).

	Conversion	**Mono-substitution**	**Di-substitution**	**Tri-substitution**
2 eq	54	~100	n.d	n.d
4 eq	100	18	67	15
6 eq	100	10	38	53

Using 2 equivalents of AcCl resulted in nearly 100% mono-substitution but the conversion was low (54%). Therefore the use of 4 and 6 equivalents were also investigated, resulting in complete conversions but also an increased amount of di- and tri-substitution. However, it was observed that the acrylation reactions were not very repeatable in terms of substitution degrees, possibly because of the rapid and exothermic reaction between TEA and AcCl, which forms an insoluble yellow

precipitate. The formation of this precipitate was dependent on the addition method of AcCl, therefore AcCl was added drop wise in portions of two equivalents from a dilute solution until Ra was consumed, as verified by TLC.

The consumption of reagents, by forming the precipitate, is believed to be the main reason for the need to use more than one eq of AcCl to form RaMonoAc. Another possible reason could be that the reaction conditions were not completely dry which results in the hydrolysis of AcCl.

Mono- and di-substitution was also observed while synthesising Ra-IAE, but tri-substitution was never detected. The absence of tri-substitution is believed to originate from the substitution method since the carbodiimide coupling reagent is not as susceptible to nucleophilic attacks as the acid chloride used for acrylation is. Hence, the sterically hindered hydroxyl group on position 10 is not reactive towards carbodiimide coupling.

According to the literature the group at position 40 (numbered positions are found in **Scheme 10**) is the most reactive, followed by the groups at position 28 and 10, respectively (Plattsburgh *et al.* 1998). This is in agreement with expectations since the hydroxyl group at position 40 is least sterically hindered and the group at position 10 the most.

In order to simplify the following synthesis steps and their analysis the mono-substituted products, RaMonoAc (**5**) and RaMonoIAE (**6a**), were isolated at high purity (100% for both derivatives) but moderate yields (35% for **5** and 65% for **6a**). The yield of **6a**, however, was superior than previously reported (57%) by (Lee *et al.* 1998). The purity of **5** and **6a** were confirmed by reversed phase HPLC analysis that showed only one signal peak for each compound (40.95 min for **5** and 41.07 for **6a** min). These peaks were slightly delayed in the hydrophobic column compared to pure Ra (37.64 min), a result from the exchange of a polar hydroxyl group to less polar Ac and IAE groups. The structural features of the derivatives were analysed by ESI-MS and the measured molecular masses agreed with the expected products. The assigned mass spectra of Ra and **6a** are given in **Figure 17.**

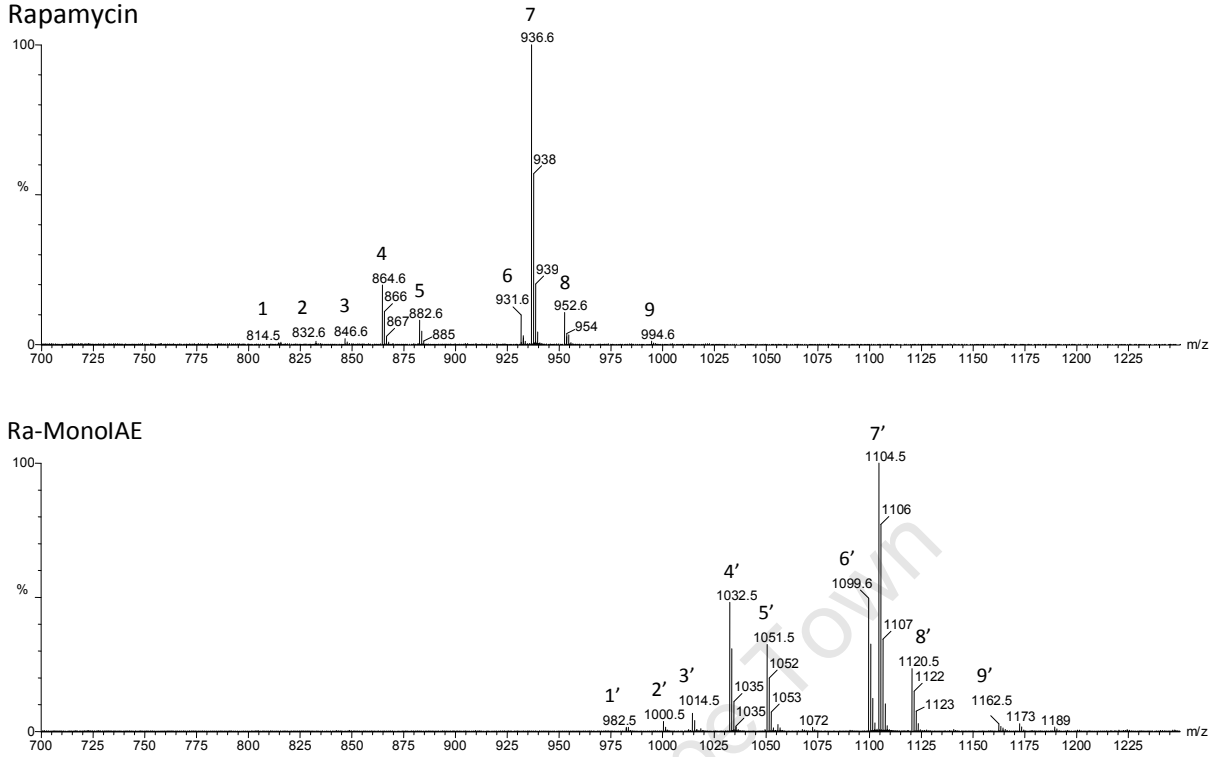

Figure 17: ESI-MS spectra of Ra and Ra-MonoIAE (**6a**). Only peaks with intensity higher than 1% of the main peaks are reported. The numbered Ra peaks correspond to the peaks denoted with a prime in the spectrum of **6a**.

Evidently Ra disintegrates to a large extent during ESI-MS analysis. Two main fragments (1 and 3), which in turn formed adducts with water (2, 4, 5 and 6), the intact drug in complex with ions (7 and 8) and another cluster (9) were repeatedly occurring (**Figure 17**, upper spectrum). These Ra fragments are also present in a previously reported Ra spectrum (Rajender *et al.* 2010). The peaks in the Ra derivative spectrum agreed with the respective products and were assigned by adding the exact mass of the functional groups (54.0 Da for Ac and 167.9 Da for IAE) to each peak in the Ra spectrum (**Figure 17**, lower spectrum).

Figure 18 shows the ^{1}H NMR spectra of Ra, RaAc (**5**) and RaIAE (**6a**). As seen in the top spectrum Ra exhibits overlapping peaks from δ =0.5 to 6.5 ppm with only a few gaps. These peaks make it difficult to identify the shifts of effected protons during synthesis and efficiently cover new peaks of the added functional groups.

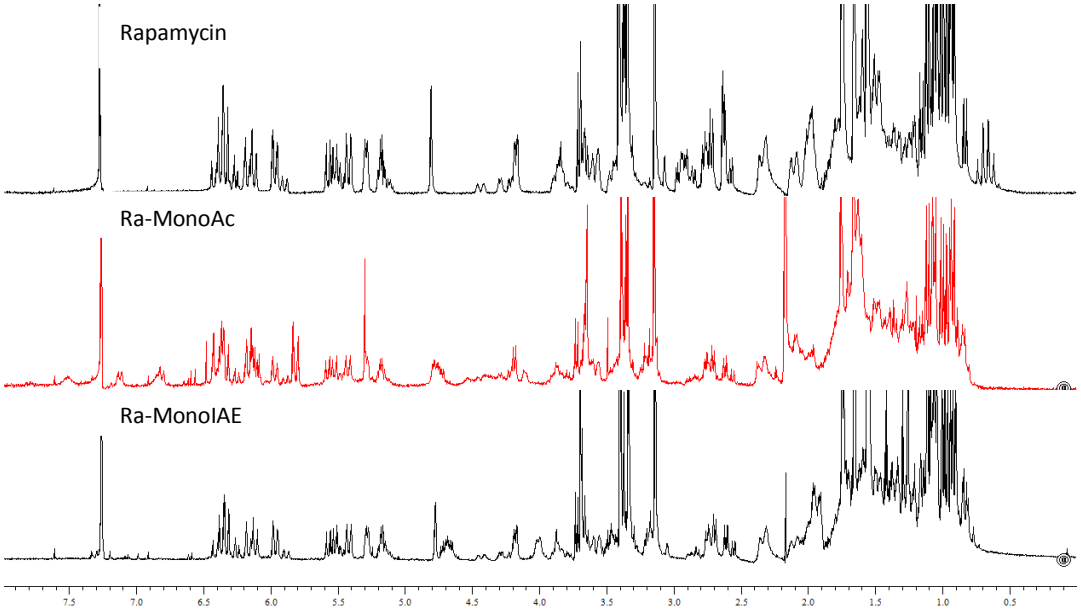

Figure 18: Stacked ^{1}H NMR (300 MHz, $CDCl_3$) spectra of rapamycin and its derivatives.

According to McAlpine *et al.* the shifts of -C*H*O*H*- at position 40 are 3.37 and 3.35 ppm respectively, but there are also five other groups of peaks assigned for that range (δ= 3.33- 3.41) making it almost impossible to identify these protons without a proper investigation involving a range of 2D experiments (McAlpine *et al.* 1991). An aggravating fact is that rapamycin is a mixture of three isomers, of which two are conformational isomers about the amide bond, which induces further overlap of the peaks (Ricciutelli *et al.* 2006). Therefore NMR was not used for the analysis of Ra derivatives and conjugates.

In the second step the RaAc and RaIAE derivatives were conjugated with dPEG-SH (**3** or **4**), which resulted in water soluble conjugates (at least 180 mg/ml). The reactions were carried out in a stoichiometric relation of X to SH groups, theoretically resulting in one drug attachment per carrier.

The amounts of Ra incorporation for RaAc-dPEG-3SH (**9**) and RaIAE-dPEG-3SH (**10**) were 79.8 and 66.6 mg/g product, respectively, which are close to the calculated value (80.9 mg Ra/g product) in case of both compounds (**Table 3**).

Table 3: Experimentally determined rapamycin contents for the Ra-PEG conjugates.

	RaAc-dPEG-3SH (9)	**RaIAE-dPEG-3SH (10)**	**Calculated value**
Ra content [mg/g product]	79.8	66.6	80.9

The Ra modification and subsequent PEGylation that make up the mono-functional approach is summarised in **Scheme 10**.

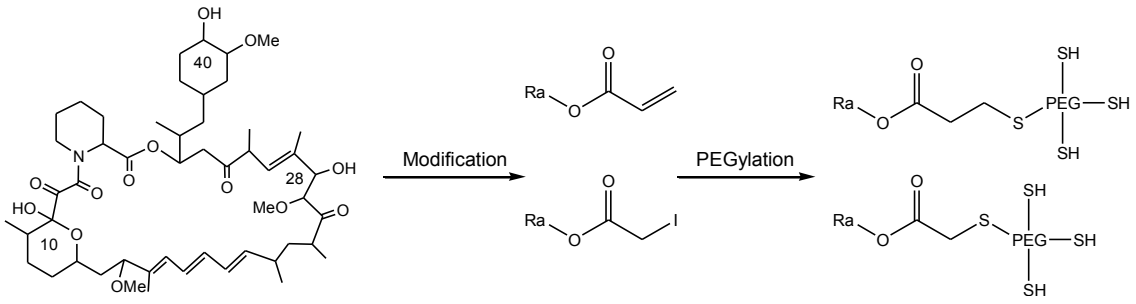

Scheme 10: Overview of the "Mono-functional Approach" towards covalent rapamycin incorporation into gels. Note that the PEG-SH links are simplified and only show the terminal bond.

Here follows a summary of the problem solving during method development of the mono-functional approach.

The RaAc derivative was initially PEGylated with 2nPEG-2SH and the conjugate was analysed by MALDI, but only a single broad peak for the carrier at 2 kDa was detected with no trace of the expected product closer to 3 kDa. Inspired by the literature (Plattsburgh *et al.* 1998; Yu *et al.* 2005) an alternative coupling route was investigated using the RaIAE derivative. The PEGylated product, RaIAE-nPEG-2SH, was analysed by MALDI but not detected, again in favour of the non-conjugated carrier at 2 kDa.

To simplify the conjugation reactions and the following product analysis as much as possible the polymeric carrier was replaced by mercaptoethanol as a substitute for PEG-SH with only one repeating unit. The products from these model reactions, using both the RaAc and RaIAE routes, were successfully confirmed by ESI-MS.

To overcome possible solvent effects resulting in a reduced availability of the reactive polymer terminals when conjugating RaX with 2nPEG-2SH, PEG-2SH of different molecular masses were synthesised. Since the protocol for synthesising nPEG-SH involves 3 steps (Hiemstra *et al.* 2007) of which the last was not successful (unpublished results), the one step esterification reaction for producing dPEG-SH was used instead. Hence, both RaAc and RaIAE were reacted with dPEG-2SH of various molecular masses. The conjugates were analysed by ESI-MS and MALDI and showed product peaks, but also a considerably amount of uncoupled dPEG-2SH. Formation of Ra conjugates with 0.6dPEG-2SH and 0.9dPEG-2SH were confirmed by MS but were not water soluble, the conjugates with 1.5dPEG-2SH and 2dPEG-2SH were water soluble but could not be confirmed by MALDI.

At this stage the opportunity to perform MALDI analysis in-house was given and it was soon obvious that the Ra-PEG conjugates were fragile and easily broke up when analysed with too high laser intensity on the MALDI. Nonetheless, by carefully tuning the intensity an intact conjugate could be monitored. However, compounds with high molecular mass, such as the 10dPEG-4SH, tend to give rise to broad and overlapping peaks, which in this case aggravate the distinction between the conjugate and its fraction (**Figure 19**).

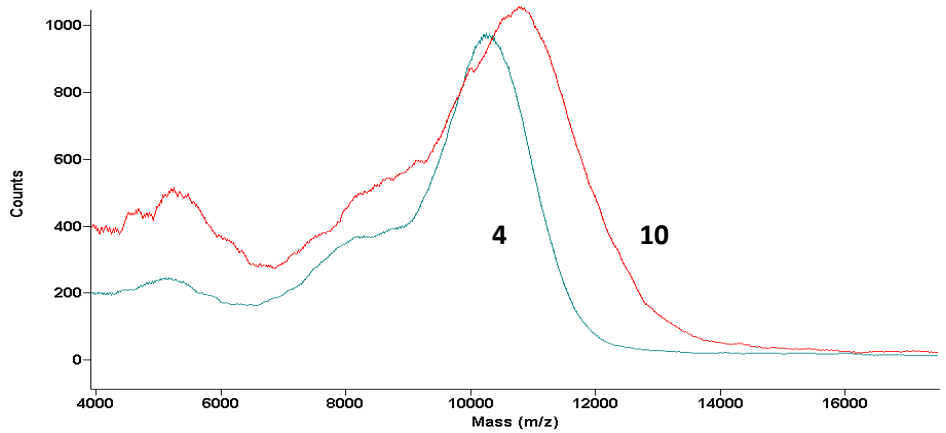

Figure 19: Overlaid MALDI spectra of 10dPEG-4SH (**4**) and RaIAE-dPEG-3SH (**10**). The laser intensity was 2270 units in both cases.

To more clearly illustrate the break-up of conjugates an example of a lower molecular mass compound is used (RaAc + 2dPEG-2SH). The product contained a mixture of unreacted (2dPEG-2SH, 2.2 kDa), mono-substituted (Ra-dPEG-SH, 3.2 kDa) and di-substituted (Ra-dPEG-Ra, 4.2 kDa) carrier (**Figure 20**). By successively increasing the laser intensities during MALDI the di-substituted Ra-dPEG-Ra compound (lower spectra) first degraded into Ra-dPEG-SH (middle spectrum) and further into 2dPEG-2SH (top spectrum).

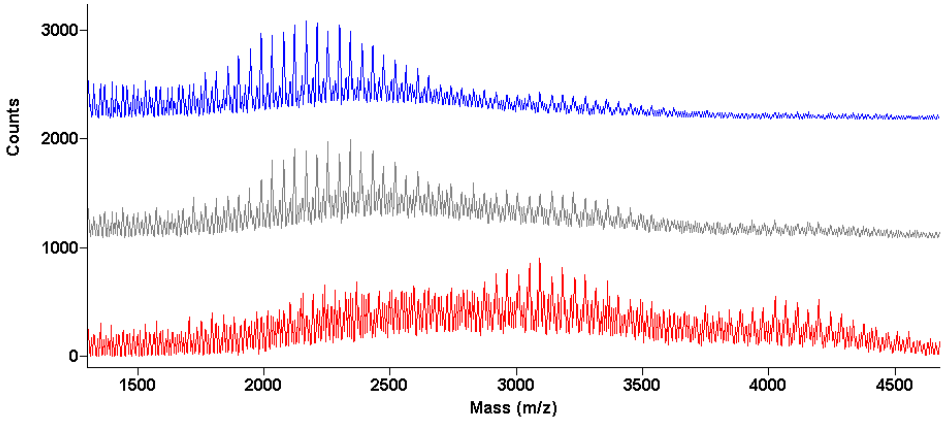

Figure 20: Stacked MALDI spectra of Ra-dPEG-SH. The laser intensities (top to bottom) were 3400, 2880 and 2780 units, respectively.

The breakdown of conjugates suggests there is a fragile bond attaching the drug with the carrier. This is encouraging since the concept of controlled drug release in this work is based on the formation of a weakened ester bond. Hence, it was assumed that these bonds break during the rather harsh conditions that MALDI presents. This hypothesis is strengthened by the literature where the breaking of ester bonds during MALDI analysis was previously observed, thus making it a likely explanation for the product degradation in this work (Elandaloussi *et al.* 2006).

3.1.4 Dendritic Approach

The mono-functional approach as presented above results in the delivery of 1 drug molecule per PEG carrier. In order to obtain higher drug loading densities dendritic multi branched structures were developed, which allow for the delivery of 2, 4 or 6 drug molecules per PEG carrier.

Only three building blocks (PEG, Dex-N_3 and acetylene monomer anhydride) were used to assemble each of the three dendritic categories (G1, 4arm and G2). The methodology used to synthesise the building blocks and dendritic compounds is presented in the following text and regarding the dendritic compounds, only one example from each step in the successive build up procedure is presented.

The preparations of the acetylene monomer anhydride (**16**) involved 6 reaction steps, which are previously published (Antoni *et al.* 2009). Therefore only the crucial reaction step where the protected trizma (**11**) was functionalised is shown (**Figure 21**).

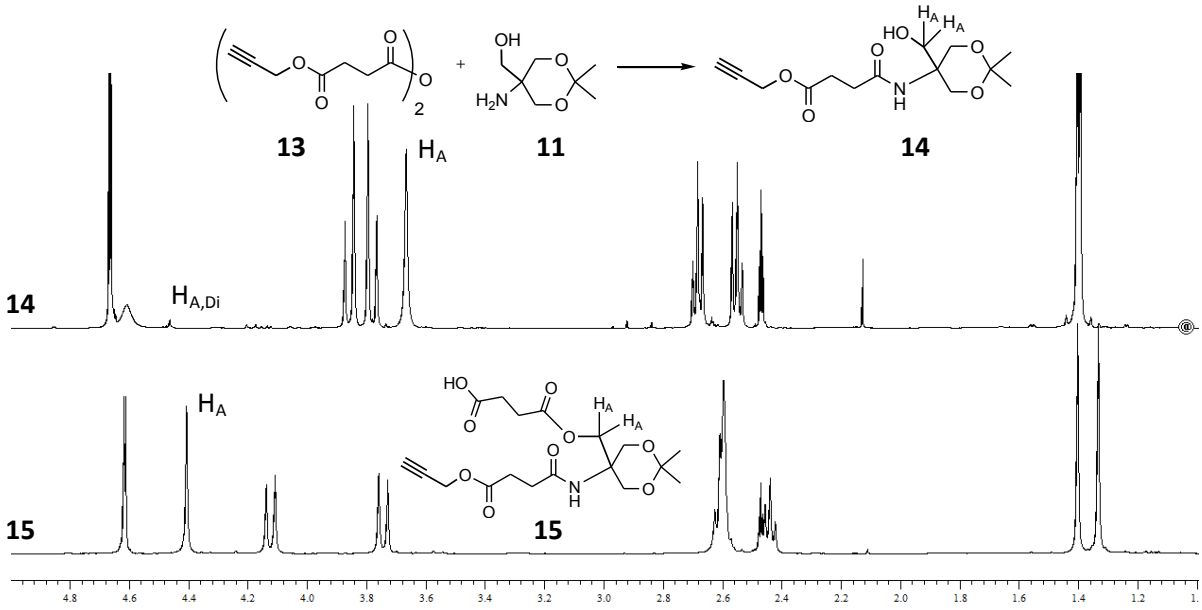

Figure 21: ^{1}H NMR (400 MHz, $CDCl_3$) spectra of acetylene (**14**) and succinate (**15**) addition to acetonide protected trizma (**11**).

The reaction scheme in **Figure 21** shows the coupling of compound **11** and **13** where the anhydride has the possibility to react with both the hydroxyl and amine group. Since the amine is more prone to nucleophilic substitution the reaction at this position was kinetically favoured by performing the reaction in an ice bath. The probability of having di-substitution was further decreased by using a deficit of the anhydride (0.8 eq) added slowly from a dilute solution.

To identify potential di-substitution of **14** the spectrum of compound **15** was used, since H_A for di-substituted **14** and compound **15** would have a similar shift. The small peak denoted $H_{A,Di}$ (δ= 4.46 ppm) corresponds relatively well with H_A of compound **15** (δ= 4.41 ppm) and by using the peak integrals a degree of mono-substitution for compound **14** higher than 98% was calculated.

Dex-N_3 (**17**) was obtained with a low yield (17%) due to a high extent of di-substitution. Dex has three hydroxyl groups; one primary (OH_{Prim}), one secondary (OH_{Sec}) and one tertiary (OH_{Tert}). The main reaction product was formed via substitution at OH_{Prim} and di-substitution occurred at OH_{Prim} and OH_{Sec}, but no reaction was observed to take place at OH_{Tert} (**Figure 22**). To explain the high degree of di-substitution for the synthesis of **17** compared to the synthesis of **14** the reactivity of the respective starting material is used. Dex has three hydroxyl groups in slightly different environments and apparently the reactivity of OH_{Prim} and OH_{Sec} is rather similar. The protected trizma on the other hand, has one amino group and one hydroxyl group where the former is the better nucleophile because of its greater electronegativity. Hence, the amount of di-substitution for protected trizma is

lower compared to Dex because of the greater range of reactivity of the competing functional groups.

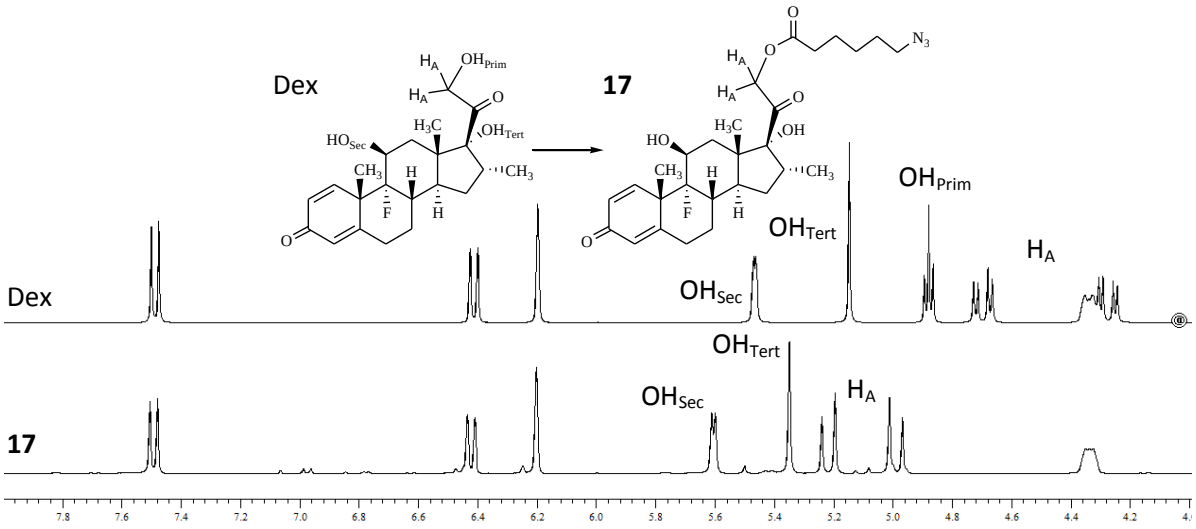

Figure 22: ^{1}H NMR (400 MHz, DMSO-d6) spectra of Dex and Dex-N_3 (**17**).

Figure 22 shows how H_A shifts downfield and OH_{Prim} disappears for the mono-substituted product compared to Dex. For the di-substituted by-product there was an additional shift of the H_B proton as seen in **Figure 23**.

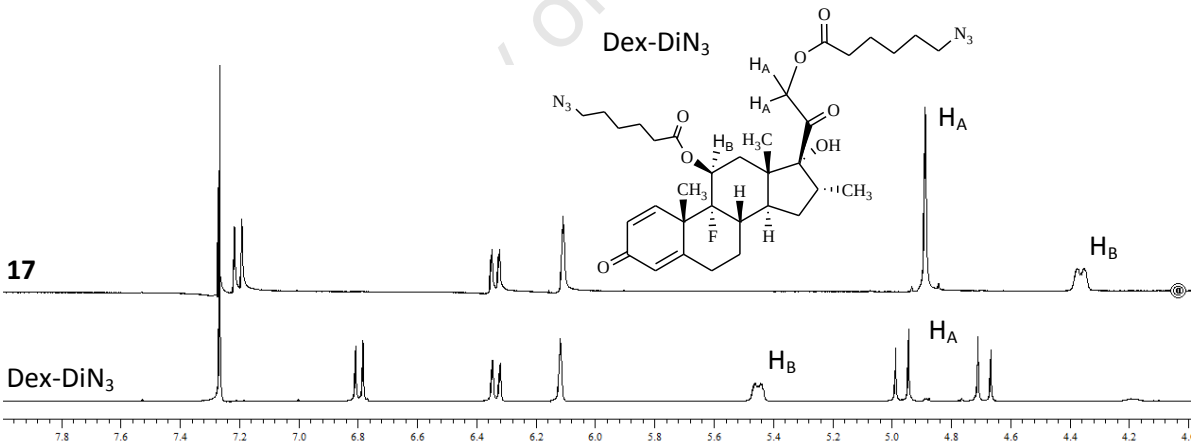

Figure 23: ^{1}H NMR (400 MHz, $CDCl_3$) spectra of Dex-MonoN_3 (**17**) and dex-DiN_3.

The acetylene monomer anhydride (**16**) was used for each generation growth in this work as depicted in **Figure 24** for PEG-2OH (due to limited space and increased clarity only one arm is drawn for the following examples).

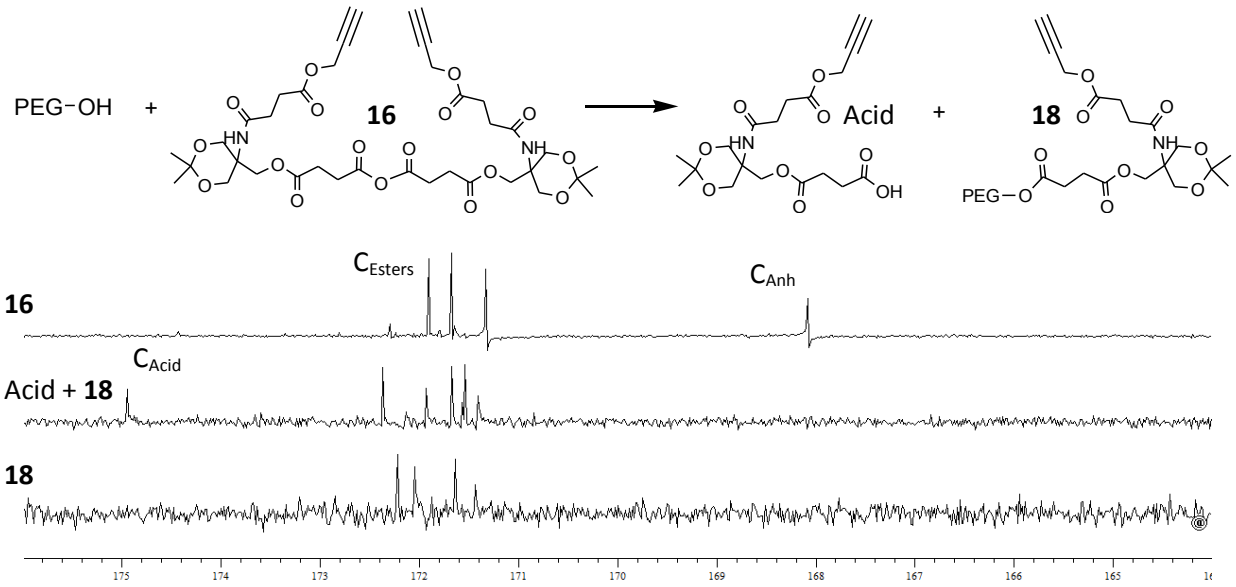

Figure 24: ^{13}C NMR (100.6 MHz, $CDCl_3$) spectra showing the consumption of acetylene monomer anhydride (**16**) during the synthesis of PEG-G1-2Act-Acet (**18**).

The reaction progress was followed by ^{13}C NMR spectroscopy. As compound **16** was totally consumed (**Figure 24**, middle spectrum; detected by the disappearance of the anhydride carbonyl carbon C_{Anh}), more of the compound was added. The lower spectrum in **Figure 24** shows the purified final product.

The following removal of acetonide protection groups was successful (yields >80%) and confirmed by ^{1}H NMR spectroscopy (**Figure 25**). However, the deprotection process often stagnated and the reaction needed to be restarted with fresh MeOH and Dowex resin for further progress. The halted reaction progress was assumed to be a result of reaching equilibrium with the released protection group, since the reaction progress in both directions in an acidic environment, such as the Dowex resin.

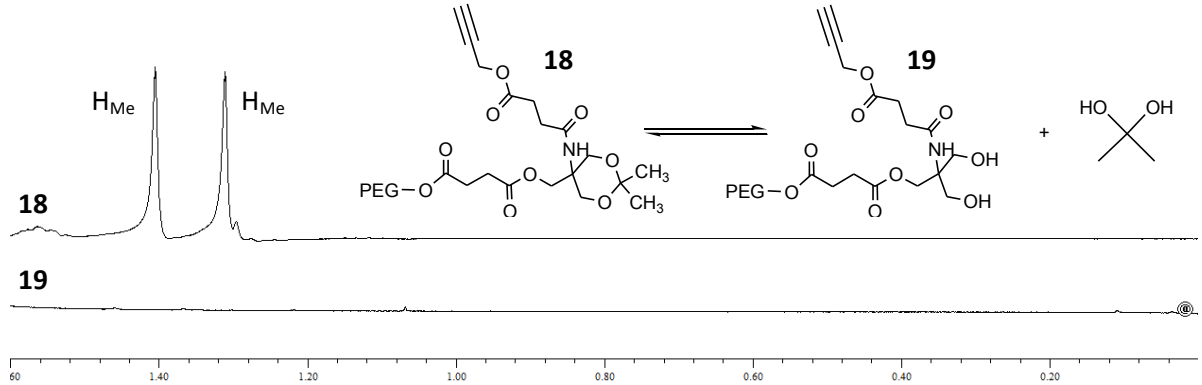

Figure 25: ^{1}H NMR (400 MHz, $CDCl_3$) spectra of PEG-G1-2Act-Acet (**18**) and PEG-G1-2Act-4OH (**19**).

In **Figure 26** the acrylation of PEG-G2-6Act-8OH (**27**) is shown and the protons of the attached acrylate group are marked H_{Ac}, H_{Cis} and H_{Trans} respectively. For some of the acrylation reactions extensive homo-polymerisation occurred as detected by sticky deposits on the walls of the reaction vessel. According to Srinivasan *et al.* self-initiated homo-polymerisation of terminal alkane acrylate groups is likely to occur (Srinivasan *et al.* 2010), therefore hydroquinone was added to quench formation of radicals. However, homo-polymerisation occurred nonetheless for some of the acrylation reactions and lowered their yields drastically.

In light of the spontaneous homo-polymerisation it would be preferred to perform the acrylation reaction as the last step, after incorporation of Dex, in order to only experience reduced yields by homo-polymerisation in one reaction step. Nonetheless, the acrylation reaction was performed before the Dex incorporation step since it was preferred to use the same batch of acrylated compounds both for the formation of "Blank" and "Trapped" gels and Dex incorporation.

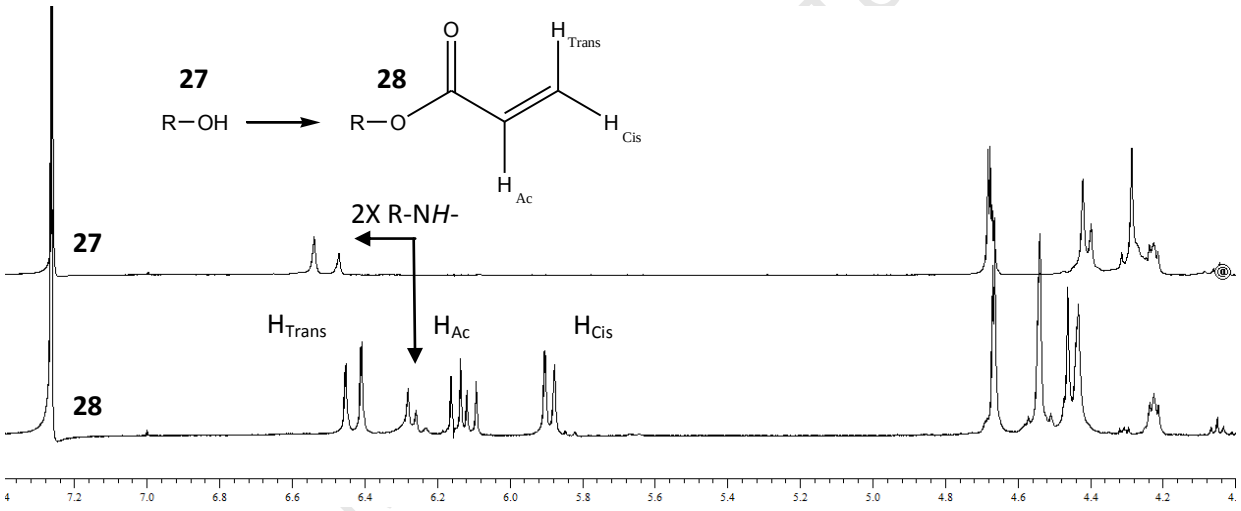

Figure 26: ^{1}H NMR (400 MHz, $CDCl_3$) spectra of PEG-G2-6Act-8OH (**27**) and PEG-G2-6Act-8Ac (**28**). R is a general denomination and represents the bulk of the molecule.

The triazole formation during Dex incorporation moved the shift of H_A downfield as illustrated in **Figure 27** for PEG-4arm-G1-4Dex-8Ac (**24**), while the change of H_B shift was less pronounced. The H_A shift of **24** is not included in the displayed range since it is part of a multiplet of several protons at δ= 2.49 ppm. H_B on the other hand is an isolated peak, slightly doubled by long range coupling to H_A, and was thus used to determine the reaction progress.

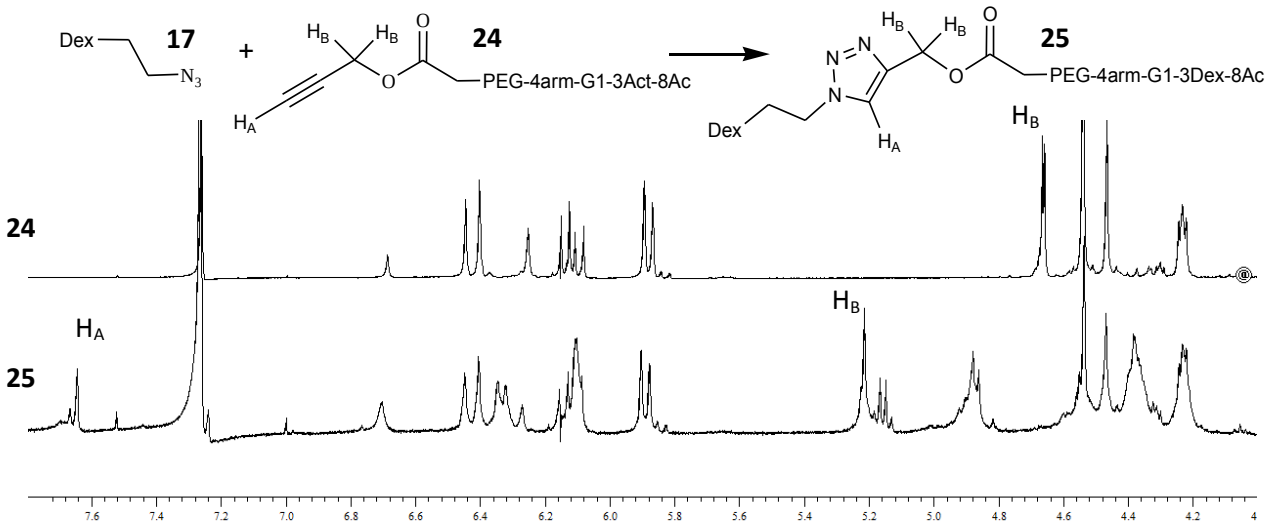

Figure 27: ^{1}H NMR (400 MHz, $CDCl_3$) spectra of PEG-4arm-G1-4Act-8Ac (**24**) and PEG-4arm-G1-4Dex-8Ac (**25**).

This HDC click reaction is dependent on copper, added as Cu (Nie *et al.*)SO_4 and reduced to Cu(I) by sodium ascorbate, to coordinate the alkyne and azide groups during the reaction progress (Hein *et al.* 2008). To obtain biocompatible compounds the amount of copper was reduced since an excessive amount in the circulatory system leads to the development of various malfunctions (Wang, T. *et al.* 2006).

The dendritic compounds were built from the terminal of PEGs in order to obtain water solubility of the final products and to facilitate purification. However, the drug carrying compounds in the 4arm and G2 categories were difficult to precipitate, hence their yields were lower than for the G1 category (G1 68%, 4arm 31% and G2 52%). Interestingly, these were also the only two compounds that were not water soluble. By considering the drug loading densities for the three dendritic categories (G1 2 Dex, 4arm 4 Dex and G2 6 Dex per 10PEG molecule) it was assumed that a too high loading density of Dex (>2 per 10PEG molecule) results in loss of water solubility of the PEG carrier. However, it is expected that the use of a bigger PEG carrier (>>10 kDa) would bring also the 4arm and G2 compounds into water solubility.

In **Figure 28**, **29** and **30** the dendritic products from the three categories used to build the gels are shown.

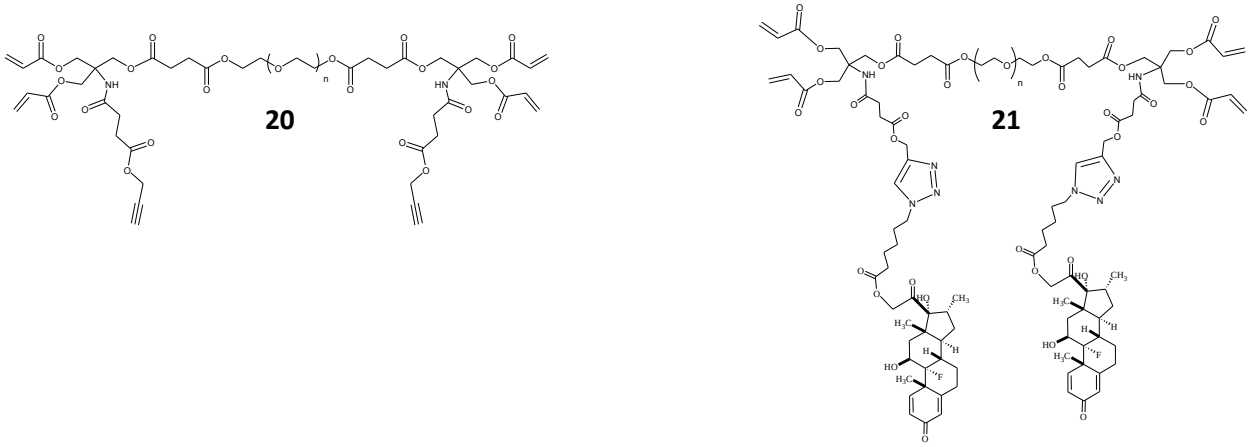

Figure 28: PEG-G1-2Act-4Ac (**20**) and PEG-G1-2Dex-4Ac (**21**).

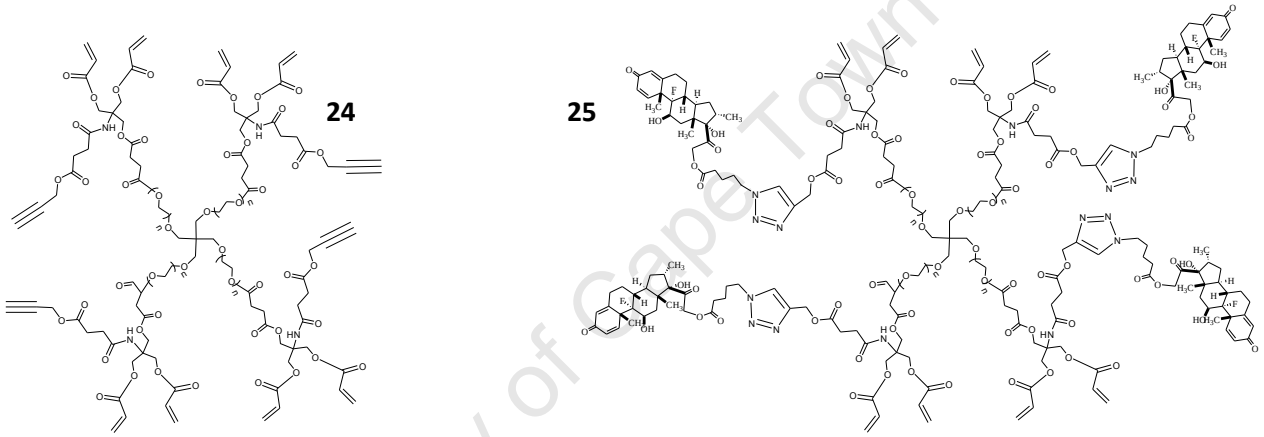

Figure 29: PEG-4arm-G1-4Act-8Ac (**24**) and PEG-4arm-G1-4Dex-8Ac (**25**).

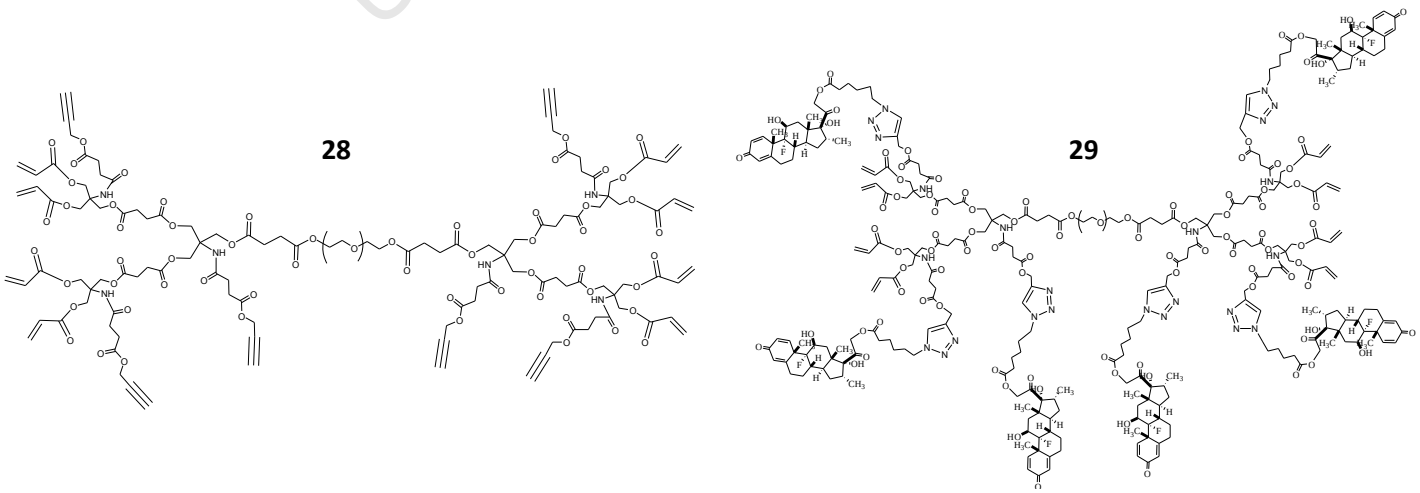

Figure 30: PEG-G2-6Act-8Ac (**28**) and PEG-G2-6Dex-8Ac (**29**).

3.2 Gel Formation Chemistries

In this work a variety of multi-arm and crosslinker combinations were used. The gel points of these combinations (percent conversion where a sufficient amount of crosslinks are created to form a continuous gel network) were calculated with **Equation 1** (**Table 4**).

Table 4: Gel points for the combinations of multi-arms and crosslinkers used for gel formation in this thesis.

Acrylate functionality	Thiol functionality	Gel point (% conversion)
4	2	58
4	4	33
8	2	38
8	4	22

The initial intention was to use conjugate addition to form all of the gels. This is the method of preference because it allows for an aqueous solution of gel building blocks to be injected *in vivo*, upon which gelling occurs spontaneously. However, compound **25** (PEG-4arm-G1-4Dex-8Ac) and **29** (PEG-G2-6Dex-8Ac) were not water soluble and could therefore not be gelled through aqueous conjugate addition. Instead, the free radical thiol-ene addition reaction in organic solvent was applied for the gelling step of the dendritic categories.

3.2.1 Conjugate Addition

Aqueous solutions of PEG-Ac compounds may have a slightly acidic pH as a result from remaining hydrochloric acid from the acrylation reaction (unpublished results).

As demonstrated in **Figure 31** the rate of conjugate addition is strongly pH dependent and a decrease in 0.5 pH units considerably prolongs the time to reach the gel point.

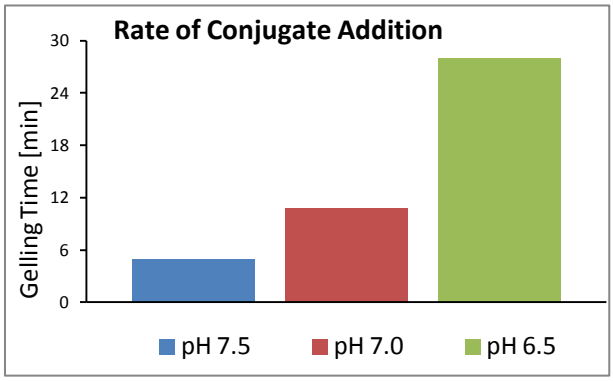

Figure 31: Gelling times for conjugate addition of 20PEG-8Ac and 2nPEG-2SH at different pH, n =1.

The pH dependence of conjugate addition originates from the acidic character of the thiol crosslinker, thus a maintained alkaline pH results in a greater degree of deprotonated thiols and a faster addition reaction (**Scheme 11**).

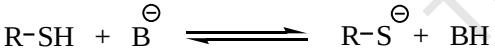

Scheme 11: Base mediated deprotonation of a thiol.

To reduce the pH lowering effect of potentially remaining hydrochloric acid in the PEG-Ac compounds, gel building blocks were dissolved in a PBS with increased buffer capacity, namely PBS-2.

The conjugate addition gels in this work reached the gel point within approximately three minutes, but were incubated for 45 minutes (100% relative humidity to prevent the gels from drying out) to allow further progress of the crosslinking. An even longer incubation time would only marginally increase the amount of crosslinks, since the gels get more rigid as more bonds form and the probability for reaction of remaining loose ends is lowered according to the Flory-Rehner theory.

3.2.2 Thiol-ene Addition

During the development of the thiol-ene gel formation protocols the relationship between concentration of building blocks and the amount of initiator was investigated. It was found that for a fixed amount of initiator a sufficiently high concentration of building blocks was required for gelling to occur, the reverse relation was also confirmed.

3.2.2.1 Conjugate versus Thiol-ene Addition

Conjugate and thiol-ene additions theoretically result in the same structural features, namely thio-ether weakened ester bonds. However, this is not the case in reality since the latter reaction gives

rise to a mixture of weakened and non-weakened ester crosslinks as a result of a side reaction (homo-polymerisation; **Scheme 1**). As a reference for 100% homo-polymerisation gels were additionally formed by photo-polymerisation in the absence of a thiol crosslinker. The resulting degradation times, for gels made by using the three crosslinking methods, are demonstrated in **Figure 32**, as it was no longer possible to measure the drug elution when the gels were too degraded for decanting supernatant. Gels made by conjugate addition, thiol-ene addition and photo-polymerisation degraded in 9, 60 and 129 days respectively. These results confirm that the close proximity of a thio-ether group make a large difference for the crosslink stability.

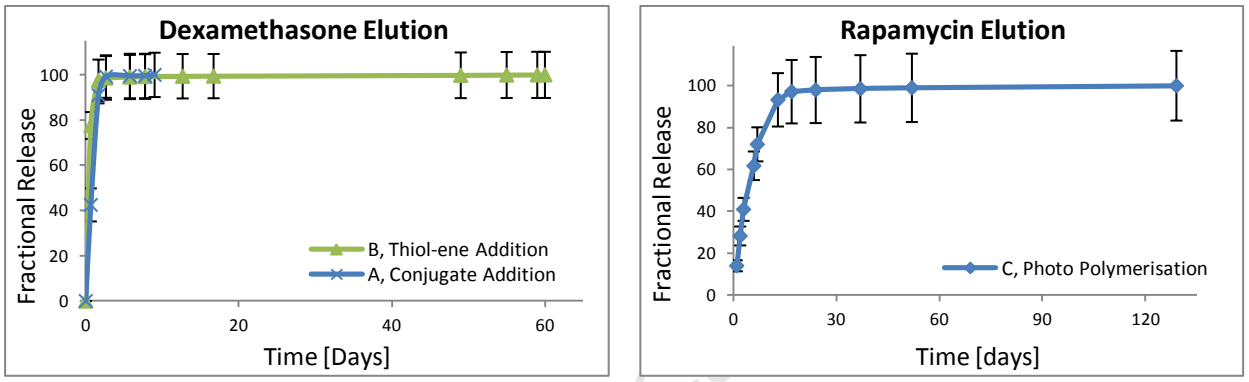

Figure 32: Three variations of 20PEG-8Ac (**1**) gels: (**A**) conjugate addition with 2dPEG-2SH at 14% in PBS-2, (**B**) thiol-ene addition with 2dPEG-2SH at 31% in THF with 10 mol% DMPA and (**C**) photo polymerisation at 20% in 50% PBS-2 in EtOH with 1 mol% DMPA and 1000 mol% NVP.

Regarding the photo-polymerised gels; UV irradiation of solutions of either **1** or DMPA in NVP did not result in gelling and a mixture of **1** and DMPA did only indicate initial gel formation after prolonged irradiation. Hence, DMPA is necessary for gelling to occur and NVP to accelerate the process.

Although a direct comparison of the elution properties of Ra and Dex is incorrect a rough indication on crosslink density may be obtained by comparing the respective times for drug elution to reach a plateau. The plateaus were reached after 3, 2 and 17 days respectively for **A**, **B** and **C** (**Figure 32**). These elution profiles suggest that the photo-polymerised gels (**C**) have a much higher crosslink density than gels formed by the other two methods, which was also expected from considering the functionalities and nature of the involved compounds. The acrylate double bond is cleaved homolytically upon UV irradiation and is thus di-functional in free radical polymerisation reactions, such as the homo-polymerisation in thiol-ene addition. Hence, method **A** is an 8 + 2 arm system, method **B** is a mixture of an 8 +2 (thiol-ene route) and a 16 + 2 (homo-polymerisation route) arm system while method **C** is a 16 + 16 arm system.

3.3 Drug Release and Hydrogel Characterisation

The six hydrogel categories were characterised with respect to drug elution properties and swelling and degradation rates of the gel scaffolds.

3.3.1 Mono-functional Approaches

The building blocks for the RaX-d4 and RaX-d2 categories were dissolved at 20% and 13%, respectively, during gelling. The difference in concentration was a result from the difference in molecular mass of the crosslinkers, because the multi-arms were always dissolved at the upper limit followed by addition of crosslinkers with different molecular masses; **3** (2 kDa) or **4** (10 kDa).

3.3.1.1 Ra-Ac/IAE, 4-armed carrier

Rapamycin elution from the RaX-d4 gels is shown in **Figure 33**. The gels, containing either RaAc-dPEG-3SH (**7**) or RaIAE-dPEG-3SH (**8**), displayed zero order drug release kinetics during a 15 days gel degradation period (**Table 5**). A similar constant and sustained zero order release was predicted by mathematical modelling, and experimentally confirmed, for degradable conjugate addition gels with a fluoroscopic probe covalently incorporated (DuBose *et al.* 2005). Following the linear release phase, the mathematical model predicts a burst of the remaining drug content prior to gel dissolution. Such trend was also observed for the release of bound drug in **Figure 33**, as the slopes of these elution curves gradually increase while the gels are degrading prior forced burst by NaOH treatment. The trend, however, was less pronounced than for DuBose and co-workers. Therefore the contribution of degradation to the release mechanism was considered to be marginal, in favour for hydrolysis of the hydrolytically labile drug-gel linker.

The hydrolytic release of bound Ra into PBS medium produced zero order elution kinetics. The situation would potentially be different if the elution instead occurred into a biologically active medium containing enzymes and/or cells, such as serum. However, Ito *et al.* (2007) created a hydrogel, based on hyaluronic acid, with Dex covalently incorporated via a pH sensitive hydrazide linker in series with an ester. The gel released the drug into a cell culture medium, with or without 10% fetal bovine serum, and there was no statistically significant difference at any time point, except for the 5^{th} day. These findings support the use of PBS as elution medium for benchmarking the chemistry in this thesis.

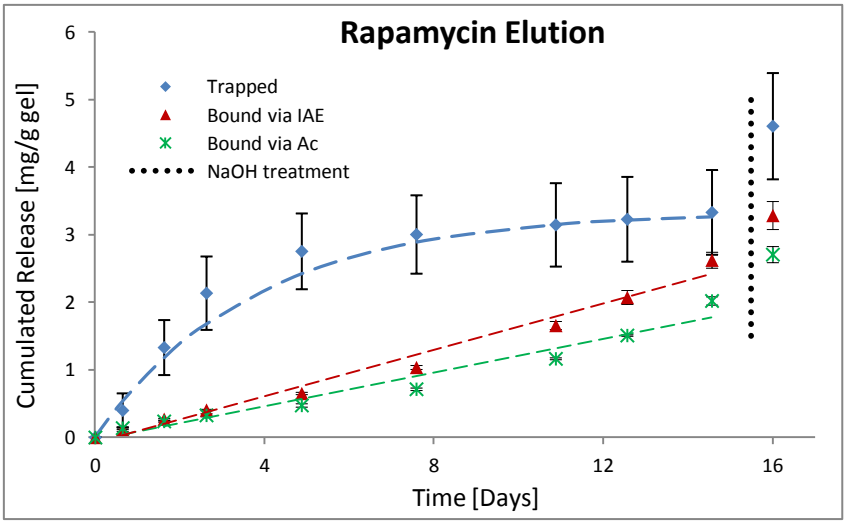

Figure 33: Experimental data (with error bars) and calculated curve fits (dashed lines) for conjugate addition gels at 20% in PBS-2. Formulation (building blocks; detected amount of drug); Trapped (20PEG-8Ac (**1**) and 10dPEG-4SH (**4**); 69%), Bound via IAE (RaIAE-dPEG-3SH (**8**), 20PEG-8Ac (**1**) and 10dPEG-4SH (**4**), 57%) and Bound via Ac (RaAc-dPEG-3SH (**7**), 20PEG-8Ac (**1**) and 10dPEG-4SH (**4**), 60%).

Gels containing **7** reached the half amount of total drug elution (prior to forced gel degradation) after 10.2 days, which is slightly slower than the 9.3 days it took for gels containing **8** to reach the same point. The two compounds are structurally very similar and the only feature that distinguishes them is the number of carbons between the thio-ether and ester moieties in the Ra-PEG link, namely two carbons (**7**) or one (**8**). However minute this difference is, it makes a distinct effect on the drug release kinetics since **7** is slightly less prone to hydrolysis than **8**.

Schoenmakers *et al.* have previously reported on a non-degradable hydrogel system that the decrease in thio-ether to ester distance for a drug-PEG conjugate from 3 to 2 carbons decreased the time to reach the half amount of total drug elution from approximately 10 to 3 days (Schoenmakers *et al.* 2004). Even though the drug release in both this thesis and the report from Schoenmakers *et al.* were primarily controlled by hydrolysis the difference in elution rates for the two gel formulations in this work is believed to be reduced by gel degradation.

Table 5: R^2-values from curve fitting of a linear line to calculated curves based on experimental data, all combinations are not applicable (n.a.), and the best curve fits are highlighted in yellow.

RaX-d4	Hixson-Crowell Equation	Korsmeyer-Peppas Equation	n	Zero Order Rate Equation	First Order Rate Equation
"Bound via Ac"	n.a.	n.a.	n.a.	0.955	0.897
"Bound via IAE"	n.a.	n.a.	n.a.	0.980	0.912
"Trapped"	0.935	0.856	0.61	0.743	0.978

Trapped Ra was released faster than bound and displayed a comparable release pattern as previously reported for degradable PEG hydrogels (van de Wetering *et al.* 2005). The elution proceeded for five days and the data fitted significantly to the first order rate equation (**Table 5**; **Figure 33**). However, the use of the Hixson-Crowell or Korsmeyer-Peppas equations did not transform the experimentally obtained release data into linear plots, hence those equations could not be used to ascribe the release mechanism to degradation, diffusion or swelling. Nevertheless, by considering the swelling (**Figure 34**) and elution (**Figure 33**) curves it was identified that swelling equilibrium was reached already on the first day while the elution of trapped Ra continued until day five. This suggests that the release was principally controlled by diffusion and not restricted by swelling. In addition, since the elution did not continue during the gel degradation period, between day 5 and 13, degradation was not considered to contribute to the elution of trapped drug.

The faster release rate of Ra from "Trapped" compared to "Bound" gels was not related to swelling or an altered architecture since these gels displayed a nearly identical swelling (**Figure 34**). The "Blank" gels however, always swelled slightly less than drug containing gels. It was also observed that "Bound" and "Trapped" gels always degraded faster than "Blank" gels, as detected by an increased difficulty to handle those gels. It is believed that the presence of hydrophobic drug affected the gel network negatively by aggravating the gel formation compared to "Blank" gels, resulting in an increased swelling. The difference in release rates for "Bound" and "Trapped" gels are thus attributed to the different release mechanisms; hydrolysis and diffusion, respectively.

In **Figure 33** approximately 60% of bound and 70% of trapped drug was detected. Incomplete drug release is commonly observed in the literature, but no general explanation has been proposed for either bound (Nuttelman *et al.* 2006; Ito *et al.* 2007) or trapped (Forrest *et al.* 2006; Kim, D. H. *et al.* 2006; Lin *et al.* 2006; Reddy *et al.* 2008) drug. For the results presented in this thesis the difference in amounts of loaded and detected drug was believed to partly origin from experimental methodology since the volume contribution of solids was not accounted for while making rather concentrated solutions.

Another possible explanation is that secondary release or dissolved PEG released from the gels quench the signal of the drug during UV quantification (unpublished results). (Ito *et al.* 2007) also speculated in the possibility that secondary release is responsible for not detecting the entire drug load.

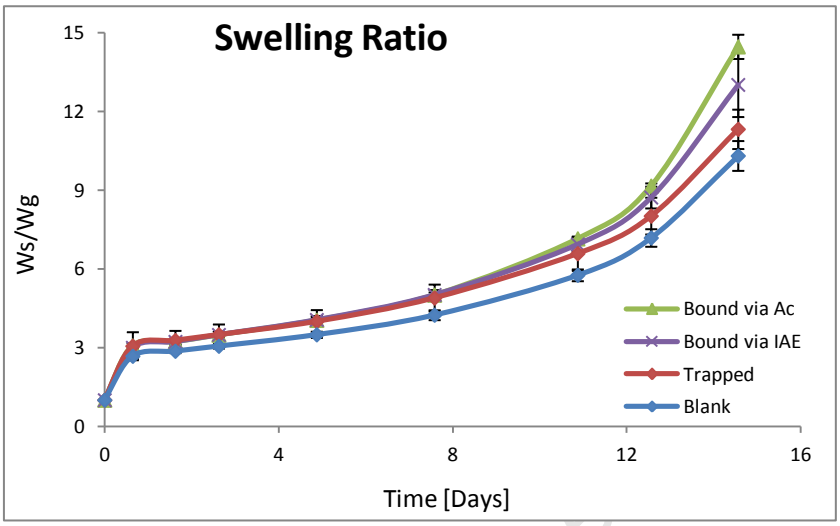

Figure 34: Conjugate addition gels at 20% in PBS-2. Formulation (building blocks); Bound via Ac (RaAc-dPEG-3SH (**7**), 20PEG-8Ac (**1**) and 10dPEG-4SH (**4**)), Bound via IAE (RaIAE-dPEG-3SH (**8**), 20PEG-8Ac (**1**) and 10dPEG-4SH (**4**)), Trapped and Blank (20PEG-8Ac (**1**) and 10dPEG-4SH (**4**)).

The swelling of the three gel formulations reached equilibrium within a few days from where further swelling occurred with increasing rates as the degradation progressed (**Figure 34**). The same swelling behaviour is previously reported for degradable PEG hydrogels (van de Wetering *et al.* 2005).

As already pointed out, the "Blank" formulations always swelled a little less and lasted a little longer than the "Bound" and "Trapped" formulations. A lower crosslink density of "Bound" compared to "Blank" gels was also confirmed by calculations of crosslink densities for selected compounds (**Figure 35**). The "Blank" formulation reached equilibrium on the first day followed by a steady decrease in crosslink density during degradation until the end point. For all time points past equilibrium the "Bound" gels showed a lower crosslink density than the "Blank". At the end point, both formulations had an average mesh size of ~230 Ångström, only that the "Bound" formulation arrived at the end point ~5 days earlier than the "Blank", which indicates a lower crosslink density.

A possible explanation for the greater swelling and lesser crosslink density of the "Bound" formulation is that the incorporated drug consumes a crosslinking site, which lowers the overall functionality. The resulting functionalities of "Bound" gels are; 8 Ac (multi-arm) + 4 SH (crosslinker) + 3 SH (drug carrier), compared to "Blank" gels; 8 Ac (multi-arm) + 4 SH (crosslinker).

Even though the ratio of Ac and SH is stoichiometric for all gels the lowering in overall functionality for the "Bound" gels might contribute to a decrease in crosslink density and increase in swelling.

That, however, does not explain the increased swelling of "Trapped" formulations compared to the "Blank". Therefore it is suggested that the drug presence disrupts gel formation, resulting in a lowered crosslink density for a yet to be discovered reason, compared to "Blank" gels.

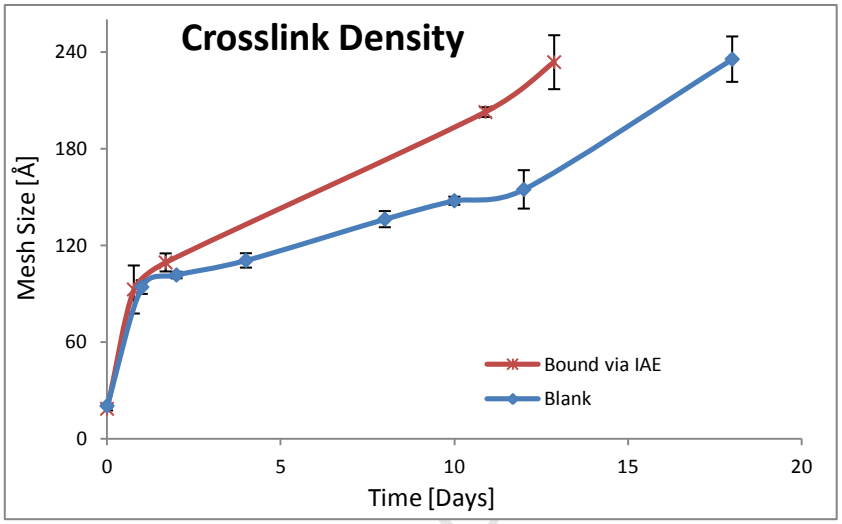

Figure 35: Conjugate addition gels at 20% in PBS-2. Formulation (building blocks); Bound via IAE (RaIAE-dPEG-3SH (**8**), 20PEG-8Ac (**1**) and 10dPEG-4SH (**4**)) and Blank (20PEG-8Ac (**1**) and 10dPEG-4SH (**4**)).

None of the journal articles reviewed during the work with this thesis compare the release of trapped and bound drug; hence there is no suitable comparison in the literature regarding the different swelling of such gel formulations.

3.3.1.2 Ra-Ac/IAE, 2-armed carrier

Several drug vehicle compositions were investigated for drug delivery in this thesis, but only the RaX-d4 and RaX-d2 categories were tested for drug elution properties. The latter gel category was made of 20PEG-8VS (**2**) crosslinked by 2dPEG-2SH and contained either RaAc-dPEG-SH (**9**) or RaIAE-dPEG-SH (**10**). The resulting drug elution from those gels is displayed in **Figure 36**.

The times to reach the half amount of total drug elution were 9.7 days for gels containing **9** and 5.1 days for gels containing **10**, which again display the effect of the structural difference for drug incorporation via Ac or IAE, respectively.

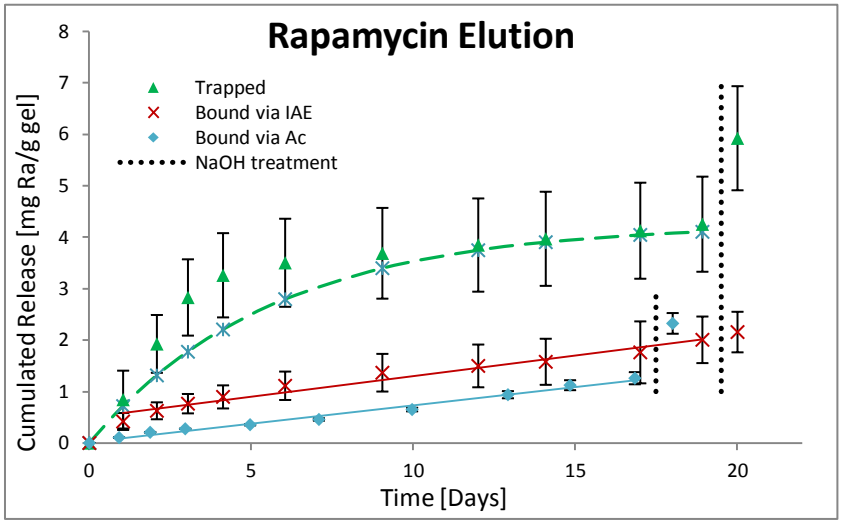

Figure 36: Experimental data (with error bars) and calculated curve fits (dashed lines) for conjugate addition gels at 13% in PBS-2. Formulation (building blocks; detected amount of drug); Trapped (20PEG-8VS (**2**) and 2dPEG-2SH; 65%), Bound via IAE (RaIAE-dPEG-SH (**10**), 20PEG-8VS (**2**) and 2dPEG-2SH, 29%) and Bound via Ac (RaAc-dPEG-SH (**9**), 20PEG-8VS (**2**) and 2dPEG-2SH, 49%).

The "Bound" formulation where Ra was incorporated via Ac agreed well with the zero order rate equation, but the elution from "Bound via IAE" gels agreed the best with the first order rate equation (**Table 6**). This unexpected release profile may be a result from a decreased quality of gel formation, as indicated by a considerable increased swelling of those gels compared to the "Bound via Ac" and "Blank" formulations (**Figure 37**). Nevertheless, the release from "Bound via IAE" gels was significantly more controlled than release from "Trapped" gels, and the elution also showed good agreement with the zero order rate equation while trapped elution data was on the border to fit the first order rate equation and burst release (**Table 6**).

Table 6: R^2-values from curve fitting of a linear line to calculated curves based on experimental data, all combinations are not applicable (n.a.), and the best curve fits are highlighted in yellow.

RaX-d2	Hixson-Crowell Equation	Korsmeyer-Peppas Equation	n	Zero Order Rate Equation	First Order Rate Equation
"Bound via IAE"	n.a.	n.a.	n.a.	0.966	0.989
"Bound via Ac"	n.a.	n.a.	n.a.	0.986	0.861
"Trapped"	0.894	0.805	0.46	0.688	0.950

The release mechanism from the "Trapped" formulation could not be established with the Hixson-Crowell or Korsmeyer-Peppas equations, because of the poor curve fitting. Nevertheless, release of trapped drug continued until day 4 (**Figure 36**) while the swelling equilibrium was reached already on day 2 (**Figure 37**), thus the elution was primarily controlled by diffusion and not restricted by swelling.

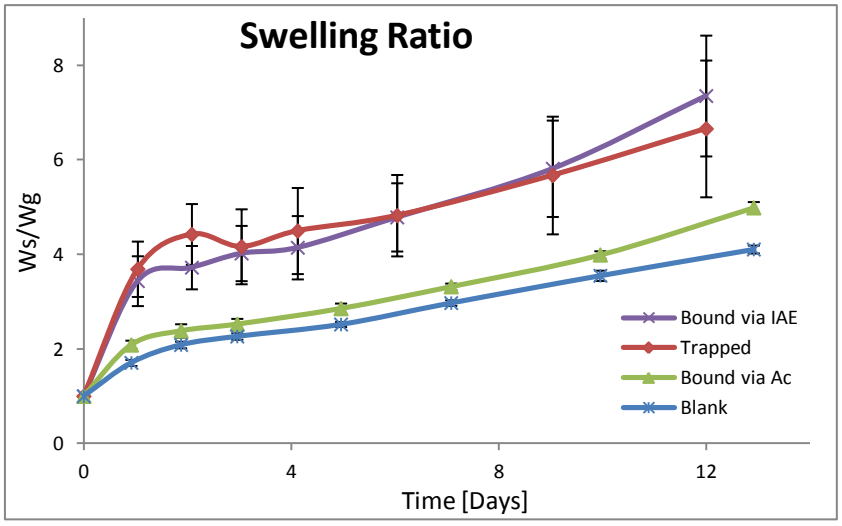

Figure 37: Conjugate addition gels at 13% in PBS-2. Formulation (building blocks); Bound via IAE (RaIAE-dPEG-SH (**10**), 20PEG-8VS (**2**) and 2dPEG-2SH), Bound via Ac (RaAc-dPEG-SH (**9**), 20PEG-8VS (**2**) and 2dPEG-2SH), Trapped and Blank (20PEG-8VS (**2**) and 2dPEG-2SH).

The RaX-d4 and RaX-d2 categories were built with different carriers, crosslinkers and multi-arms for the following reasons;

Ra has low water solubility and a PEG carrier of 1.5 kDa (1.5dPEG-2SH) was just sufficient to render the drug soluble. Even though **3** (2 kDa) was investigated as a carrier in the RaX-d2 category it was preferred to keep a larger margin to the 1.5 kDa limit, hence **4** (10 kDa) was used in the main RaX-d4 category within the mono-functional approach. Another argument for using **4** in favour of **3** is the higher risk of Ra saturation by di-substitution of the 2-armed carrier, resulting in a non-soluble conjugate and no Ac groups left for hydrogel incorporation. For the 4-armed carrier on the other hand, a di- or tri-substitution would not ruin its function, since such conjugates would still be water soluble and have at least one Ac group left for gel incorporation.

The carrier and crosslinker were always the same in order to make the gel formulations as similar as possible. Consequently, the crosslinkers were different for the RaX-d4 and RaX-d2 categories.

As earlier described, during synthesis of the Ac and VS functionalised multi-arms there was a substantial amount of self-initiated polymerisation for the latter compound. In order to avoid possible homo-polymerisation of PEG-8VS during gel preparations the PEG-8Ac compound was preferred.

3.3.1.3 RaDilAE, no carrier

During synthesis of RaMonoAc (**5**) and RaMonoIAE (**6a**) the di-substituted by-products were isolated and characterised. These compounds have two sites available for further modification, hence

RaDiIAE (**6b)** was copolymerised into a gel without previous conjugation to 10dPEG-4SH or 2dPEG-2SH.

The degradation time of 12 days (**Figure 38**) was slightly longer than for similar gels reported in the literature, where the gels (15PEG-4Ac crosslinked by 3nPEG-2SH at 40%) degraded in 8 days, even though the contrary was expected due to the nature of the respective crosslinks (Elbert *et al.* 2001). The use of Ra-2IAE as crosslinker is believed to turn the immediate proximity of the crosslink relatively hydrophobic, hence decreasing the rate of hydrolysis. A similar argumentation has previously been presented in the literature for explaining a prolonged degradation time of PEG gels (Schoenmakers *et al.* 2004).

The resulting gels contained a large proportion of Ra and 17.2 mg Ra/g gel was detected, compared to 3.3 and 2.2 mg Ra/g gel, respectively, for the RaMonoIAE gels in the RaX-d4 and RaX-d2 categories. A disadvantage however, is that non-PEGylated Ra is not water soluble and gelling must occur in a mixture of organic and aqueous solvents, thus making these gels improper for *in situ* gelling.

The elution of bound Ra from the RaX-d4 (**Figure 33**) and RaDiIAE (**Figure 38**) categories revealed similar profiles for the first seven days. Thereafter the RaX-d4 gels continued the zero order release while RaDiIAE gels took on an exponential profile (R^2 =0.987).

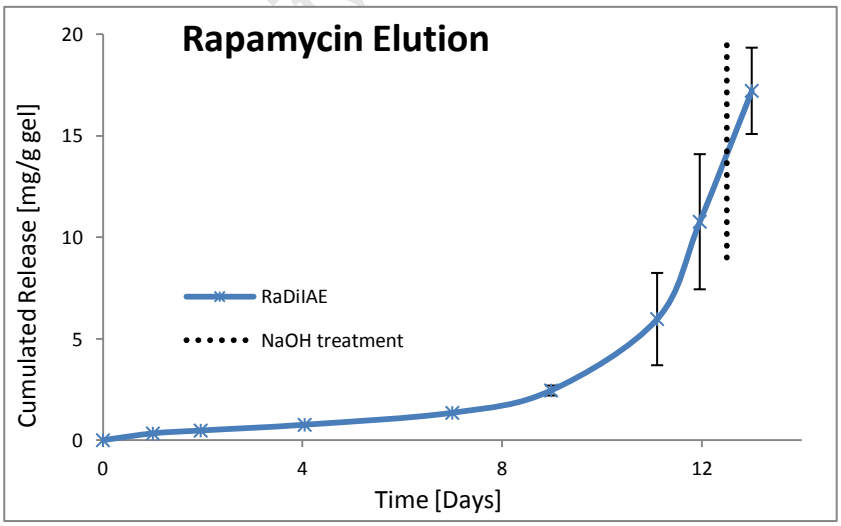

Figure 38: Gelling through nucleophilic substitution at 18% in MeCN and $NaHCO_3$ (2:1). Formulation (building blocks; detected amount of drug); RaDiIAE (RaDiIAE (**6b**) and 10dPEG-4SH (**4**); 47%).

If the release profile of RaDiIAE gels is divided into an initial zero order release (day 1-7) followed by a burst (day 7-12), the elution can be explained by gel dissolution as previously reported (DuBose *et*

al. 2005). As **Figure 38** and **39** demonstrate the drastic increase in Ra release appeared simultaneously as the swelling started to increase. The biphasic release however, was much more pronounced than the results from DuBose *et al.* and this discrepancy is believed to origin from the inherent gel properties. DuBose *et al.* also showed that the biphasic character decreased in favour for zero order release when the crosslink density was increased. Therefore, the profile in **Figure 38** is believed to have had a higher proportion of the zero order phase if the gel had a higher crosslink density and degraded slower.

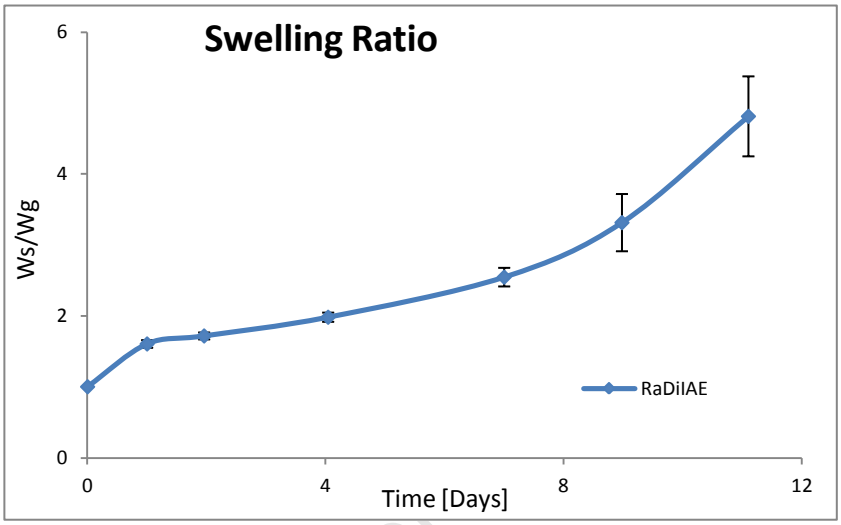

Figure 39: Gelling through nucleophilic substitution at 18% in MeCN and $NaHCO_3$ (2:1). Formulation (building blocks); RaDilAE (RaDilAE (**6b**) and 10dPEG-4SH (**4**)).

Due to lack of suitable control compounds (similar to **6b**, but drug deficient) the "Blank" and "Trapped" formulations had to be omitted in this case. Normally, supernatant from the "Blank" gels was used as background reading during UV quantification of released drug for the corresponding "Trapped" and "Bound" formulations. Since no "Blank" gels were made in this experiment a mixture of PBS-1 and EtOH was used instead for the "Blank" supernatant. This approximation is justified by comparing the obtained background level (0.074 ±0.005) with the level of "Blank" RaX-d4 gels (0.070 ±0.006), which are essentially the same.

The gelling of **6a** and **4** was the final proof that drug-PEG conjugates actually form, because if gelling of RaDilAE and PEG-4SH occurs then the reaction of RaMonoIAE and PEG-4SH also takes place, even though MALDI analysis provided inconclusive information.

3.3.2 Dendritic Approaches

Discussions regarding reasons for zero order release from "Bound" and first order release from "Trapped" formulations, difference in elution profile between bound and trapped drug, incomplete drug release and swelling trends of the three gel formulations as presented for the mono-functional approach are also valid here and will not be repeated.

Since these formulations are unique, there is a void in the literature of applicable comparisons regarding elution and swelling characteristics.

3.3.2.1 First Generation, 2-armed backbone

G1 was the only category within the dendritic approach where the compound remained water soluble after Dex incorporation. The solubility limit was approximately 130 mg/ml PBS-2 and consequently gelling at a similar concentration as for the mono-functional categories was possible. The G1 category was gelled by both conjugate and thiol-ene additions.

3.3.2.1.1 Gelling Through Conjugate Addition

The hydrolytically released drug from the "Bound" formulation displayed a constant zero order release profile during the entire elution period (**Figure 40**, **Table 7**), independently of swelling and degradation (**Figure 42**).

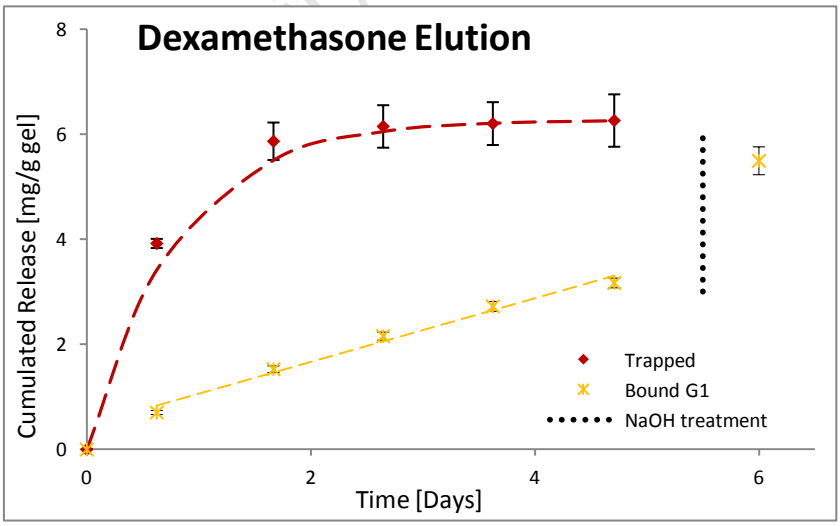

Figure 40: Experimental data (with error bars) and calculated curve fits (dashed lines) for conjugate addition gels at 19% in PBS-2. Formulation (building blocks; detected amount of drug); Trapped (PEG-G1-4Ac-2Act (**20**) and 10nPEG-4SH; 71%) and Bound G1 (PEG-G1-4Ac-2Dex (**21**) and 10nPEG-4SH; 49%).

Drug incorporation using the HDC click reaction resulted in a triazole containing link between the drug and the gel network (**Figure 41**). The ester connecting to the drug is followed by five methylene

groups and is not weakened by electron withdrawing groups. Instead the next following ester is believed to be weakened by the triazole moiety, since this ester has a two carbon distance to electronegative nitrogen, making it likely that the released drug is still connected to the triazole linker.

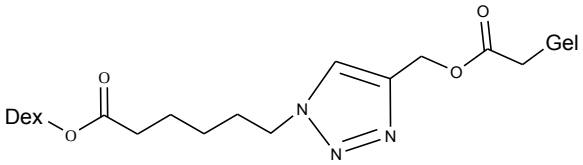

Figure 41: Details of the drug-gel link for the dendritic approach.

However, a Dex-OH_{Prim} conjugate still has biological activity (Rebuffat *et al.* 2002), which was also confirmed by an *in vitro* cell assay shown later in this text.

The release mechanism of trapped drug could not be established by the Hixson-Crowell and Korsmeyer-Peppas equations, but was considered to be primarily controlled by diffusion after comparing the elution and swelling curves (**Figure 40** and **42**). The first order rate equation, on the other hand, agreed well with the trapped data (**Table 7**).

Unexpectedly, the "Trapped" gels were dissolved at day 5 while "Bound" gels were still rather intact, hence there was no alkali treatment of the "Trapped" formulation (**Figure 40**).

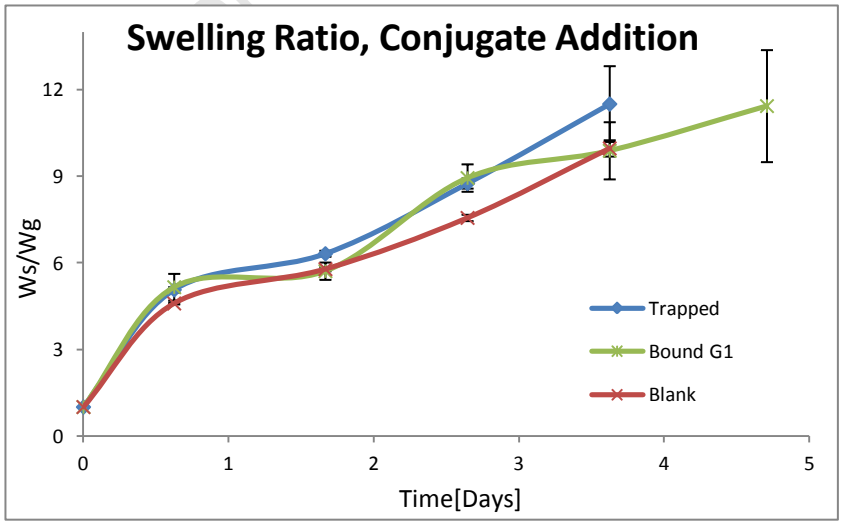

Figure 42: Conjugate addition gels at 19% in PBS-2. Formulation (building blocks); Trapped and Blank (PEG-G1-4Ac-2Act (**20**) and 10nPEG-4SH) and Bound G1 (PEG-G1-4Ac-2Dex (**21**) and 10nPEG-4SH).

Table 7: R^2-values from curve fitting of a linear line to calculated curves based on experimental data, all combinations are not applicable (n.a.), and the best curve fits are highlighted in yellow.

G1		Hixson-Crowell Equation	Korsmeyer-Peppas Equation	n	Zero Order Rate Equation	First Order Rate Equation
Conj. Add.	"Bound"	n.a.	n.a.	n.a.	0.986	0.968
	"Trapped"	0.938	0.855	0.23	0.635	0.968
Thiol-ene	"Bound"	n.a.	n.a.	n.a.	0.986	0.925
	"Trapped"	0.795	0.773	0.08	0.534	0.758

3.3.2.1.2 Gelling Through Thiol-ene Addition

Regarding the G1 compounds gelled by thiol-ene addition; the elution of hydrolytically released drug followed a zero order profile between day 1 and 11, but elution data from the "Trapped" formulation did not agree with any of the used models and was thus considered to be of burst character (**Figure 43** and **Table 7**).

For gelling through thiol-ene addition the general aim was to dissolve the dendritic compounds at high concentrations in order to keep the amount of potentially toxic initiator low and the UV irradiation time short. Nonetheless, to keep the concentration of G1 gels similar for the two gelling methods the concentration of G1 thiol-ene gels was decreased to a minimum, which resulted in the need of an increased amount of initiator (10 mol%) for gelling to occur.

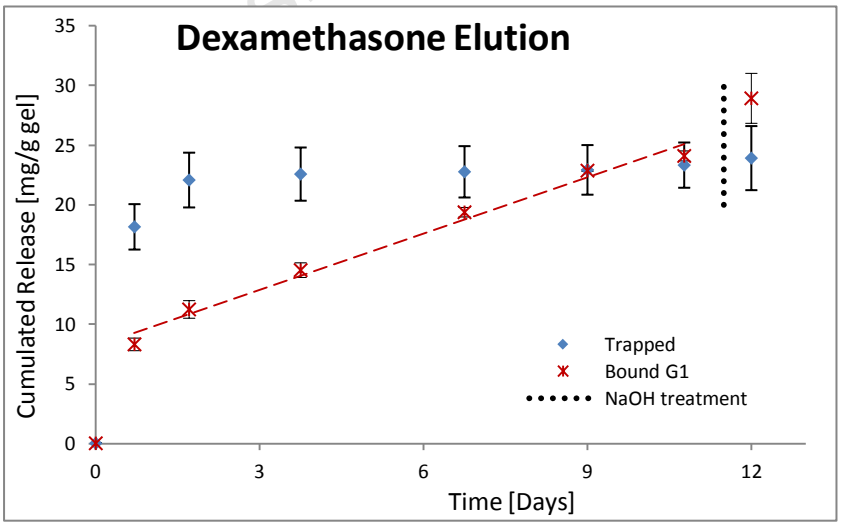

Figure 43: Experimental data (with error bars) and a calculated curve fit (dashed line) for thiol-ene addition gels at 38% in THF with 10 mol% Irgacure 2959. Formulation (building blocks; detected amount of drug); Trapped (PEG-G1-4Ac-2Act (**20**) and 10nPEG-4SH; 79%) and Bound G1 (PEG-G1-4Ac-2Dex (**21**) and 10nPEG-4SH; 60%).

Even though the same batch of PEG-G1-4Ac-2Dex (**21**) was used to form gels via conjugate (**Figure 40**) or thiol-ene addition (**Figure 43**), the bound drug in the latter case set off with a minor burst release. An initial burst followed by zero order release was also observed for the 4arm category and in some of the experiments with the G2 category (not shown). The obvious reason for a burst release is the presence of non-covalently bound drug diffusing from the gel immediately upon immersion. However, any potentially unbound drug is not believed to originate as a contamination in the product since the burst releases were only occasional. A possible explanation is that the drug is released during gel formation procedures, resulting in a small amount of drug being trapped in the gel matrix. Possibly the drug was cleaved off by the UV irradiation during gelling, because the initial burst release of bound drug was not observed in the mono-functional approach.

Despite the fact that incorporation of hydrophobic drugs is expected to increase the hydrophobicity of the hydrogel, and consequently lower its swelling, the "Bound" gels showed an increased swelling compared to the other two gel formulations. Nonetheless, the three gel formulations had similar degradation times (**Figure 44**), which was interpreted as an indication that the gels have roughly the same crosslink density. A comparison of the collected raw data provides the information that W_g of "Bound" gels was approximately half the value compared to the other formulations, but W_s was nearly equal for the three formulations. Therefore it was believed that these "Bound" gels lost more solvent through evaporation during preparations, hence a lowered W_g and a higher swelling ratio. An alternative explanation is if the increased swelling was a result of lower crosslink density, in such case degradation would also be faster, which was not observed.

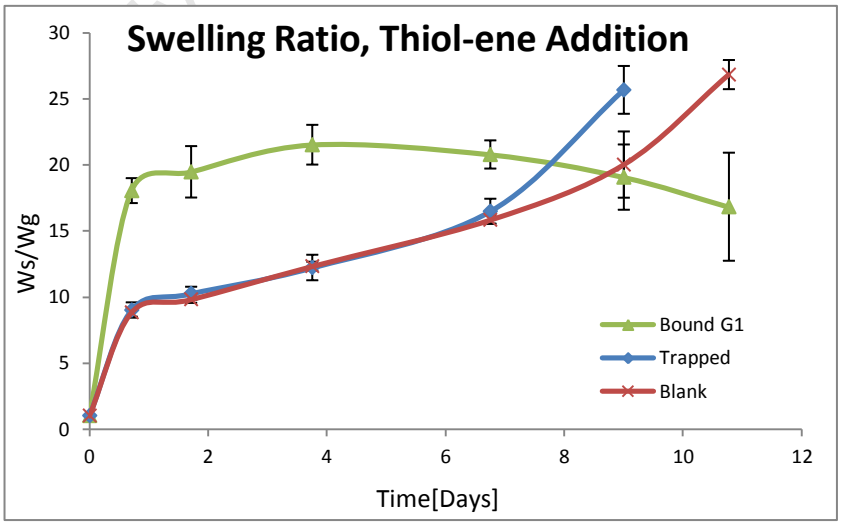

Figure 44: Thiol-ene addition gels at 38% in THF with 10 mol% Irgacure 2959. Formulation (building blocks); Bound G1 (PEG-G1-4Ac-2Dex (**21**) and 10nPEG-4SH), Trapped and Blank (PEG-G1-4Ac-2Act (**20**) and 10nPEG-4SH).

G1 gels crosslinked by conjugate addition degraded faster than those made by thiol-ene addition (5 and 11 days respectively). Even though the concentrations of gel building blocks were different for the two gelling methods, 19 and 38% respectively, it was assumed that formation of non-weakened ester bonds during the thiol-ene addition prolonged the degradation time for these gels. Combining previous and published results strengthens this assumption. Previously shown in **Figure 32**, an 8 + 2 arm system of PEG derivatives was gelled via either conjugate (at 14%) or thiol-ene (at 31%) additions with a resulting 7-fold difference in degradation time (8 and 59 days respectively). In contrast, Mason *et al.* and Dubose *et al.* describe that a doubling in concentration (25 to 50% and 10 to 20%, respectively) only prolonged the degradation time 2-fold or by 25% for hydrolytically degradable gels made by photo-polymerisation of PLA-*b*-PEG-*b*-PLA-2Ac building blocks or conjugate addition of 20PEG-8Ac and dithiothreitol (Mason *et al.* 2001; DuBose *et al.* 2005). In light of these experiments it is believed that the gels made by thiol-ene addition degraded more slowly than those made by conjugate addition as a result of an increased bond stability, and only marginally because of an increased crosslink density.

It was also observed that the degradation time for G1 gels formed by conjugate addition was shorter than for the RaX-d4 and RaX-d2 gels, as summarised in **Table 8**. By considering the functionality of gel building blocks for gels at similar concentrations a lucid picture of the resulting degradation rates is developed.

Table 8: A comparison of blank conjugate addition gels regarding composition and resulting properties.

Gel Category	Functionality	Concentration of Building Blocks	Degradation Time [Days]
RaX-d4	8 + 4	20%	15
RaX-d2	8 + 2	14%	9
G1	4 + 4	19%	4

The category with the most crosslinking sites of the multi-arm and crosslinker combined (RaX-d4) produced the most durable gels and the G1 category, with the least combined number of sites, degraded the fastest. Despite that the RaX-d4 and G1 categories were gelled at a slightly higher concentration than the RaX-d2 category, the latter gels followed the trend and degraded faster than RaX-d4 but slower than the G1 category. Hence, the fewer crosslinking sites for the G1 gels, compared to the other conjugate addition gels, resulted in a faster degradation rate.

3.3.2.2 First Generation, 4-armed backbone

After a minor burst the covalently bound drug was released in a zero order mode between day 1 and 27 (**Figure 45**, **Table 9**). In contrast, the entire elution of trapped drug was released with a burst during the first few days.

Table 9: R^2-values from curve fitting of a linear line to calculated curves based on experimental data, all combinations are not applicable (n.a.), and the best curve fits are highlighted in yellow.

4arm	Hixson-Crowell Equation	Korsmeyer-Peppas Equation	n	Zero Order Rate Equation	First Order Rate Equation
"Bound"	n.a.	n.a.	n.a.	0.998	0.854
"Trapped"	0.632	0.584	0.17	0.301	0.783

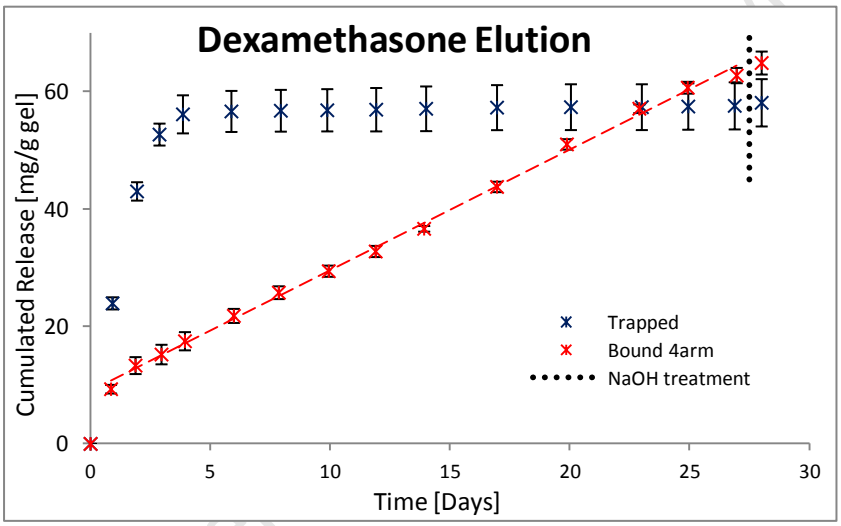

Figure 45: Experimental data (with error bars) and a calculated curve fit (dashed line) for thiol-ene addition gels at 69% in THF with 5 mol% Irgacure 2959. Formulation (building blocks; detected amount of drug); Trapped (PEG-4arm-G1-8Ac-4Act (**24**) and 2dPEG-2SH; 67%) and Bound 4arm (PEG-4arm-G1-8Ac-4Dex (**25**) and 2dPEG-2SH; 87%).

The 4arm compounds were dissolved at their upper solubility limit at 400 mg/ml THF and consequently the amount of initiator needed for gelling could be kept low (5 mol%).

Each arm of the compounds in the G1 and 4arm categories is structurally identical, but the different number of arms resulted in either 4 or 8 crosslinking sites for the compounds in the respective category and gave the gels dissimilar properties, as presented here for the thiol-ene gels.

As expected from considering gel parameters, gels in the 4arm category degraded slower than the corresponding G1 thiol-ene gels (27 and 11 days respectively). There are two reasons for this; firstly, the 4arm gels were made at a higher concentration of building blocks (69%) compared to the G1

category (38%) and secondly, the 4arm gels were made in an 8 + 2 arm system while G1 gels were of a 4 + 4 arm system. Both reasons result in a higher crosslink density for the 4arm gels and, hence, slower degradation.

A consequence of an increased number of crosslinks is a denser gel, which swells less. This was confirmed by comparing the swelling ratios of "Blank" formulations at equilibrium for the G1 (**Figure 44**) and 4arm (**Figure 46**) categories, which were 10 and 4 respectively.

These two categories had different drug loading capacities; 2 and 4 Dex molecules per carrier for the G1 and 4arm category respectively. The different loadings were clearly mirrored by the amount of detected drug released from the two categories; 29 mg Dex/g gel (**Figure 43**) and 65 mg Dex/g gel (**Figure 45**) for the G1 and 4arm categories respectively.

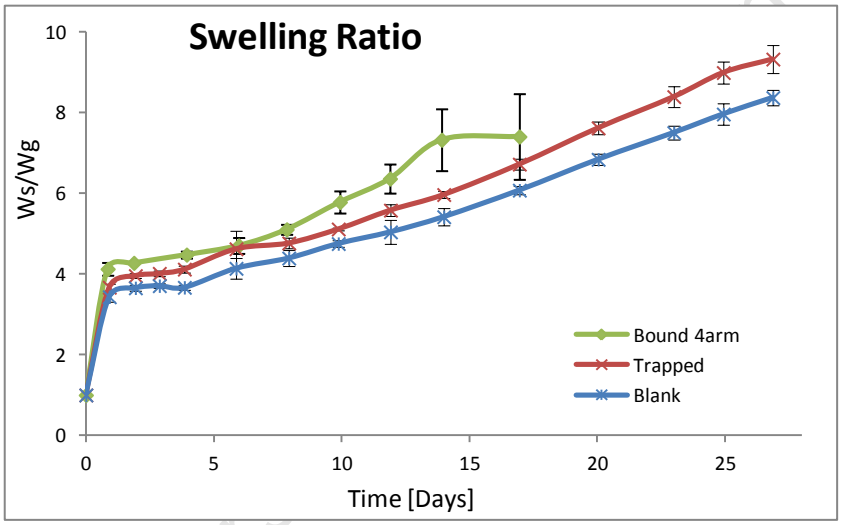

Figure 46: Thiol-ene addition gels at 69% in THF with 5 mol% Irgacure 2959. Formulation (building blocks); Bound 4arm (PEG-4arm-G1-8Ac-4Dex (**25**) and 2dPEG-2SH), Trapped and Blank (PEG-4arm-G1-8Ac-4Act (**24**) and 2dPEG-2SH).

Compound **25** was reprecipitated prior to the crosslink density experiment in order to remove impurities from spontaneous crosslinking. As already mentioned, the compounds with high Dex loading (4arm and G2 categories) were difficult to precipitate in diethyl ether and at this occasion the product came out poorly with reduced quality of gel formation as a result, hence mesh size determination of 4arm gels was omitted.

3.3.2.3 Second Generation, 2-armed Backbone

The "Bound" formulation in the G2 category displayed a zero order drug release, until the degrading gels were treated with alkali to force the last amount of Dex to release with a burst (**Table 10**, **Figure 47**).

Table 10: R^2-values from curve fitting of a linear line to calculated curves based on experimental data, all combinations are not applicable (n.a.), and the best curve fits are highlighted in yellow.

G2	Hixson-Crowell Equation	Korsmeyer-Peppas Equation	n	Zero Order Rate Equation	First Order Rate Equation
"Bound"	n.a.	n.a.	n.a.	0.979	0.945
"Trapped"	0.880	0.844	0.38	0.599	0.950

The G2 compounds were less soluble than the 4arm compounds and were dissolved at 300 mg/ml THF, but 5% of initiator was still sufficient for gelling to occur.

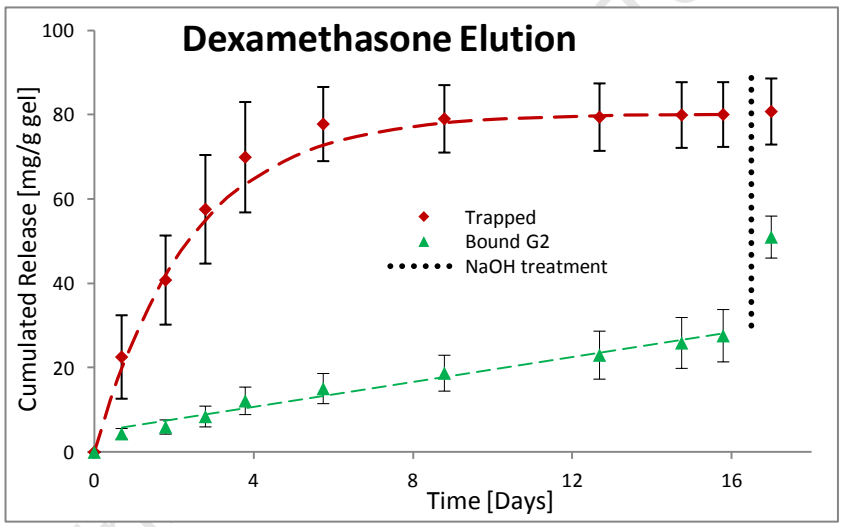

Figure 47: Experimental data (with error bars) and calculated curve fits (dashed lines) for thiol-ene addition gels at 50% in THF with 5 mol% Irgacure 2959. Formulation (building blocks; detected amount of drug); Trapped (PEG-G2-8Ac-6Act (**28**) and 2dPEG-2SH; 77%) and Bound G2 (PEG-G2-8Ac-6Dex (**29**) and 2dPEG-2SH; 37%).

Although a lower total amount of Dex was detected (51 mg/g gel) compared to the "Bound" formulation in the 4arm category (65 mg/g gel; **Figure 45**), the G2 gels had the highest drug loading density of the three dendritic categories developed in this work, namely 138 mg Dex/g gel. The corresponding values for the G1 and 4arm categories are 48 and 75 mg Dex/g gel, respectively. The lower amount of detected Dex has already been suggested to originate from the gelling protocol and secondary release.

The release of trapped drug followed a first order profile, but the elution mechanism could not be established by the Hixson-Crowell and Korsmeyer-Peppas equations (**Table 10**). Nonetheless, by comparing the elution and swelling curves, the elution was considered to be controlled by diffusion (**Figure 47** and **48**).

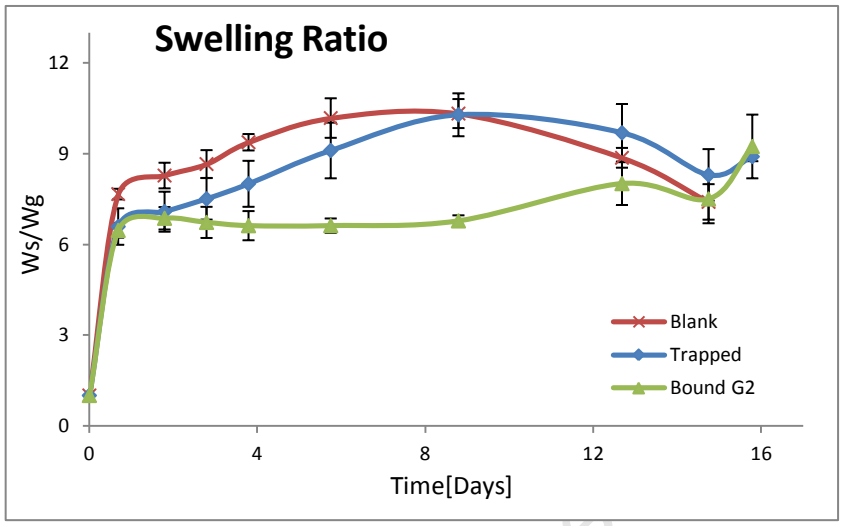

Figure 48: Thiol-ene addition gels at 50% in THF with 5 mol% Irgacure 2959. Formulation (building blocks); Blank and Trapped (PEG-G2-8Ac-6Act (**28**) and 2dPEG-2SH) and Bound G2 (PEG-G2-8Ac-6Dex (**29**) and 2dPEG-2SH).

Once again the close relationship between crosslink density, swelling and degradation is demonstrated experimentally. By comparing the "Blank" formulations of respective category it is found that the 4arm gels, made at a concentration of 69% with an equilibrium swelling of 4, degraded in 27 days (**Figure 46**) while G2 gels, which were made at a lower concentration (50%) had a higher equilibrium swelling (8) and shorter degradation period (15 days; **Figure 48**). Both formulations were of an 8 + 2 arm system.

The "Bound" formulation swelled somewhat less than the "Blank" and "Trapped" formulations (**Figure 48**) and the calculated relative mesh size was much lower than for the "Blank" formulation (**Figure 49**). Although both parameters indicate a higher crosslink density for the "Bound" formulation all three formulations degraded within a similar period of time and, hence, their crosslink densities were probably similar.

This assumption is supported by regarding the water solubility of the building blocks. Compound **29** is not water soluble and consequently gels build from compound **29** are less hydrophilic then gels build from the water soluble compound **28**. Therefore the "Bound G2" gels have a disfavoured interaction with water leading to a lower degree of swelling than for the "Blank" gels. The variables in **Equation 7** and **8** are based on swelling, and the equations could be simplified

to $\zeta \propto \text{swelling}^{-1}$. Consequently, the lower degree of swelling for the "Bound" formulation, caused by hydrophobicity, transforms via **Equation 7** and **8** into a smaller increase of mesh size than for the "Blank" formulation.

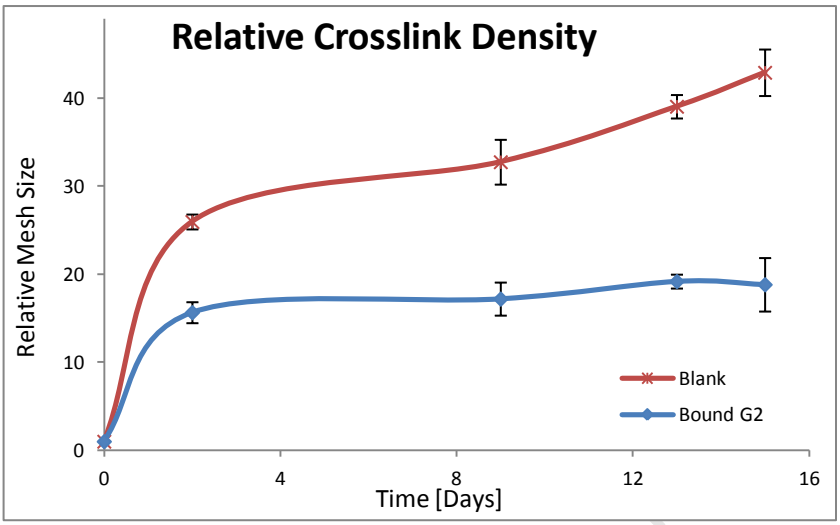

Figure 49: Thiol-ene addition gels at 50% in THF with 5 mol% Irgacure 2959 (n =2). Formulation (building blocks); Blank (PEG-G2-8Ac-6Act (**28**) and 2dPEG-2SH) and Bound G2 (PEG-G2-8Ac-6Dex (**29**) and 2dPEG-2SH).

3.3.3 Summary

In **Table 11** gelling parameters for the "Bound" formulation of each category and the resulting gel properties are summarised.

Table 11: Parameters and results for "Bound" gels.

	Gel Concentration [% W/V]	**Functionality of Drug-Carrier Unit**	**Added Building Blocks**	**Equilibrium Swelling** W_s/W_g	**Amount of Detected Drug** % of loaded	mg/g gel	**Degradation Time** [Days]
RaAc-d4	20	3	20PEG-8Ac 10dPEG-4SH	3	60	2.7	15
RaIAE-d4					57	3.3	
RaAc-d2	13	1	20PEG-8VS 2dPEG-2SH	2	49	2.3	17
RaIAE-d2				4	29	2.2	19
RaDilAE	18	2	10dPEG-4SH	2	47	17	11
G1 (Conjugate addition)	19	4	10nPEG-4SH	5	49	6	5
G1 (Thiol-ene addition)	38			18	60	29	11
4arm	69	8	2dPEG-2SH	4	87	65	27
G2	50	8	2dPEG-2SH	8	37	51	16

3.4 Reporter Assays

Supernatant from the “Blank”, “Trapped” and “Bound” gel formulations of the mono-functional and dendritic approaches were tested on appropriate cell types in order to verify maintained biological activity of the released drugs.

3.4.1 Rapamycin

In **Figure 50** the reduction of cell proliferation after treatment with known amounts of Ra is shown. The reduction was smaller than expected and the proliferation was only reduced to 77% for the treatment with 2000 µg Ra/l cell medium (left hand side graph).

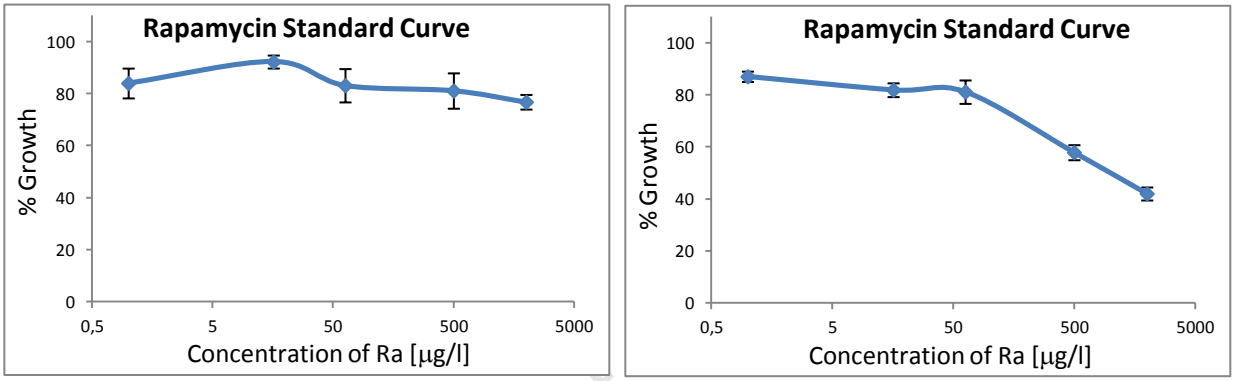

Figure 50: Influence of rapamycin on smooth muscle cell proliferation, n =3.

In the literature however, a treatment of 100 µg Ra/l cell medium reduced the proliferation to approximately 65-70% (Reddy *et al.* 2008; Yallapu *et al.* 2008). The results in the literature were obtained by UV quantification of a formazan dye formed by adding an assay reagent to cell samples. The results in this work were obtained by measuring the luminescence from adenosine 5-triphosphate (ATP) dependent luciferase activity obtained by another cell assay. Since the outcome from both assays is proportional to the number of living cells it was assumed that the measured reduction in cell proliferation should be similar.

The discrepancy is believed to originate from the recommended protocol (10 min incubation time in T_{room} with only initial shaking) where the incubation of cells and cell viability reagent is not sufficient for thorough cell lyses to occur. For samples with not fully lysed cells only a partial amount of the present cells are measured and the results are inaccurate. Therefore the experiment was repeated, and by using a modified protocol the monitored reduction of proliferation was more pronounced (**Figure 50**, right hand side graph), probably as a result of increased cell lyses.

The Ra concentration in the prepared cell treatments was within the linear range (63 -2000 µg /l) of the standard curve (**Table 12**).

Table 12: UV quantified concentrations of eluted rapamycin from the RaIAE-d4 category.

Supernatant Treatments	Elution Day	µg Ra/l media
"Bound" gels	2	220
	5	410
	11	1020
	15	950
"Trapped" gels	2	1370
	3	1170
	5	870
	15	160

The resulting cell growth from treating cells with Ra containing supernatants is shown in **Figure 51**. Treatment with supernatant from the "Blank" gels, to start with, resulted in a reduced proliferation at both time points (~80%). This is however considered to be within the experimental error since the reduction for cell treatment with low amounts of Ra in the standard curve (**Figure 50**, right hand side graph) levelled out at a similar value.

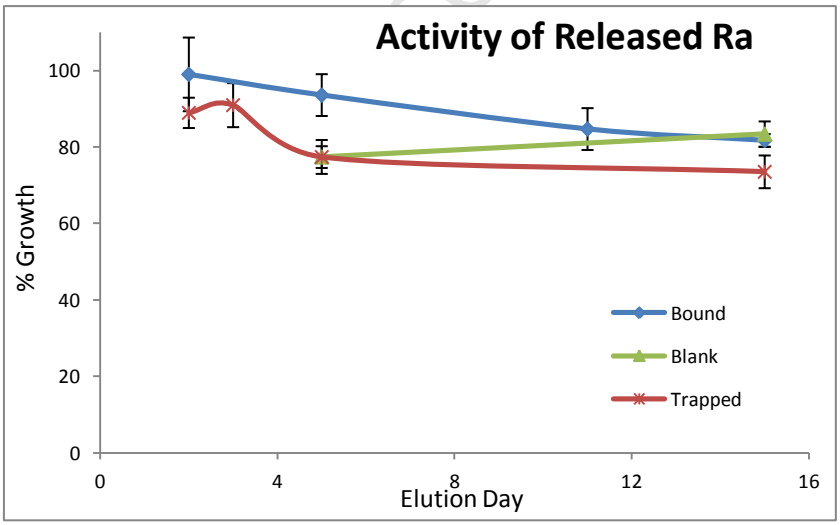

Figure 51: Cell treatment with supernatant from the three RaIAE-d4 gel formulations.

Unexpectedly though, the resulting cell growth from treatment with supernatant from the "Bound" gels were in the same range as the "Blank" treatment. The conclusion would have been that the eluted Ra was inactive if not for the results of the "Trapped" treatment. The eluted Ra from these gels also revealed low or no activity towards the cells even though the "Trapped" Ra was the very same unmodified drug that was used for the standard curve where it effectively reduced proliferation. The difference in cell treatment methodology between the standard curve and the

eluted drugs is that the former treatment was made up in MeOH and diluted with PBS-1 and media while the drug in the latter case was eluted in PBS-1 and diluted with MeOH and media. Thus, it was assumed that there is an, as yet undefined, parameter in the gel supernatants that inhibits the effect of Ra or impedes the assay. To uncover the particular situation further investigation is required.

3.4.2 Dexamethasone

Figure 52 shows how Dex, in a dose dependent manner, induced luciferase expression as measured by a standard luciferase assay. Both the lowest (10^{-8} M) and highest (10^{-6} M) concentrations for linear response were in the same range as previously reported results (Wilson *et al.* 2002).

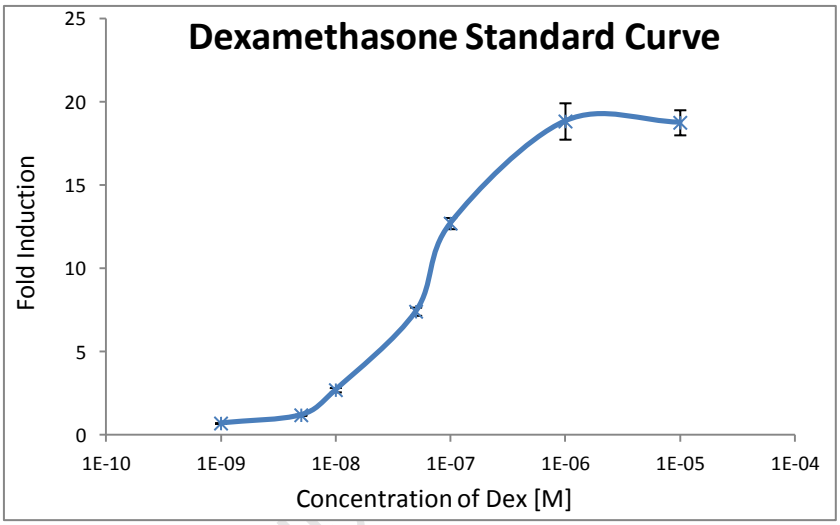

Figure 52: Dexamethasone induced luciferase expression, n =3.

Supernatant from the G1 conjugate addition gel formulations were tested for maintained biological activity (**Figure 53**). The degradation products from the "Blank" gels did not increase the luciferase expression compared to untreated cells. Dex containing supernatant from the "Trapped" formulation was active, but the activity was decreasing and was all but absent on day 5. "Bound" gels on the other hand eluted Dex at a relatively constant rate, which was also reflected by the measured activity of "Bound" gel supernatant.

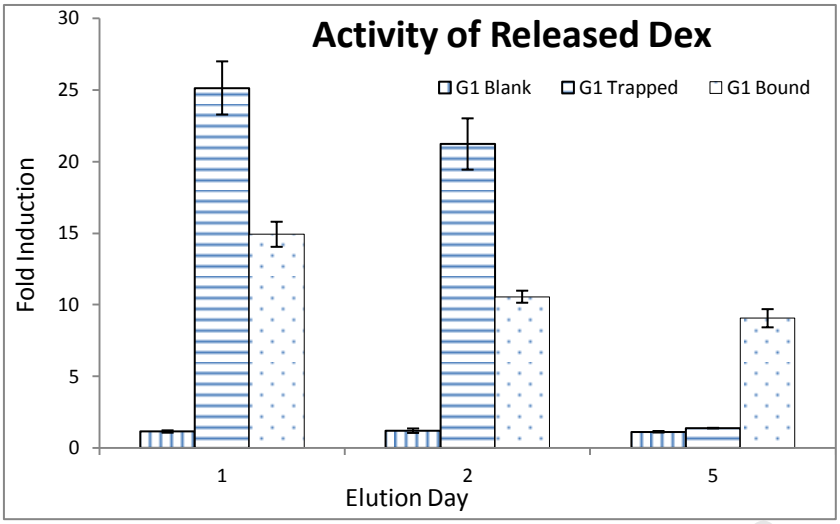

Figure 53: Cell treatment with supernatant from the G1 conjugate addition gel formulations (n =3).

By considering **Figure 54** it is evident that supernatant from "Bound" gels, in case of both 4arm and G2, is active at a nearly constant level from the first days of drug elution all the way to gel dissolution, where supernatant from "Trapped" gels is inactive.

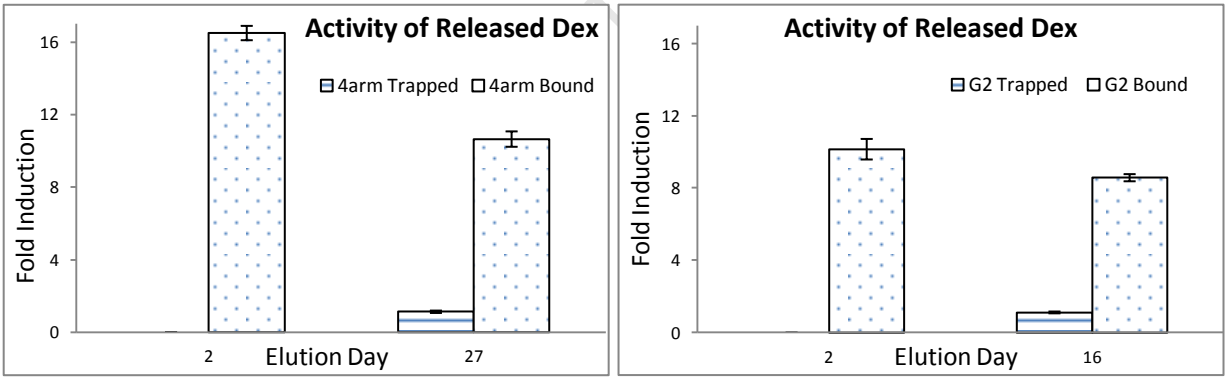

Figure 54: Cell treatment with supernatant from the 4arm and G2 categories, respectively (n =3).

To avoid any potentially negative effect on cells from THF the supernatant from day 1 was not tested for the 4arm and G2 categories. Supernatant was instead tested for day two and also for the last day of drug elution, prior to alkali treatment, for the "Bound" formulations, while "Trapped" supernatant was only tested for the last day.

The activity measurement of supernatant from "Blank" 4arm and G2 gels was omitted. Since all dendritic categories were built from the same building blocks, only with different geometries, it was assumed that the released degradation products from "Blank" G1 gels were identical to those

released from the 4arm and G2 categories. Therefore supernatant from "Blank" G1 gels is also representative for the 4arm and G2 categories.

The primary hydroxyl group of Dex was used for the drug conjugation in this work. Even though this hydroxyl group interacts with the glucocorticoid receptor (Bledsoe *et al.* 2002) it does not contribute to the biological activity of Dex (Gruneich *et al.* 2004) and is therefore a favourable site for conjugation. As previously mentioned, Dex is believed to be released while still attached to a few methylene groups followed by a triazole. However, (Rebuffat *et al.* 2002) confirmed by an *in vitro* competition binding assay that Dex conjugated at the primary hydroxyl still demonstrates affinity to a rat glucocorticoid receptor.

The amount of Dex in the supernatants either measured by UV or calculated from the fold inductions, were in the same range (**Table 13**).

Table 13: Comparison of Dex concentrations in supernatant obtained by either UV-measurements (Sen *et al.*) or fold inductions (F.I.). Concentrations are given in mg/l supernatant. For fold inductions too high for the linear range of the standard curve the corresponding concentration is marked by a dash.

		G1 Conjugate Addition			**4arm**		**G2**	
		Day 1	*Day 2*	*Day 5*	*Day 2*	*Day 27*	*Day 2*	*Day 16*
"Bound"	**UV**	8	11	5	18	8	7	6
	F.I.	47	33	26	51	33	29	26
"Trapped"	**UV**	75	31	0	74	0	79	1
	F.I.	-	-	0	-	0	-	0

Concentrations in gel supernatant exceeding the aqueous solubility limit of Dex are attributed to the secondary release mechanism where Dex is released while still linked to a piece of PEG keeping the drug in solution.

4 CONCLUSIONS

The results in this thesis confirm the hypothesis that zero order release kinetics is obtainable from injectable and degradable hydrogels by covalently attaching the drug to the hydrogel matrices.

Regarding the specific aims stated in the introduction (chapter 1.5), each corresponding conclusion is listed in the following text.

Building blocks:

Multi-arms, crosslinkers, drug derivatives and drug conjugates were successfully synthesised with moderate to excellent yields and the product structures were confirmed by appropriate analytical methods. The drug loading density was varied by design of the carriers and was 1 Ra per carrier for the mono-functional approach and 2, 4 or 6 Dex molecules per carrier for the dendritic approach. However, the loading of 4 or 6 Dex molecules per carrier were too high to maintain water solubility of the carrier.

Hydrogels:

Conjugate and thiol-ene addition reactions were investigated for gelling of the building blocks. For conjugate addition the gelling rate was shown to be pH dependent. Conditions for thiol-ene addition were optimised by tuning the concentration of building blocks, amount of initiator and irradiation time. Differences between the gelling methods were investigated and assessed to mainly consist of a large proportion of homo-polymerisation for the thiol-ene addition, which results in slower gel degradation.

Gel degradation was tuned by using multi-arms modified with either Ac or VS groups crosslinked by either dPEG-SH or nPEG-SH, by varying the number of crosslinking sites and by using different crosslinking methods. The gels made in this work showed a range of degradation times between 5 and 129 days.

Drug elution:

The elution profiles of covalently incorporated drugs were of zero order for both the mono-functional and dendritic approaches and were sustained for 5-28 days depending on the individual gel formulation. Additionally, by incorporating Ra via either an IAE or Ac linker the elution rate was moderately, but significantly, different, prolonging the time to reach the half amount of total drug

elution from 9.3 to 10.2 days and from 5.1 to 9.7 days, for the RaX-d4 and RaX-d2 formulations respectively. Dex released from the dendritic gels showed a preserved biological activity which was roughly constant during the entire elution period for the "Bound" formulations but declining for the "Trapped" formulations, which corresponds well with the drug elution profiles obtained by UV measurements.

The release mechanism of "Trapped" drugs could not be described by the Hixson-Crowell or Korsmeyer-Peppas equations, but by comparing elution and swelling curves the release was considered to be controlled by diffusion. The "Trapped" release followed either first order or burst release kinetics

Thus, the hydrogel concepts developed in this work are promising tools for controlled drug delivery in general and local delivery of Ra and Dex with the potential to ameliorate cardiovascular healing in particular. Additionally, from a rigorous search in the present literature it is concluded that the work in this thesis is a substantial and significant contribution to the field of controlled drug delivery in terms of (**A**) slow release of Ra obtained by covalent incorporation into hydrogels, (**B**) the use of unique PEG-based dendrimers to incorporate Dex into a hydrogel and (**C**) zero order sustained release of Dex at physiological pH.

4.1 Complementary Work

The content in this thesis is a strong foundation from which further research has the potential to be developed, such work might for instance include the following topics;

- To develop hydrogels with a slower degradation rate by combining 20PEG-8VS and 10dPEG-4SH or by tuning the weakening of ester crosslinks with other functional groups than thio-ethers. This will prevent the interruption of drug elution by gel dissociation.
- To further develop these drug delivery concepts by combining the simple synthesis of the mono-functional approach with the multivalency and orthogonal properties of the dendritic approach.
- To continue the evaluation of the drug eluting and gel degradation properties in a biologically active medium, such as fetal bovine serum.
- To evaluate the developed hydrogels *in vivo*, initially for inflammatory response, and if biocompatibility is good, also for post MI amelioration and graft patency.
- To include other drugs, such as atorvastatin, in the slow release concepts developed in this thesis.

5 ACKNOWLEDGEMENTS

Many persons contributed to the development and completion of this thesis and I would like to show these persons my sincere gratitude.

During dull times when failed experiments and unsolved problems darkened my mood there was always a smile and cheerful encouragement to receive from dear Irina My, which to a great part inspired me to continue.

General acknowledgement is directed to Onderneming and my neighbors for making Cape Town my home, to Welmoed, Vergelegen, Seidelberg and all the other wine estates around Cape Town for the merry times provided, to Devil's Peak for its beauty and the ocean for the adventures.

UCT-side

Most of all I want to put all light on my excellent supervisor Dr. **Deon Bezuidenhout** who in an encouraging and supportive manner guided me through this work. Many thanks are directed to Prof. Peter Zilla for accepting me as a PhD student in the Cardiovascular Research Unit and finding financial aid for a majority of the project. The many hours in the lab were brightened by good company of Anel Oosthuysen who is sincerely accredited for valuable input on method development and for daily giving a helping hand. Mona Bracher is greatly thanked for help with preparing cells, planning and interpreting cell experiments. Dr. Karen Kadner is acknowledged for assistance on determining pH dependence of conjugate addition.

Late Prof. Wolf Brandt (Dept. of Molecular & Cellular Biology) and Dr. Marietjie Stander (University of Stellenbosch, Central Analytical Facilities) were both great assets for access, development and interpretation of several analysis methods. Dr. Gareth Arnott (Stellenbosch University, Dept. Chemistry & Polymer Science) is accredited for input during problem solving of the mono-functional approach.

KTH-side

The knowledge and experience accumulated by **Yvonne Hed** were essential to develop the dendritic approach and she was also a major support and a good friend during long lab hours. Yvonne was involved in several of the synthesis; particularly she produced the azide anhydride, purified compound **15**, deprotected compound **20** and acrylated compound **21**. Prof. Anders Hult earns my

sincere gratefulness for finding complementary funds to finish the project in Cape Town and for welcoming me to his lab at KTH. Dr. Michael Malkoch is thanked for sharing his dendritic chemistry, valuable input on planning the dendritic approach and sharing his experience. Thanks are directed to Kim Öberg for aiding my project at KTH and preparing compounds for subcutaneous implants at UCT and to Prof. Mats Johansson for guidance in the field of thiol-ene chemistry.

Apart from the respective university institutions economic aid was also obtained from my parents Stefan and Bianca Ahrenstedt and the following private funds: Gålöstiftelsen and Lars Hiertas Stiftelse.

6 APPENDIX I; ATORVASTATIN

An additional drug considered for gel incorporation in this PhD project was Atorvastatin (At), a member of the statin class of drugs. This drug was chosen on behalf of its documented ability to balance cholesterol levels (Schachter 2004), reduce atherosclerosis (Blumenthal 2000) and inhibit tumour cell growth (Bellosta *et al.* 2000). In addition, statins have the ability to reduce plasma levels of C-reactive protein, a general marker for systemic inflammation and a predictor of cardiovascular events (Ridker *et al.* 2002). In a study by Ridker *et al.* the statin treatment of apparently healthy patients with normal cholesterol levels but elevated levels of C-reactive protein reduced the occurrence of cardiovascular events by 50% compared to the placebo group (Ridker *et al.* 2008).

The collective benefits of statin treatment on cardiovascular diseases strengthened the motivation for developing a platform for controlled delivery of At.

Atorvastatin was successfully isolated from commercial tablets sold for oral delivery and was analysed by MS (**Figure 55**).

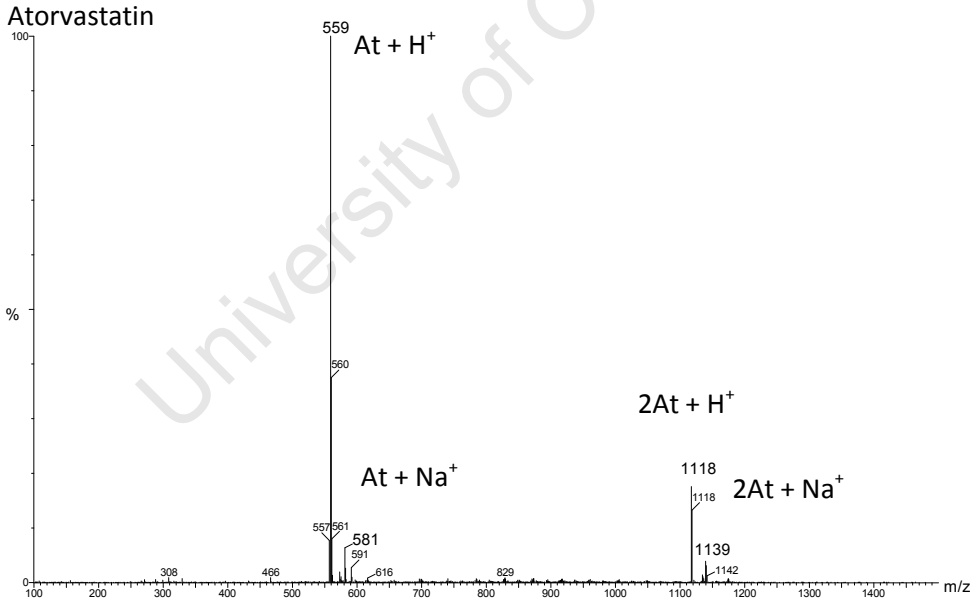

Figure 55: ESI-MS of isolated atorvastatin.

However, it was observed in some cases that the compound underwent spontaneous ring-closing during handling as detected by loss of H_2O in the MS spectra (**Scheme 12**). This was not considered a major problem since the ring-closed derivative was assumed to ring-open again in contact with aqueous solutions, such as blood. But, in order to maximise the amount of ring-opened At during

isolation small amounts of water was always added to the organic solvents during the purification steps.

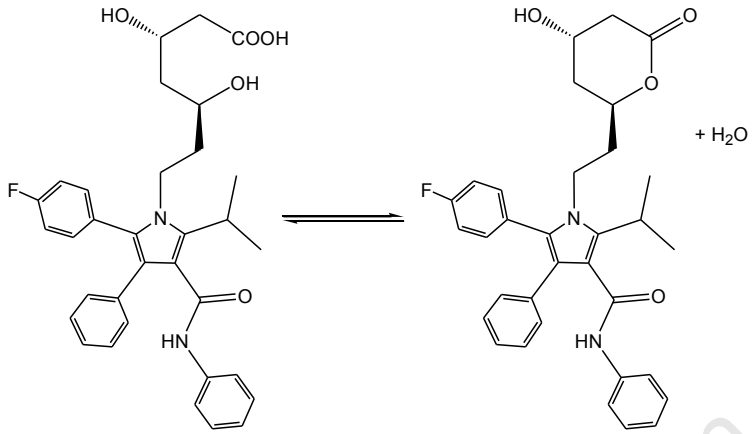

Scheme 12: Reversible ring-closing of atorvastatin.

The isolated drug was further acrylated for subsequent PEGylation, but the acrylation reaction however, was quenched by presence of water and therefore required the use of dry solvents which resulted in acrylation of both the ring-closed and ring-opened derivatives. In addition, the ring-opened derivative was acrylated at both hydroxyl positions (**Scheme 13**).

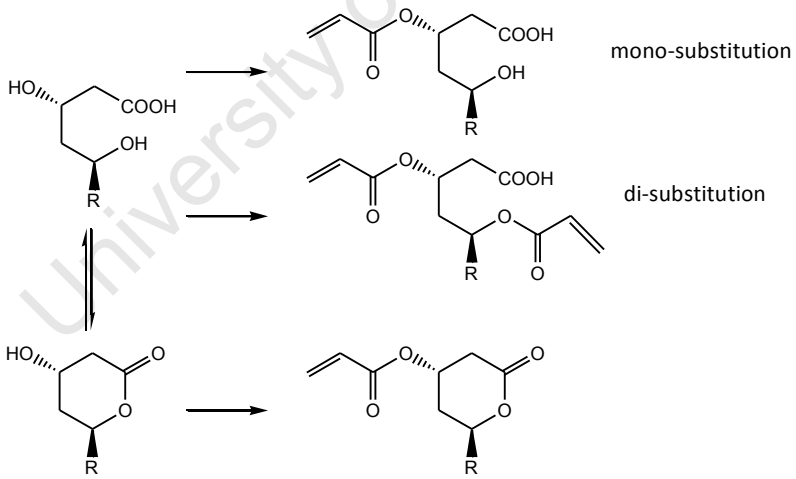

Scheme 13: Acrylation of atorvastatin results in a mixture of three compounds, R represents the main body of the drug.

At this stage the PEGylation protocol was not fully developed because the product degradation during analysis was not yet identified. Therefore this project was put on hold in favour of development of the PEGylation methods of Ra and Dex.

REFERENCES

Ahn, S., Kasi, R. M., Kim, S., Sharma, N. and Zhou, Y. "**Stimuli-responsive polymer gels**." *Soft Matter*, **2008**, 4, 1151-1157

Aimetti, A. A., Machen, A. J. and Anseth, K. S. "**Poly(ethylene glycol) hydrogels formed by thiol-ene photopolymerization for enzyme-responsive protein delivery**." *Biomaterials*, **2009**, 30, 30, 6048-54

Alexis, F., Venkatraman, S. S., Rath, S. K. and Boey, F. "**In vitro study of release mechanisms of paclitaxel and rapamycin from drug-incorporated biodegradable stent matrices**." *J Controlled Release*, **2004**, 98, 1, 67-74

Andreadis, S. T. and Geer, D. J. "**Biomimetic approaches to protein and gene delivery for tissue regeneration**." *Trends in Biotechnology*, **2006**, 24, 7, 331-7

Andreopoulos, F. M., Beckman, E. J. and Russell, A. J. "**Light-induced tailoring of PEG-hydrogels properties**." *Biomaterials*, **1998**, 19, 1343-1352

Anseth, K. S., Bowman, C. N. and Brannon-Peppas, L. "**Mechanical properties of hydrogels and their experimental determination**." *Biomaterials*, **1996**, 17, 17, 1647-57

Antoni, P., Hed, Y., Nordberg, A., Nyström, D., von Holst, H., Hult, A. and Malkoch, M. "**Bifunctional dendrimers: from robust synthesis and accelerated one-pot postfunctionalization strategy to potential applications**." *Angewandte Chemie International Edition*, **2009**, 48, 12, 2126-30

Baeyens, V., Kaltsatos, V., Boisrame, B., Varesio, E., Veuthey, J. L., Fathi, M., Balant, L. P., Gex-Fabry, M. and Gurny, R. "**Optimized release of dexamethasone and gentamicin from a soluble ocular insert for the treatment of external ophthalmic infections**." *J Control Release*, **1998**, 52, 1-2, 215-20

Bahney, C. S., Lujan, T. J., W., H. C., Bottlang, M., West, J. L. and Johnstone, B. "**Visible light photoinitiation of mesenchymal stem cell-laden bioresponsive hydrogels**." *European Cells and Materials*, **2011**, 22, 43-45

Bellosta, S., Ferri, N., Bernini, F., Paoletti, R. and Corsini, A. "**Non-lipid-related effects of statins**." *Annals of Medicine*, **2000**, 32, 3, 164-76

Benton, J. A., Fairbanks, B. D. and Anseth, K. S. "**Characterization of valvular interstitial cell function in three dimensional matrix metalloproteinase degradable PEG hydrogels**." *Biomaterials*, **2009**, 30, 34, 6593-603

Bestard, O., Cruzado, J. M. and Grinyo, J. M. "**Inhibitors of the mammalian target of rapamycin and transplant tolerance**." *Transplantation*, **2009**, 87, 8 Suppl, S27-9

Blair, S. N., Kohl, H. W., 3rd, Paffenbarger, R. S., Jr., Clark, D. G., Cooper, K. H. and Gibbons, L. W. "**Physical fitness and all-cause mortality. A prospective study of healthy men and women**." *Journal of the American Medical Association*, **1989**, 262, 17, 2395-2401

Bledsoe, R. K., Montana, V. G., Stanley, T. B., Delves, C. J., Apolito, C. J., McKee, D. D., Consler, T. G., Parks, D. J., Stewart, E. L., Willson, T. M., Lambert, M. H., Moore, J. T., Pearce, K. H. and Xu, H. E. "**Crystal structure of the glucocorticoid receptor ligand binding domain reveals a novel mode of receptor dimerization and coactivator recognition**." *Cell*, **2002**, 110, 1, 93-105

Blom, D. J. and Fith, J. C. "**A clinical approach to dyslipidaemia**." *Journal of the South African Heart Association*, **2005**, 2, 3, 20-31

Blumenthal, R. S. "**Statins: Effective antiatherosclerotic therapy**." *American Heart Journal*, **2000**, 139, 4, 577-583

Boluyt, M. O., Li, Z. B., Loyd, A. M., Scalia, A. F., Cirrincione, G. M. and Jackson, R. R. "**The mTOR/p70(S6K) signal transduction pathway plays a role in cardiac hypertrophy and influences expression of myosin heavy chain genes in vivo**." *Cardiovascular Drugs and Therapy*, **2004**, 18, 4, 257-267

Brunzell, J. D., Davidson, M., Furberg, C. D., Goldberg, R. B., Howard, B. V., Stein, J. H. and Witztum, J. L. "**Lipoprotein management in patients with cardiometabolic risk: consensus statement from the American Diabetes Association and the American College of Cardiology Foundation**." *Diabetes Care*, **2008**, 31, 4, 811-22

Buss, S. J., Muenz, S., Riffel, J. H., Malekar, P., Hagenmueller, M., Weiss, C. S., Bea, F., Bekeredjian, R., Schinke-Braun, M., Izumo, S., Katus, H. A. and Hardt, S. E. "**Beneficial effects of Mammalian target of rapamycin inhibition on left ventricular remodeling after myocardial infarction**." *Journal of the American College of Cardiology*, **2009**, 54, 25, 2435-46

Cascone, M. G., Pot, P. M., Lazzeri, L. and Zhu, Z. "**Release of dexamethasone from PLGA nanoparticles entrapped into dextran/poly(vinyl alcohol) hydrogels**." *J Mater Sci Mater Med*, **2002**, 13, 3, 265-9

Castro, D. and Pacetti, S. D. (2010). Poly(butylmethacrylate) and rapamycin coated stent. **7 691 401**.

Chandra, J., Dua, T., Narayan, S., Jain, V., Sharma, S. and Dutta, A. K. "**Dexamethasone therapy in chronic ITP**." *Indian Pediatr*, **2000**, 37, 6, 647-50

Chen, M. C., Tsai, H. W., Liu, C. T., Peng, S. F., Lai, W. Y., Chen, S. J., Chang, Y. and Sung, H. W. "**A nanoscale drug-entrapment strategy for hydrogel-based systems for the delivery of poorly soluble drugs**." *Biomaterials*, **2009**, 30, 11, 2102-11

Cheng, Y., Xu, Z., Ma, M. and Xu, T. "**Dendrimers as drug carriers: applications in different routes of drug administration**." *Journal of Pharmaceutical Sciences*, **2008**, 97, 1, 123-43

Cohn, J. N. and Tognoni, G. "**A Randomized Trial of the Angiotensin-Receptor Blocker Valsartan in Chronic Heart Failure**." *N Engl J Med*, **2001**, 345, 1667-1675

Cole, T. J. "**Glucocorticoid action and the development of selective glucocorticoid receptor ligands**." *Biotechnol Annu Rev*, **2006**, 12, 269-300

Cramer, N. B. and Bowman, C. N. "**Kinetics of thiol-ene and thiol-acrylate photopolymerizations with real-time fourier transform infrared**." *Journal of Polymer Science: Part A: Polymer Chemistry*, **2001**, 39, 3311-3319

Cramer, N. B., Reddy, S. K., O'Brien, A. K. and Bowman, C. N. "**Thiol-ene photopolymerization mechanism and rate limiting step: changes for various vinyl functional group chemistries**." *Macromolecules*, **2003**, 36, 7964-7969

Cruickshank, J. M. "**Beta blockers in hypertension**." *Lancet*, **2010**, 376, 415-416

Diaz, D., Morin, E., Schön, E., Budin, G., Wagner, A. and Remy, J. "**Tailoring drug release profile of low-molecular weight hydrogels by supramolecular co-essembly thiol-ene orthogonal coupling**." *J Mat Chem*, **2010**, 21, 641-644

Dobner, S., Bezuidenhout, D., Govender, P., Zilla, P. and Davies, N. "**A synthetic non-degradable polyethylene glycol hydrogel retards adverse post-infarct left ventricular remodeling**." *Journal of Cardiac Failure*, **2009**, 15, 7, 629-36

DuBose, J. W., Cutshall, C. and Metters, A. T. "**Controlled release of tethered molecules via engineered hydrogel degradation: model development and validation**." *Journal of Biomedical Materials Research Part A*, **2005**, 74, 1, 104-16

Ehrbar, M., Metters, A., Zammaretti, P., Hubbell, J. A. and Zisch, A. H. "**Endothelial cell proliferation and progenitor maturation by fibrin-bound VEGF variants with differential susceptibilities to local cellular activity**." *Journal of Controlled Release*, **2005**, 101, 1-3, 93-109

Elandaloussi, E. H., Somogyi, A., Buyle Padias, A., Bates, R. B. and Hall Jr, H. K. "**Resequencing of Comonomer Units of Well-Defined Vectra Oligomers during MALDI-TOF Mass Spectral Measurements**." *Macromolecules*, **2006**, 39, 6913-6923

Elbert, D. L., Pratt, A. B., Lutolf, M. P., Halstenberg, S. and Hubbell, J. A. "**Protein delivery from materials formed by self-selective conjugate addition reactions**." *Journal of Controlled Release*, **2001**, 76, 1-2, 11-25

Ertl, G. and Frantz, S. "**Healing after myocardial infarction**." *Cardiovascular Research*, **2005**, 66, 1, 22-32

Farr, M., Garvey, K., Bold, A. M., Kendall, M. J. and Bacon, P. A. "**Significance of the hydrogen ion concentration in synovial fluid in rheumatoid arthritis**." *Clinical and Experimental Rheumatology*, **1985**, 3, 2, 99-104

Fittkau, M. H., Zilla, P., Bezuidenhout, D., Lutolf, M. P., Human, P., Hubbell, J. A. and Davies, N. "**The selective modulation of endothelial cell mobility on RGD peptide containing surfaces by YIGSR peptides**." *Biomaterials*, **2005**, 26, 2, 167-74

Flory, P. J. and Rehner, R. J. "**Statistical mechanics of crosslinked polymer networks. II Swelling** " *Journal of Chemical Physics*, **1943**, 11, 512-520

Forrest, M. L., Won, C., Malick, A. W. and Kwon, G. S. "**In vitro release of the mTOR inhibitor rapamycin from poly(ethylene glycol)-b-poly((epsilon-caprolactone) micelles**." *J Controlled Release*, **2006**, 110, 370-377

Freemantle, N., Cleland, J., Young, P., Mason, J. and Harrison, J. "**beta blockade after myocardial infarction: systematic review and meta regression analysis**." *British Medical Journal*, **1999**, 318, 1730-1737

Frokjaer, S. and Otzen, D. E. "**Protein drug stability: a formulation challenge**." *Nature Reviews Drug Discovery*, **2005**, 4, 4, 298-306

Ganji, F. and Farahani-Vasheghani, E. "**Hydrogels in controlled drug delivery systems**." *Iranian Polymer Journal*, **2009**, 18, 1, 63-88

Gaumann, A., Schlitt, H. J. and Geissler, E. K. "**Immunosuppression and tumor development in organ transplant recipients: the emerging dualistic role of rapamycin**." *Transplant International*, **2008**, 21, 3, 207-17

Gombotz, W. R. and Pettit, D. K. "**Biodegradable polymers for protein and peptide drug delivery**." *Bioconjugate Chemistry*, **1995**, 6, 4, 332-51

Greenberg, B., Quinones, M. A., Koilpillai, C., Limacher, M., Shindler, D., Benedict, C. and Shelton, B. "**Effects of Long-term Enalapril Therapy on Cardiac Structure and Function in Patients With Left Ventricular Dysfunction; Results of the SOLVD Echocardiography Substudy** " *Circulation*, **1995**, 91, 2573-2581

Gruneich, J. A., Price, A., Zhu, J. and Diamond, S. L. "**Cationic corticosteroid for nonviral gene delivery**." *Gene Therapy*, **2004**, 11, 8, 668-74

Gurtner, G. C., Werner, S., Barrandon, Y. and Longaker, M. T. "**Wound repair and regeneration**." *Nature*, **2008**, 453, 7193, 314-21

Guvendiren, M. and Burdick, J. A. "**The control of stem cell morphology and differentiation by hydrogel surface wrinkles**." *Biomaterials*, **2010**, 31, 6511-6518

Hamidi, M., Azadi, A. and Rafiei, P. "**Hydrogel nanoparticles in drug delivery**." *Advanced Drug Delivery Reviews*, **2008**, 60, 15, 1638-49

Haraguchi, K. "**Nanocomposite hydrogels**." *Current Opinion in Solid State and Materials Science*, **2007**, 11, 47-54

Harrison, D. E., Strong, R., Sharp, Z. D., Nelson, J. F., Astle, C. M., Flurkey, K., Nadon, N. L., Wilkinson, J. E., Frenkel, K., Carter, C. S., Pahor, M., Javors, M. A., Fernandez, E. and Miller, R. A. "**Rapamycin fed late in life extends lifespan in genetically heterogeneous mice**." *Nature*, **2009**, 460, 7253, 392-5

He, C., Kim, S. W. and Lee, D. S. "**In situ gelling stimuli-sensitive block copolymer hydrogels for drug delivery**." *J Controlled Release*, **2008**, 127, 3, 189-207

Hein, C. D., Liu, X. M. and Wang, D. "**Click chemistry, a powerful tool for pharmaceutical sciences**." *Pharmaceutical Research*, **2008**, 25, 10, 2216-2230

Hennink, W. E. and van Nostrum, C. F. "**Novel crosslinking methods to design hydrogels**." *Advanced Drug Delivery Reviews*, **2002**, 54, 1, 13-36

Hiemstra, C., van der Aa, L. J., Zhong, Z., Dijkstra, P. J. and Feijen, J. "**Novel in Situ Forming, Degradable Dextran Hydrogels by Michael Addition Chemistry: Synthesis, Rheology, and Degradation**." *Macromolecules*, **2007**, 40, 4, 1165-1173

Hoffman, A. S. "**Hydrogels for biomedical applications**." *Advanced Drug Delivery Reviews*, **2002**, 54, 1, 3-12

Hong, R., Han, G., Fernandez, J. M., Kim, B. J., Forbes, N. S. and Rotello, V. M. "**Glutathione-mediated delivery and release using monolayer protected nanoparticle carriers**." *Journal of the American Chemical Society*, **2006**, 128, 4, 1078-9

Horta, A. and Pastoriza, M. A. "**The interaction parameter of crosslinked networks and star polymers**." *European Polymer Journal*, **2005**, 41, 2793-2802

Hossainy, S. F. A., Stewart, G., Williams, M. A., Royal, J., Consigny, P. M., Happ, D. M., Scheinpflug, K. and Hu, T. (2012). 40-O-(2-hydroxy)ethyl-rapamycin coated stent. **8 173 199**

Howard, M. D., Ponta, A., Eckman, A., Jay, M. and Bae, Y. "**Polymer Micelles with Hydrazone-Ester Dual Linkers for Tunable Release of Dexamethasone**." *Pharmaceutical Research*, **2011**, 28, 10, 2435-2446

Huang, X. and Brazel, C. S. "**On the importance and mechanisms of burst release in matrix-controlled drug delivery systems**." *J Controlled Release*, **2001**, 73, 2-3, 121-36

Hubbell, J. A. "**Synthetic biodegradable polymers for tissue engineering and drug delivery**." *Current Opinion in Solid State & Materials Science*, **1998**, 3, 246-251

Ihre, H. R., Padilla De Jesus, O. L., Szoka, F. C., Jr. and Frechet, J. M. "**Polyester dendritic systems for drug delivery applications: design, synthesis, and characterization**." *Bioconjugate Chemistry*, **2002**, 13, 3, 443-52

Ito, T., Fraser, I. P., Yeo, Y., Highley, C. B., Bellas, E. and Kohane, D. S. "**Anti-inflammatory function of an in situ cross-linkable conjugate hydrogel of hyaluronic acid and dexamethasone**." *Biomaterials*, **2007**, 28, 10, 1778-86

Jo, Y. S., Gantz, J., Hubbell, J. A. and Lutolf, M. P. "**Tailoring hydrogel degradation and drug release via neighboring amino acid controlled ester hydrolysis**." *Soft Matter*, **2009**, 5, 440-446

Jolly, C., Hessler, R., Dhanasingh, A. and Groll, J. (2009). Hydrogel-Filled Drug Delivery Reservoirs. **20100121422**.

Kadner, K., Dobner, S., Franz, T., Bezuidenhout, D., Sirry, M. S., Zilla, P. and Davies, N. H. "**The beneficial effects of deferred delivery on the efficiency of hydrogel therapy post myocardial infarction**." *Biomaterials*, **2012**, 33, 2060-2066

Katz, A. M. "**Maladaptive growth in the failing heart: The cardiomyopathy of overload**." *Cardiovascular Drugs and Therapy*, **2002**, 16, 3, 245-249

Khandare, J. and Minko, T. "**Polymer–drug conjugates: Progress in polymeric prodrugs**." *Progress in Polymer Science*, **2006**, 31,

Kim, D. H. and Martin, D. C. "**Sustained release of dexamethasone from hydrophilic matrices using PLGA nanoparticles for neural drug delivery**." *Biomaterials*, **2006**, 27, 15, 3031-7

Kim, I. H., Kong, H. S., Choi, B. I., Kim, Y. S., Kim, H. J., Yang, Y. W., Jung, Y. J. and Kim, Y. M. "**Synthesis and in vitro properties of dexamethasone 21-sulfate sodium as a colon-specific prodrug of dexamethasone**." *Drug Dev Ind Pharm*, **2006**, 32, 3, 389-97

Ko, H., Hambly, B. D., Eris, J. M., Levidiotis, V., Wyburn, K., Wu, H., Chadban, S. J. and Yin, J. L. "**Dentritic cell derived IL-18 production is inhibited by rapamycin and sanglifehrin A, but not cyclosporine A**." *Transplant Immunology*, **2008**, 20, 1-2, 99-105

Koenig, E., Leibig, J., Rieber, T., Theisen, U., Siebert, U., Gothe, R. and Klauss, V. "**Randomized comparison of dexamethasone-eluting stents with bare metal stent implantation in patients with acute coronary syndrome: Serial angiographic and sonographic analysis**." *American Heart Journal*, **2009**, 153, 6, 971-979

Kuribayashi, M. and Tokumoto, S. (2006). Hydrogel composition. **20070020325**.

Køber, L., Torp-Pedersen, C., Carlsen, J. E., Bagger, H., Eliasen, P., Lyngborg, K., Videbæk, J., Cole, D. S., Auclert, L., Pauly, N. C., Aliot, E., Persson, S. and Camm, A. J. "**A Clinical Trial of the Angiotensin-Converting–Enzyme**

Inhibitor Trandolapril in Patients with Left Ventricular Dysfunction after Myocardial Infarction." *N Engl J Med*, **1995**, 333, 1670-1676

Lee, H.-K. and Zhu, T. (1998). Water Soluble Rapamycin Esters. A. H. P. Corporation. U.S.A. **5 780 462**.

Lee, H. J., Park, K. D., Park, H. D., Lee, W. K., Han, D. K., Kim, S. H. and Kim, Y. H. "**Platelet and bacterial repellence on sulfonated poly(ethylene glycol)-acrylate copolymer surfaces**." *Colloids and Surfaces B: Biointerfaces*, **2000**, 18, 3-4, 355-370

Li, J. and Kao, W. J. "**Synthesis of polyethylene glycol (PEG) derivatives and PEGylated-peptide biopolymer conjugates**." *Biomacromolecules*, **2003**, 4, 4, 1055-67

Lin, C. C. and Anseth, K. S. "**PEG hydrogels for the controlled release of biomolecules in regenerative medicine**." *Pharmaceutical Research*, **2009**, 26, 3, 631-43

Lin, C. C. and Metters, A. T. "**Hydrogels in controlled release formulations: network design and mathematical modeling**." *Advanced Drug Delivery Reviews*, **2006**, 58, 12-13, 1379-408

Liu, M., Farrant, R. D., Nicholson, J. K. and Lindon, J. C. "**Selective Detection of 1H NMR Resonances of CHn Groups Using a Heteronuclear Maximum-Quantum Filter and Pulsed Field Gradients** " *Journal of Magnetic Resonance, Series B*, **1995**, 106, 3, 270-278

Liu, X., Quan, L., Tian, J., Laquer, F. C., Ciborowski, P. and Wang, D. "**Synthesis of click PEG-Dexamethasone conjugates for the treatment of rheumatoid arthritis**." *Biomacromolecules*, **2010**, 11, 2621-2628

LoPachin, R. M., Barber, D. S. and Gavin, T. "**Molecular mechanisms of the conjugated alpha,beta-unsaturated carbonyl derivatives: relevance to neurotoxicity and neurodegenerative diseases**." *Toxicological Sciences*, **2008**, 104, 2, 235-49

Lowenberg, M., Verhaar, A. P., van den Brink, G. R. and Hommes, D. W. "**Glucocorticoid signaling: a nongenomic mechanism for T-cell immunosuppression**." *Trends Mol Med*, **2007**, 13, 4, 158-63

LU, W., LI, F. and MAHATO, R. I. "**Poly(ethylene glycol)-Block-Poly(2-methyl-2-benzoxycarbonyl- propylene Carbonate) Micelles for Rapamycin Delivery: In Vitro Characterization and Biodistribution**." *JOURNAL OF PHARMACEUTICAL SCIENCES*, **2011**, 100, 6, 2418-2429

Lu, W., Li, F. and Mahato, R. I. "**Poly(ethylene glycol)-block-poly(2-methyl-2-benzoxycarbonyl-propylene carbonate) micelles for rapamycin delivery: in vitro characterization and biodistribution**." *J Pharm Sci*, **2011**, 100, 6, 2418-29

Lundberg, P., Bruin, A., Klijnstra, J. W., Nystrom, A. M., Johansson, M., Malkoch, M. and Hult, A. "**Poly(ethylene glycol)-based thiol-ene hydrogel coatings-curing chemistry, aqueous stability, and potential marine antifouling applications**." *ACS Applied Materials & Interfaces*, **2010**, 2, 3, 903-12

Lutolf, M. P., Tirelli, N., Cerritelli, S., Cavalli, L. and Hubbell, J. A. "**Systematic modulation of Michael-type reactivity of thiols through the use of charged amino acids**." *Bioconjugate Chemistry*, **2001**, 12, 6, 1051-6

Malkoch, M., Vestberg, R., Gupta, N., Mespouille, L., Dubois, P., Mason, A. F., Hedrick, J. L., Liao, Q., Frank, C. W., Kingsbury, K. and Hawker, C. J. "**Synthesis of well-defined hydrogel networks using click chemistry**." *Chemical Communications*, **2006**, 26, 2774-6

Martellini, F., Higa, O. Z., Takacs, E., Safranj, A., Yoshida, M., Katakai, R. and Carenza, M. "**Thermally reversible gels based on acryloyl-L-proline methyl ester as drug delivery systems**." *Radiation Physics and Chemistry*, **1999**, 55, 185-192

Mason, M. N., Metters, A. T., Bowman, C. N. and Anseth, K. S. "**Predicting Controlled-Release Behavior of Degradable PLA-b-PEG-b-PLA Hydrogels**." *Macromolecules*, **2001**, 34, 4630-4635

Mathers, C. D., Bernard, C., Iburg, K. M., Inoue, M., Ma Fat, D., Shibuya, K., Stein, C., Tomijima, N. and Xu, H. "**Global Burden of Disease: data sources, methods and results**." *http://www.who.int/healthinfo/bod/en/index.html* **2004**,

McAlpine, J. B., Swanson, S. J., Jackson, M. and Whittern, D. N. "**Revised NMR assignments for rapamycin**." *Journal of Antibiotics*, **1991**, 44, 6, 688-690

McCarthy, T. J., Hayes, E. P., Schwartz, C. S. and Witz, G. "**The reactivity of selected acrylate esters toward glutathione and deoxyribonucleosides in vitro: structure-activity relationships**." *Fundamental and Applied Toxicology*, **1994**, 22, 4, 543-8

McGuigan, L. J., Cook, D. J. and Yablonski, M. E. "**Dexamethasone, D-penicillamine, and glaucoma filter surgery in rabbits**." *Invest Ophthalmol Vis Sci*, **1986**, 27, 12, 1755-7

McMullen, J. R., Sherwood, M. C., Tarnavski, O., Zhang, L., Dorfman, A. L., Shioi, T. and Izumo, S. "**Inhibition of mTOR signaling with rapamycin regresses established cardiac hypertrophy induced by pressure overload**." *Circulation*, **2004**, 109, 24, 3050-5

McMurray, J., J., O., K., S., B., G. C., P., H., L., M. E., B., O., S., Y. and A, P. M. "**Effects of candesartan in patients with chronic heart failure and reduced left-ventricular systolic function taking angiotensin-converting-enzyme inhibitors: the CHARM-Added trial**." *Lancet*, **2003**, 362, 767-771

Metters, A. and Hubbell, J. "**Network formation and degradation behavior of hydrogels formed by Michael-type addition reactions**." *Biomacromolecules*, **2005**, 6, 1, 290-301

Miller, D. C., Haberstroh, K. M. and Webster, T. J. "**Mechanism(s) of increased vascular cell adhesion on nanostructured poly(lactic-co-glycolic acid) films**." *Journal of Biomedical Materials Research Part A*, **2005**, 73, 4, 476-84

Morice, M. C., Serruys, P. W., Sousa, J. E., Fajadet, J., Ban Hayashi, E., Perin, M., Colombo, A., Schuler, G., Barragan, P., Guagliumi, G., Molnar, F. and Falotico, R. "**A randomized comparison of a sirolimus-eluting stent with a standard stent for coronary revascularization**." *The New England Journal of Medicine*, **2002**, 346, 23, 1773-80

Nagi, A. S. (1998). Rapamycin formulations for oral administration

Navath, R. S., Kurtoglu, Y. E., Wang, B., Kannan, S., Romero, R. and Kannan, R. M. "**Dendrimer-drug conjugates for tailored intracellular drug release based on glutathione levels**." *Bioconjugate Chemistry*, **2008**, 19, 12, 2446-55

Nelson, D. M., Ma, Z., Fujimoto, K. L., Hashizume, R. and Wagner, W. R. "**Intra-myocardial biomaterial injection therapy in the treatment of heart failure: Materials, outcomes and challenges**." *Acta Biomaterialia*, **2011**, 7, 1-15

Ng, M. K. and Celermajer, D. S. "**Glucocorticoid treatment and cardiovascular disease**." *Heart*, **2004**, 90, 8, 829-30

Nie, T., Baldwin, A., Yamaguchi, N. and Kiick, K. L. "**Production of heparin-functionalized hydrogels for the development of responsive and controlled growth factor delivery systems**." *Journal of Controlled Release*, **2007**, 122, 3, 287-296

Norton, L. W., Koschwanez, H. E., Wisniewski, N. A., Klitzman, B. and Reichert, W. M. "**Vascular endothelial growth factor and dexamethasone release from nonfouling sensor coatings affect the foreign body response**." *J Biomed Mater Res A*, **2007**, 81, 4, 858-69

Nuttelman, C. R., Tripodi, M. C. and Anseth, K. S. "**Dexamethasone-functionalized gels induce osteogenic differentiation of encapsulated hMSCs**." *Journal of Biomedical Materials Research Part A*, **2006**, 76, 1, 183-95

Nuttelman, C. R., Tripodi, M. C. and Anseth, K. S. "**Dexamethasone-functionalized gels induce osteogenic differentiation of encapsulated hMSCs**." *J Biomed Mater Res A*, **2006**, 76, 1, 183-95

Ossipov, D. A., Piskounova, S. and Hilborn, J. "**Poly(vinyl alcohol) Cross-Linkers for in Vivo Injectable Hydrogels**." *Macromolecules*, **2008**, 41, 3971-3982

Padilla De Jesus, O. L., Ihre, H. R., Gagne, L., Frechet, J. M. and Szoka, F. C., Jr. "**Polyester dendritic systems for drug delivery applications: in vitro and in vivo evaluation**." *Bioconjugate Chemistry*, **2002**, 13, 3, 453-61

Pan, Y., Zheng, J. M., Zhao, H. Y., Li, Y. J., Xu, H. and Wei, G. "**Relationship between drug effects and particle size of insulin-loaded bioadhesive microspheres**." *Acta Pharmacologica Sinica*, **2002**, 23, 11, 1051-1056

Pang, Y. N., Zhang, Y. and Zhang, Z. R. "**Synthesis of an enzyme-dependent prodrug and evaluation of its potential for colon targeting**." *World Journal of Gastroenterology*, **2002**, 8, 5, 913-7

Patil, S. D., Papadmitrakopoulos, F. and Burgess, D. J. "**Concurrent delivery of dexamethasone and VEGF for localized inflammation control and angiogenesis**." *J Control Release*, **2007**, 117, 1, 68-79

Peppas, N. A., Hilt, J. Z., Khademhosseini, A. and Langer, R. "**Hydrogels in Biology and Medicine: From Molecular Principles to Bionanotechnology**." *Advanced Materials*, **2006**, 18, 1345-1360

Plattsburgh, H. L. and Monroe, T. Z. (1998). Water Soluble Rapamycin Esters. A. H. P. Corporation. U.S.A. **5780462**.

Proud, C. G. "**Ras, PI3-kinase and mTOR signaling in cardiac hypertrophy**." *Cardiovascular Research*, **2004**, 63, 3, 403-413

Qiao, M., Chen, D., Ma, X. and Liu, Y. "**Injectable biodegradable temperature-responsive PLGA-PEG-PLGA copolymers: synthesis and effect of copolymer composition on the drug release from the copolymer-based hydrogels**." *International Journal of Pharmaceutics*, **2005**, 294, 1-2, 103-12

Rajender, G. and Narayanan, N. G. "**Liquid chromatography-tandem mass spectrometry method for determination of Sirolimus coated drug eluting nano porous carbon stents**." *Biomedical Chromatography*, **2010**, 24, 3, 329-334

Rebuffat, A. G., Nawrocki, A. R., Nielsen, P. E., Bernasconi, A. G., Bernal-Mendez, E., Frey, B. M. and Frey, F. J. "**Gene delivery by a steroid-peptide nucleic acid conjugate**." *FASEB Journal*, **2002**, 16, 9, 1426-+

Reddy, M. K., Vasir, J. K., Sahoo, S. K., Jain, T. K., Yallapu, M. M. and Labhasetwar, V. "**Inhibition of apoptosis through localized delivery of rapamycin-loaded nanoparticles prevented neointimal hyperplasia and reendothelialized injured artery**." *Circulation: Cardiovascular Interventions*, **2008**, 1, 3, 209-16

Reeve, M. S., McCarthy, S. P., Downey, M. J. and Gross, R. A. "**Polylactide Stereochemistry: Effect on Enzymatic Degradability**." *Macromolecules*, **1994**, 27, 825-831

Ricciutelli, M., Di Martino, P., Barboni, L. and Martelli, S. "**Evaluation of rapamycin chemical stability in volatile-organic solvents by HPLC**." *Journal of Pharmaceutical and Biomedical Analysis*, **2006**, 41, 3, 1070-4

Richter, A., Paschew, G., Klatt, S., Lienig, J., Arndt, K.-F. and Adler, H.-j. P. "**Review on Hydrogel-based pH Sensors and Microsensors**." *Sensors*, **2008**, 8, 561-581

Ridker, P. M., Danielson, E., Fonseca, F. A. H., Genest, J., Gotto, A. M., Kastelein, J. J. P., Koenig, W., Libby, P., Lorenzatti, A. J., MacFadyen, J. G., Nordestgaard, B. G., Shepherd, J., Willerson, J. T. and J., G. R. "**Rosuvastatin to Prevent Vascular Events in Men and Women with Elevated C-Reactive Protein**." *The New England Journal of Medicine*, **2008**, 359, 21, 2195-2207

Ridker, P. M., Rifai, N., Rose, L., Buring, J. E. and Cook, N. R. "**Comparison of C-reactive protein and low-density lipoprotein cholesterol levels in the prediction of first cardiovascular events**." *N Engl J Med*, **2002**, 347, 20, 1557-65

Roberts, M. J., Bentley, M. D. and Harris, J. M. "**Chemistry for peptide and protein PEGylation**." *Adv Drug Deliv Rev*, **2002**, 54, 4, 459-76

Rydholm, A. E., Anseth, K. S. and Bowman, C. N. "**Effects of neighboring sulfides and pH on ester hydrolysis in thiol-acrylate photopolymers**." *Acta Biomater*, **2007**, 3, 4, 449-55

Rydholm, A. E., Reddy, S. K., Anseth, K. S. and Bowman, C. N. "**Development and Characterization of Degradable Thiol-Allyl Ether Photopolymers**." *Polymer (Guildf)*, **2007**, 48, 15, 4589-4600

Sakakibara, K., Liu, B., Hollenbeck, S. and Kent, K. C. "**Rapamycin inhibits fibronectin-induced migration of the human arterial smooth muscle line (E47) through the mammalian target of rapamycin**." *American Journal of Physiology-Heart and Circulatory Physiology*, **2005**, 288, 6, H2861-H2868

Scarborough, P., Bhatnagar, P., Wickramasinghe, K., Smolina, K., C., M. and M., R. (2010). Coronary heart disease statistics 2010 edition. London, British Heart Foundation.

Schachter, M. "**Chemical, pharmacokinetic and pharmacodynamic properties of statins: an update**." *Fundamental & Clinical Pharmacology*, **2004**, 19, 117-125

Schmelzle, T. and Hall, M. N. "**TOR, a central controller of cell growth**." *Cell*, **2000**, 103, 2, 253-62

Schoenmakers, R. G., van de Wetering, P., Elbert, D. L. and Hubbell, J. A. "**The effect of the linker on the hydrolysis rate of drug-linked ester bonds**." *Journal of Controlled Release*, **2004**, 95, 2, 291-300

Schultz, C. L. (2003). Growth factor delivery system for the healing of wounds and the prevention of inflammation and disease. **20030203001**.

Segers, V. F. and Lee, R. T. "**Stem-cell therapy for cardiac disease**." *Nature*, **2008**, 451, 7181, 937-42

Sen, M. and Guven, O. "**Prediction of the swelling of amphiphilic hydrogels and the determination of average molcular weight between cross-links**." *Computational and Theoretical Polymer Science*, **2000**, 11, 475-482

Sharp, Z. R., Strong, J. R., Galvan, V., Oddo, S. and Wheeler, H. G. (2012). INHIBITION OF MAMMALIAN TARGET OF RAPAMYCIN.

Shioi, T., McMullen, J. R., Tarnavski, O., Converso, K., Sherwood, M. C., Manning, W. J. and Izumo, S. "**Rapamycin attenuates load-induced cardiac hypertrophy in mice**." *Circulation*, **2003**, 107, 12, 1664-70

Shiojima, I., Sato, K., Izumiya, Y., Schiekofer, S., Ito, M., Liao, R., Colucci, W. S. and Walsh, K. "**Disruption of coordinated cardiac hypertrophy and angiogenesis contributes to the transition to heart failure**." *Journal of Clinical Investigation*, **2005**, 115, 8, 2108-18

Shoaib, M. H., Tazeen, J., Merchant, H. A. and Yousuf, R. I. "**Evaluation of drug release kinetics from ibuprofen matrix tablets using HPMC**." *Pakistan Journal of Pharmaceutical Sciences*, **2006**, 19, 2, 119-124

Siepmann, J., Kranz, H., Peppas, N. A. and Bodmeier, R. "**Calculation of the required size and shape of hydroxypropyl methylcellulose matrices to achieve desired drug release profiles**." *International Journal of Pharmaceutics*, **2000**, 201, 2, 151-64

Siepmann, J. and Peppas, N. A. "**Modeling of drug release from delivery systems based on hydroxypropyl methylcellulose (HPMC)**." *Advanced Drug Delivery Reviews*, **2001**, 48, 2-3, 139-57

Siepmann, J. and Peppas, N. A. (2011). Higuchi equation: Derivation, applications, use and misuse. Int J Pharm.

Singer, A. J. and Clark, R. A. "**Cutaneous wound healing**." *New England Journal of Medicine*, **1999**, 341, 10, 738-46

Song, Z., Feng, R., Sun, M., Guo, C., Gao, Y., Li, L. and Zhai, G. "**Curcumin-loaded PLGA-PEG-PLGA triblock copolymeric micelles: Preparation, pharmacokinetics and distribution in vivo.**" *Journal of Colloid and Interface Science*, **2011**, 354, 1, 116-123

Srinivasan, S., Lee, M. W., Grady, M. C., Soroush, M. and Rappe, A. M. "**Self-initiation mechanism in spontaneous thermal polymerization of ethyl and n-butyl acrylate: a theoretical study**." *Journal of Physical Chemistry A*, **2010**, 114, 30, 7975-83

Stojkovic, S., Ostojic, M., Nedeljkovic, M., Stankovic, G., Beleslin, B., Vukcevic, V., Orlic, D., Arandjelovic, A., Kostic, J., Dikic, M. and Tomasevic, M. "**Systemic rapamycin without loading dose for restenosis prevention after coronary bare metal stent implantation**." *Catheterization and Cardiovascular Interventions*, **2010**, 75, 3, 317-25

Stojkovic, S., Ostojic, M., Nedeljkovic, M., Stankovic, G., Beleslin, B., Vukcevic, V., Orlic, D., Arandjelovic, A., Kostic, J., Dikic, M. and Tomasevic, M. "**Systemic rapamycin without loading dose for restenosis prevention after coronary bare metal stent implantation**." *Catheter Cardiovasc Interv*, **2010**, 75, 3, 317-25

Ulbrich, K., Etrych, T., Chytil, P., Pechar, M., Jelinkova, M. and Rihova, B. "**Polymeric anticancer drugs with pH-controlled activation**." *International Journal of Pharmaceutics*, **2004**, 277, 1-2, 63-72

Wadhwa, R., Lagenaur, C. F. and Cui, X. T. "**Electrochemically controlled release of dexamethasone from conducting polymer polypyrrole coated electrode**." *J Control Release*, **2006**, 110, 3, 531-41

van de Wetering, P., Metters, A. T., Schoenmakers, R. G. and Hubbell, J. A. "**Poly(ethylene glycol) hydrogels formed by conjugate addition with controllable swelling, degradation, and release of pharmaceutically active proteins**." *Journal of Controlled Release*, **2005**, 102, 3, 619-627

Wang, T. and Guo, Z. "**Copper in medicine: homeostasis, chelation therapy and antitumor drug design**." *Current Medicinal Chemistry*, **2006**, 13, 5, 525-37

Wang, X., Venkatraman, S. S., Boey, F. Y., Loo, J. S. and Tan, L. P. "**Controlled release of sirolimus from a multilayered PLGA stent matrix**." *Biomaterials*, **2006**, 27, 32, 5588-95

Vanhoutte, D., Schellings, M., Pinto, Y. and Heymans, S. "**Relevance of matrix metalloproteinases and their inhibitors after myocardial infarction: a temporal and spatial window**." *Cardiovascular Research*, **2006**, 69, 3, 604-13

Waranis, R. P., Harrison, M. M., Leonard, T. W. and Enever, R. P. (1996). Rapamycin formulation for IV injection. **5 530 006**.

Venkatraman, S. and Boey, F. "**Release profiles in drug-eluting stents: issues and uncertainties**." *Journal of Controlled Release*, **2007**, 120, 3, 149-60

Veronese, F. M. and Pasut, G. "**PEGylation, successful approach to drug delivery**." *Drug Discov Today*, **2005**, 10, 21, 1451-8

Veronese, F. M. and Pasut, G. "**PEGylation, successful approach to drug delivery**." *Drug Discovery Today*, **2005**, 10, 21, 1451-8

West, K. R. and Otto, S. "**Reversible covalent chemistry in drug delivery**." *Current Drug Discovery Technologies*, **2005**, 2, 3, 123-60

Villa, A. E., Guzman, L. A., Chen, W., Golomb, G., Levy, R. J. and Topol, E. J. "**Local delivery of dexamethasone for prevention of neointimal proliferation in a rat model of balloon angioplasty**." *J Clin Invest*, **1994**, 93, 3, 1243-9

Wilson, V. S., Bobseine, K., Lambright, C. R. and Gray, L. E., Jr. "**A novel cell line, MDA-kb2, that stably expresses an androgen- and glucocorticoid-responsive reporter for the detection of hormone receptor agonists and antagonists**." *Toxicological Sciences*, **2002**, 66, 1, 69-81

Viswanath, S., Bartelt, L., Leanna, R., Rasmussen, M., Dhaon, M., Henry, R., Borchardt, T., Chen, S. and Zhang, G. (2008). Methods of Manufacturing Crystalline Forms of Rapamycin Analogs. **7 820 812**.

Woghiren, C., Sharma, B. and Stein, S. "**Protected thiol-polyethylene glycol: a new activated polymer for reversible protein modification**." *Bioconjugate Chemistry*, **1993**, 4, 5, 314-8

Yallapu, M. M., Vasir, J. K., Jain, T. K., Vijayaraghavalu, S. and Labhasetwar, V. "**Synthesis, characterization and antiproliferative activity of rapamycin-loaded poly(N-isopropylacrylamide)-based nanogels in vascular smooth muscle cells**." *Journal of Biomedical Nanotechnology*, **2008**, 4, 1, 16-24

Yeh, C. C., Hou, M. F., Wu, S. H., Tsai, S. M., Lin, S. K., Hou, L. A., Ma, H. and Tsai, L. Y. "**A study of glutathione status in the blood and tissues of patients with breast cancer**." *Cell Biochemistry and Function*, **2006**, 24, 6, 555-9

Yoon, J. J., Kim, J. H. and Park, T. G. "**Dexamethasone-releasing biodegradable polymer scaffolds fabricated by a gas-foaming/salt-leaching method**." *Biomaterials*, **2003**, 24, 13, 2323-9

Yu, K., Lucas, J., Zhu, T., Zask, A., Gaydos, C., Toral-Barza, L., Gu, J., Li, F., Chaudhary, I., Cai, P., Lotvin, J., Petersen, R., Ruppen, M., Fawzi, M., Ayral-Kaloustian, S., Skotnicki, J., Mansour, T., Frost, P. and Gibbons, J. "**PWT-458, a novel pegylated-17-hydroxywortmannin, inhibits phosphatidylinositol 3-kinase signaling and suppresses growth of solid tumors**." *Cancer Biology & Therapy*, **2005**, 4, 5, 538-45

Zacchigna, M., Cateni, F., Di Luca, G., Voinovich, D., Perissutti, B., Drioli, S. and Bonora, G. M. "**Synthesis of a new mPEG-dexamethasone conjugate and preliminary bioavailability studies in rabbits**." *Journal of Drug Delivery Science and Technology*, **2008**, 18, 3, 155-159

Zisch, A. H., Lutolf, M. P., Ehrbar, M., Raeber, G. P., Rizzi, S. C., Davies, N., Schmokel, H., Bezuidenhout, D., Djonov, V., Zilla, P. and Hubbell, J. A. "**Cell-demanded release of VEGF from synthetic, biointeractive cell ingrowth matrices for vascularized tissue growth**." *Faseb Journal*, **2003**, 17, 15, 2260-2

Zolnik, B. S. and Burgess, D. J. "**Evaluation of in vivo-in vitro release of dexamethasone from PLGA microspheres**." *J Control Release*, **2008**, 127, 2, 137-45